ORGANIC-FUNCTIONALIZED MOLECULAR SIEVES (OFMS'S): A NEW CLASS OF MATERIALS

Thesis by

Christopher W. Jones

In Partial Fulfillment of the Requirements

for the Degree of

Doctor of Philosophy

California Institute of Technology

Pasadena, California

1999

(submitted May 28, 1999)

to my parents,

Elbert W. Jones Jr. and Mary Lou Jones

and my grandparents,

Milton C. Portmann Jr. and Eleanor Hill Portmann,

Elbert W. Jones and Mary Ann Jones

ACKNOWLEDGMENTS

I have learned more about myself, life, and science during my four years at Caltech than I would have ever dreamt possible. This is largely due to the superb learning environment created by Professor Mark E. Davis in his laboratories. Everything about the Davis Laboratories is first class: my colleagues, the resources, and the forward-looking drive that continuously pushes the boundaries of the field. Most importantly, Mark has an unwavering interest in and support for the intellectual and personal growth of his students. I can not imagine a better place to study.

I would like to thank my thesis committee, Dr. Jay Labinger, Professor George Gavalas, Professor Rick Flagan and Professor Dave Tirrell for their interest and helpful insights into my work.

Many members of the Davis Group helped make my transition into the lab a smooth one. Chris Dartt and Shervin Khodabandeh were instrumental in teaching me about zeolite synthesis. Larry Beck introduced me to solid state NMR and was quite generous with his time in helping me learn the technique. Hector Gonzalez was always willing to give well-thought-out organic chemistry advice when I needed it and chat about sports when science was the last thing I wanted to think about. I had great discussions with Katsuyuki Tsuji, both in the lab and on the golf course. Alex Katz was both helpful with his knowledge of organic and silica chemistry and entertaining with his musical abilities and sense of humor. All of my chemical engineering student cohorts in the Davis Group have been great colleagues and friends.

Dr. Stacey Zones and Dr. C. Y. Chen at Chevron have been great mentors and friends. I appreciate the interest in my personal and professional growth that both have shown over the last four years.

Many friends at Caltech have made my years here very memorable. In particular, I will never forget: surviving the New Year's Eve Window-Gate Scandal with Rob Griffin; incessant right-hand turns at Mammoth Mountain with Jason Kenney; multi-hour football scouting missions with Mike Vicic; Korean BBQ and endless faculty search discussions with Gyeong Soon Hwang; laughing along with Mina Sierou and Jeff Eldredge as Michele Ostraat screams at the TV during the X-Files or Millenium; camping in the San Gabriel Mountains with Peter Adams and Amy Rigsby; hours and hours and hours of studying for the transport qualifier with Mike "Grashof Number" Gordon; all of my time with my various football, softball and basketball teams and the hockey team. Others who contributed to my great experience at Caltech include Ken Carlgren, Tim Van Reken, Ann McAdam, and Cheryl Anderson.

All of my accomplishments are a direct reflection of the support I have always received from my family. My parents have sacrificed for many years for me and have shaped me into who I am today. They instilled in me a love for knowledge and a strong work ethic that has enabled me to accomplish anything I set my mind to. My brothers Bill and Brian along with my large extended family of grandparents, aunts, uncles and cousins have created a strong and supportive 'home base' that I have always relied upon in good times and bad. My California family in Orange and San Diego Counties provided a great home away from home that served as a respite from the busy world of Caltech.

Many people prior to my matriculation at Caltech have contributed to my desire to pursue a PhD in chemical engineering. Mentors such as Levi T. Thompson, H. Scott Fogler, Marcy Osgood and Ross Graham all motivated and encouraged my quest for knowledge. Colleagues such as Ken Benjamin, Dave Beuther, Paul Graham, Rich Otten, Jennifer Tipa and Wendyann Wright were always extremely supportive.

The person to whom I am most indebted is Shaney Lokken. She has always been willing to listen to me banter about my studies and tirelessly has supported all of my efforts in every endeavor. She enabled me to keep sight of what is really important in life and not become overwhelmed with the rigors of my research. My successes were sweeter and my lows did not seem quite as bad, thanks to her.

It is sad that this chapter of my life has to end, but another will begin, building off my experiences of the past 4 years.

ABSTRACT

Throughout the last two decades, there has been a tremendous interest and growth in molecular sieve science. In particular, substantial attention has been paid to the development of new molecular sieves for catalytic applications, as molecular sieves have the unique ability to promote reactions in a shape-selective manner. To increase the variety of reactions that can be catalyzed by molecular sieves, recent efforts have focused on generating new types of active sites in molecular sieves by incorporating transition metals into the silicate framework or by supporting metal-based species within the micropores. Despite this, there are still many chemistries that can not be carried out over molecular sieve catalysts where significant benefit could be gained if the reaction were to be accomplished in a shape-selective manner. To address this problem, I have prepared a new class of molecular sieves that contain intracrystalline organic functionalities [denoted organic-functionalized molecular sieves (OFMS's)]. Previous attempts to synthesize silicate-based molecular sieves with organic functionalities within the micropores have focused on grafting organic groups onto pre-formed zeolites. However, this is not a viable route to the production of OFMS's that can function as shape-selective catalysts, as the organic groups preferentially functionalize the external crystal surface. Here, the problems with this approach are circumvented by preparing OFMS's by direct synthesis.

Attempts to synthesize OFMS's directly both in the presence and absence of organic structure-directing agents (SDA's) are described. Pure-silica beta zeolites containing a variety of intracrystalline organic groups are synthesized using tetraethylammonium fluoride (TEAF) as the SDA. Porosity is generated by removing the occluded TEAF by solvent-extraction techniques. Following extraction, the exposed organic functionalities are further altered by chemical techniques, e.g., amines to imines, phenethyl groups to phenethylsulfonic acid groups. The ability to perform

shape-selective acid catalysis (phenethylsulfonic acid) and shape-selective formation of imines from amines indicates that the organic moieties reside largely in the micropores of the molecular sieve. Several preparation variables have an impact on the nature of the resulting OFMS's, the most of important of which are the synthetic method, silicon source, and extraction method. The effects of these synthetic factors on the crystal size and morphology, porosity and hydrophobicity of the products are discussed.

TABLE OF CONTENTS

Chapter One *Introduction and Objectives*

Chapter Two *Investigations into the Synthesis OFMS's*
  from Hydrophilic, Organic SDA-free Gels

Chapter Six   *Conclusions*

LIST OF TABLES

LIST OF FIGURES

Chapter One

Chapter Two

Chapter Three

Chapter Four

Chapter Five

LIST OF PUBLICATIONS

"Organic-Functionalized Molecular Sieves (OFMS's): II Synthesis, Characterization and the Transformation of OFMS's with Non-Polar Functional Groups into Solid Acids."

C. W. Jones, K. Tsuji, and M. E. Davis *Microporous Mesoporous Mater.* (submitted).

"Organic-Functionalized Molecular Sieves (OFMS's): I Synthesis and Characterization of OFMS's with Polar Groups."

K. Tsuji, C. W. Jones, and M. E. Davis *Microporous Mesoporous Mater.* (in press).

"Reactions of M-Xylene Over Zeolites with Intersecting Medium and Large Pores Part 2: Aluminum Population in Structures with CON Topology."

C. W. Jones, S. I. Zones, and M. E. Davis *Microporous Mesoporous Mater.* 28 (1999) 471-481.

"M-Xylene Reactions over Zeolites with Unidimensional Pore Systems."

C. W. Jones, S. I. Zones, and M. E. Davis *Appl. Catal. A.* 181 (1999) 289-303.

"Organic-Functionalized Molecular Sieves: A New Class of Shape Selective Catalysts."

C. W. Jones, K. Tsuji, and M. E. Davis in *Proceedings of the 12th International Zeolite Conference*, Materials Research Society, 1479-1486, 1999.

"Synthesis, Characterization and Structure Solution of CIT-5, a New High Silica Molecular Sieve."

M. Yoshikawa, P. Wagner, M. Lovallo, K. Tsuji, T. Takewaki, C. Y. Chen, L. W. Beck, C. Jones, M. Tsapatsis, S. I. Zones, and M. E. Davis *J. Phys. Chem.* 102 (1998) 7139-7147.

"Organic-Functionalized Molecular Sieves as Shape-Selective Catalysts."

C. W. Jones, K. Tsuji, and M. E. Davis *Nature* 383 (1998) 52-54.

U.S. Patent Application

K. Tsuji, C. W. Jones, and M. E. Davis;

Provisional Application 60/057,652 Filed August 25, 1997

Provisional Application 60/083,787 Filed May 1, 1998

CHAPTER ONE

Introduction and Objectives

1.1 Introduction

Molecular sieves are crystalline solids that contain pores that are similar in size to small organic molecules (roughly 2-10 Å in diameter). The porous nature of these materials imparts molecular sieves with a large internal surface area and hence the ability to adsorb a variety of gases or liquids. Because these materials are crystalline, the pores throughout the materials are uniform. This enables molecular sieves to selectively adsorb molecules of specific sizes or shapes; hence, the name molecular sieve.

Perhaps the simplest example of a molecular sieve is a microporous, pure-silicate such as silicalite. Silicalite is composed of an infinitely extending three-dimensional network of SiO_4 tetrahedra linked to give the periodic structure described in Figure 1.1. Substitution of some of the silicon atoms by aluminum atoms produces a molecular sieve with an anionic framework as described in Figure 1.2. These microporous aluminosilicates, also called zeolites, require a balancing cation for charge neutralization of the framework. These cations reside within the micropores of the zeolite and hence are accessible to adsorbed species. When the cations are protons, the zeolites are solid acids that are capable of promoting acid catalyzed reactions within the micropores of the molecular sieve crystals.

A wide variety of catalytically active sites can be incorporated into the micropores of zeolites. As indicated above, substitution of some silicon atoms by trivalent atoms such as aluminum or gallium produces a cation exchange site. By altering the balancing cation, a variety of types of active sites can be produced. For example, ion exchange with alkali cations such as sodium, potassium or cesium produces an active site with basic character [1]. In addition, exchange with transition metals such as Co^{2+} also can create sites with unique catalytic capabilities [2]. Another approach to creating active sites is to deposit an extra-framework species within the molecular sieve micropores. For example, small metal oxide clusters [3] or small metal

particles [4] can be supported within the micropores of zeolites. Additionally, incorporation of other tetravalent atoms into the framework (substitution for silicon) such as titanium [5] or vanadium [6] can produce sites active for oxidation and oxidative dehydrogenation, respectively.

Because the catalytically active sites are in the constrained environment of the micropores, zeolites and molecular sieves are capable of promoting reactions to give a different selectivity than typical homogeneous catalysts. The ability to sterically alter the course of a catalytic reaction, to impart "shape-selectivity" on a reaction in a uniform manner, makes molecular sieves unique in the realm of heterogeneous catalysis.

There are three different types of shape-selectivity that are widely discussed [7]. The first type of shape-selectivity is called reactant shape-selectivity. In this case, the size of the micropores of the catalyst will not allow large molecules to enter the zeolite and react. However, smaller molecules that are capable of diffusing into the molecular sieve react over the active sites. An example of this type of shape-selectivity is illustrated in Figure 1.3 a, where linear alkanes are selectively cracked and the larger branched alkanes are too large to enter the micropores of the zeolite catalyst. Product shape-selectivity also occurs over zeolites and molecular sieves. An example of this type of shape-selectivity is shown in Figure 1.3 b. In the alkylation of toluene with methanol over an acidic catalyst, the expected major products are ortho, meta and para-xylene. When this reaction is carried out over zeolite catalysts, p-xylene is preferentially produced at the expense of the bulkier meta and ortho isomers. The third type of shape-selectivity, transition state selectivity, is depicted in Figure 1.3 c. In this case, both the reactants and products can fit within the micropores of the molecular sieve but the necessary reaction transition state is too large to be accommodated within the pores.

Zeolites are currently used extensively in a variety of industrial catalytic processes [8]. Most of these processes, such as those listed in Table 1.1, are gas-

phase catalytic conversions important to the petrochemical industry. While zeolites are currently among the most important classes of catalysts for industrial, gas-phase catalytic production of bulk chemicals and petrochemicals, the future will bring an increase in the use of molecular sieves in liquid phase catalytic processes important to the fine chemical and pharmaceutical industries. Recently, liquid phase catalytic processes based on molecular sieve catalysts have been implemented for the production of fine chemicals. For example, Enichem has produced catechol and hydroquinone over the last decade using a microporous, titanosilicate catalyst TS-1 [9]. Also, Rhone Poulenc has developed a liquid phase process for the acylation of anisole using zeolite beta in the liquid phase [10].

Despite the vast array of types of active sites that can be introduced into molecular sieves by the methods discussed above, there are still many reactions that can not be carried out over zeolites and molecular sieves. In many cases, the ability to run a reaction in a shape-selective manner would result in significant economic (cost reduction) and environmental (reduction of unwanted by-products) impact. For example, the ability to nitrate aromatics in a shape-selective manner using nitric acid in the liquid phase would bring significant improvements to the production of dinitrobenzene. Currently, a distribution of dinitrobenzenes (mostly m-dinitrobenzene) are produced by homogeneous catalysis and the isomers are then separated, as shown in Scheme 1.1 below. The ability to produce p-dinitrobenzene in high-yield by utilizing the shape-selective acid sites of a zeolite would be a beneficial technological advance. Unfortunately, this chemistry can not be performed over an aluminosilicate acid catalyst due to an inability to nitrate the deactivated aromatic nitrobenzene in the unfavorable para position. Additionally, there is the problem that the zeolitic aluminum is not very stable in nitric acid and can be leached from the molecular sieve. The creation of an active site that is stable in the presence of nitric acid and with increased acidity relative

to a zeolite within the micropores of a molecular sieve would circumvent these problems.

$$HNO_3 \qquad H_2O$$

MINOR   MINOR   MAJOR
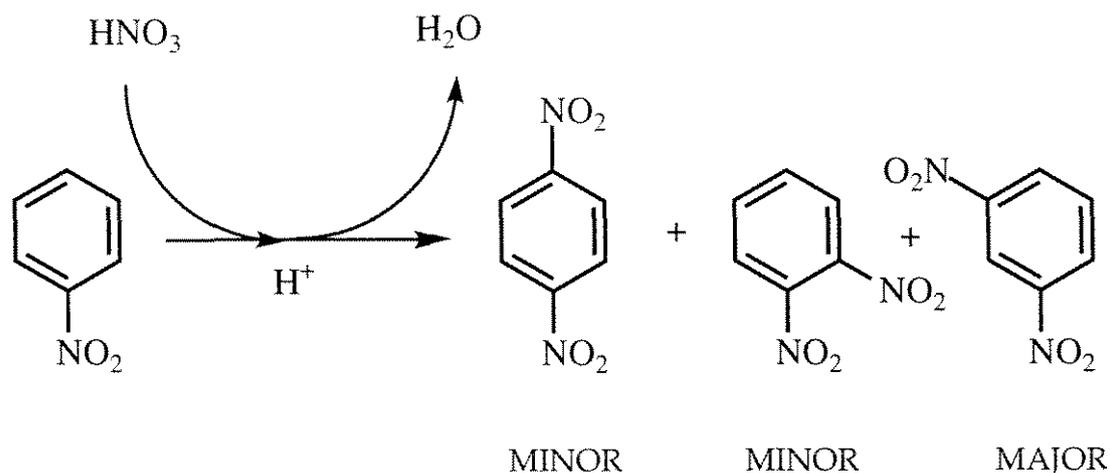
Scheme 1.1

Hence, as the above-example illustrates, there remains a need to develop new methods of creating active sites within the micropores of molecular sieves. A wide variety of active site types can currently be created as outlined above. However, all of the methods rely on active sites based on metal centers. The creation of molecular sieves with active sites based on organic species, organic-functionalized molecular sieves (OFMS's), would significantly broaden the range of active sites in molecular sieves and therefore reaction chemistries amenable to promotion in a shape-selective manner. If an organic residue can be covalently attached to the framework, by a silicon-carbon bond for example, the diversity of organic chemistry could then be used to create active sites tailored for specific reactions of interest. Figure 1.4 illustrates the concept of creating an OFMS active site.

1.2 OFMS Synthesis

There are two synthetic routes available for the synthesis of OFMS's. The first route involves the functionalization of pre-synthesized molecular sieves with organic species by using grafting techniques. The second route is to synthesize the entire molecular sieve from precursor species such that it contains organic functional groups already tethered to the framework.

Grafting techniques have been used successfully by a number of researchers to functionalize mesoporous (pore diameter > 20 Å) silicate materials with organic species. Cauvel and coworkers first showed that catalytically active organic species could be easily grafted onto the pore walls of mesoporous MCM-41-type materials [11]. Attempts have been made to develop OFMS materials using grafting techniques as well. In 1988, Bein and coworkers studied the interaction of organosilanes with acidic zeolites by solid-state NMR and showed that the organosilanes are covalently grafted onto the zeolite [12]. Brunel and coworkers attempted to functionalize zeolite NaY and HY with organosilanes by grafting in 1995 [13]. They found that the organosilanes preferentially functionalize the external surface, giving very little functionalization of the target area, the micropores. Subsequently, Ahmad and Davis studied the functionalization of the molecular sieve SSZ-33 by grafting and found similar results [14]. Unlike the facile grafting of organosilanes onto the walls of mesoporous materials, grafting of organosilanes onto microporous materials such as zeolites (pore diameter < 10 Å) results in blockage of the relatively small pores and prevents significant incorporation of organic groups on the interior of the crystals.

These results indicate that grafting will not likely result in a viable route to organic-functionalized molecular sieves with shape-selective properties. Hence, production of OFMS's by direct synthesis seems a more suitable approach.

Zeolites and molecular sieves are generally synthesized from a mixture containing a silica source (and an aluminum source in the case of zeolites), a

mineralizing agent (OH⁻ or F⁻), water and in some cases an organic structure-directing agent (SDA) such as tetrapropylammonium hydroxide [15]. Figure 1.5 illustrates the general synthetic strategy. Synthesis of molecular sieves in the absence of an organic structure directing agent generally requires the inclusion of a non-silicon tetrahedral atom in the synthesis mixture and thus incorporation of that species into the framework of the molecular sieve (substitution of some Si by Al, B, Ga, etc.). Hence, synthesis of an OFMS from a starting gel free of an organic SDA will result in a hydrophilic structure containing an anionic framework. For liquid phase catalytic applications where substrate adsorption and product desorption are critical, hydrophobic molecular sieves are preferred due to their more favorable partitioning abilities.

Zeolites and molecular sieves synthesized from a starting mixture that includes an organic SDA generally have no microporosity in the as-synthesized form. This is because the organic SDA is occluded within the micropores as shown in Figure 1.5. Hence, the SDA must be removed to generate porosity. The standard technique for removal of SDA's from molecular sieves is to calcine the materials at high temperatures in air, thereby combusting the organic species and leaving the pores of the inorganic framework free of condensed species. This approach is not amenable to the synthesis of OFMS materials because the calcination step would also remove the intended organic functionality. Hence, synthesis of OFMS's from a gel containing an organic SDA requires two things. First, there must be sufficient space within the micropores for incorporation of the intended organic functional group and second, the SDA must be removed by means other than calcination.

1.3   Objectives

The last two decades has seen a large increase in the development of zeolite and molecular sieve science. New non-silicon atoms such as titanium [5], vanadium [6], and iron [16] have been incorporated into the frameworks of silicate molecular sieves.

Even entirely new classes of materials, such as the aluminophosphate (ALPO) molecular sieves, have been developed [17]. Despite this, as described in the previous sections, there are still many reaction chemistries that would bring significant economic, environmental and technological benefit to society if they could be carried out in a shape-selective manner. Development of molecular sieves with a new type of active center, a center based on an organic species, would create an new class of catalytic materials where the type and strength of the active site could be designed using the common techniques of organic chemistry.

The primary objective of this work is to develop a strategy for the synthesis of organic-functionalized molecular sieves. The problem has been addressed by synthesizing OFMS's directly from molecular precursors to circumvent the problems that other researchers have encountered when trying to graft organic species onto pre-formed zeolites [13,14]. Synthetic routes for the synthesis of OFMS's that both did and did not require an organic SDA were evaluated, with the investigations leading to the synthesis of the first OFMS's. Additional objectives include probing the generality of the techniques, demonstration of shape-selective properties, and demonstration of the potential to modify the functional groups using organic chemical techniques.

Chapter 2 describes efforts to synthesize OFMS's using a synthetic strategy that did not include an organic SDA. Chapter 3 provides a conceptual demonstration of the approach that was developed to synthesize the first OFMS catalyst. Pure-silica zeolite beta was synthesized in the presence of phenethyltrimethoxysilane using tetraethlammonium fluoride as a SDA to produce a molecular sieve with intracrystalline phenylsulfonic acid groups. Chapter 4 extends the synthetic strategy described in Chapter 3 to include other organic functional groups, specifically moieties containing basic functionalities. Chapter 5 details the synthesis and characterization of the phenyl-functionalized OFMS introduced in Chapter 3. Chapter 6 provides a summary and discusses the impact of this work on the fields of molecular sieve science and catalysis.

1.4 References

[1]   H. Hattori *Chem. Rev.* 95 (1995) 537-558.

[2]   Y. J. Li and J. N. Armor *J. Catal.* 173 (1998) 511-518.

[3]   P. E. Hathaway and M. E. Davis *J. Catal.* 116 (1989) 263-278.

[4]   E. J. Creyghton and R. S. Downing *J. Mol. Catal. A* 134 (1998) 47-61.

[5]   M. Taramasso and B. Notari U. S. Patent 4,410,501, 1983.

[6]   T. Inui, D. Medhanavyn, P. Praserthdam, K. Fukuda, T. Ukawa, A.
       Sakamoto, and A. Miyamoto *Appl. Catal* 18 (1985) 311-324; M. S. Rigutto
       and H. van Bekkum *Appl. Catal. A* 68 (1991) L1-L7.

[7]   S. M. Sciscery *Zeolites* 4 (1984) 202-213.

[8]   (a) S. T. Sie in *Studies in Surface Science and Catalysis 85* (J. C. Jansen, et
       al. Eds.) Elsevier, Amsterdam, 1994; (b) A. Dyer, *An Introduction to Zeolite
       Molecular Sieves*; John Wiley & Sons: New York, 1988.

[9]   U. Romano, A. Esposito, F. Maspero, and C. Neri in *Studies in Surface
       Science and Catalysis 55* (G. Senti and F. Trifiro, Eds.) Elsevier, Amsterdam,
       1990.

[10]   M. Spagnol, L. Gilbert, E. Benazzi, and C. Marcilly Patent PCT, Int. Appl.
       WO 96 35,655, 1996; M. Spagnol, L. Gilbert, R. Jacqout, H. Guillot, P. J.
       Tirel, and A. LeGovic in *Proceedings of the 4th International Symposium on
       Heterogeneous Catalysis and Fine Chemicals*, Basel, 1996.

[11]   D. Brunel, A. Cauvel, F. Fajula, and F. DiRenzo in *Studies in Surface
       Science and Catalysis 97* (L. Bonneviot et al., Eds.) Elsevier, Amsterdam,
       1995.

[12]   T. Bein, R. F. Carver, R. D. Farlee, and G. D. Stucky *J. Am. Chem. Soc.* 110
       (1988) 4546-4553.

[13]   A. Cauvel, D. Brunel, F. DiRenzo, P. Moreau, and F. Fajula in *Studies in Surface Science and Catalysis 94* (H. K. Beyer, et al., Eds.) Elsevier, Amsterdam, 1995.

[14]   W. R. Ahmad and M. E. Davis, unpublished results.

[15]   R. F. Lobo, S. I. Zones, and M. E. Davis *J. Inclus. Phenom. Mol.* 21 (1995) 47-78.

[16]   L. M. Kustov, V. B. Kazansky, and P. Ratnasamy *Zeolites* 7 (1987) 79-83.

[17]   S. T. Wilson, B. M. Lok, C. M. Messina, T. R. Cannan, and E. M. Flanagan *J. Am. Chem. Soc.* 104 (1982) 1146-1147.

[18]   E. G. Derouane in *Studies in Surface Science and Catalysis 5* (B. Emilik et al. Eds.) Elsevier, Amsterdam, 1980.

Table 1.1 **Commercial zeolite-based catalytic processes in hydrocarbon processing industries (adapted from reference 8a).**

Catalytic Cracking
Hydrocracking
Isomerization of Light Paraffins
Reformate Upgrading
Distillate and Luboil Dewaxing
Aromatic Alkylation
Gasoline from Methanol
Light Olefins from Methanol
Gasoline and Middle Distillates from Light Olefins
Deep Hydrogenation of Diesel Fuel
Isobutene Production from Normal Butenes
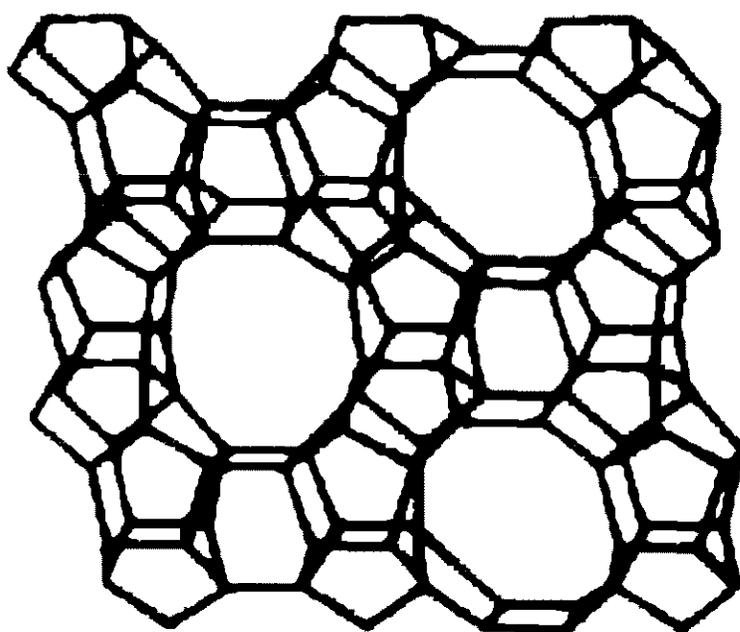
Figure 1.1 Schematic diagram of silicalite structure. Line intersections are silicon atoms. Line mid-points are oxygen atoms.
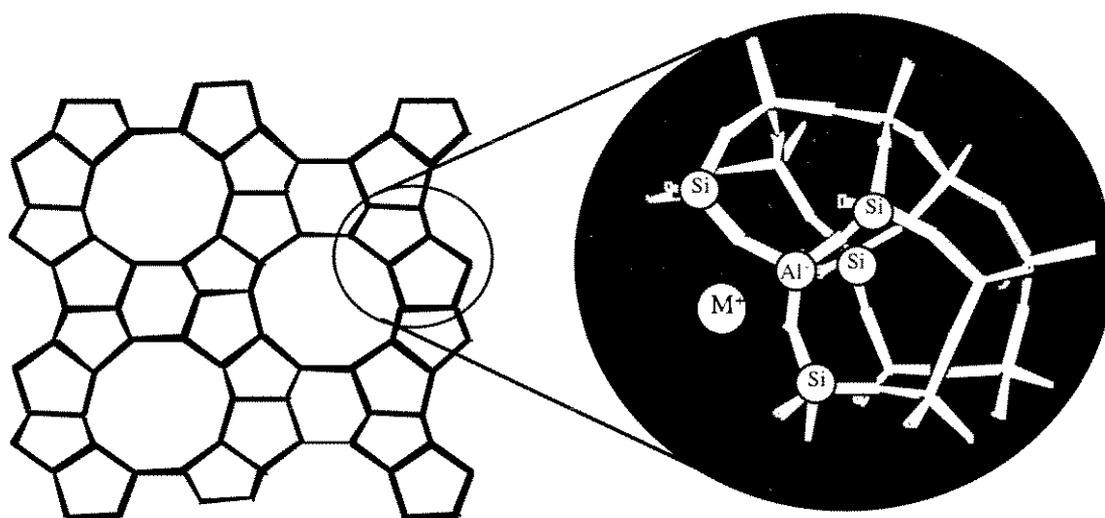
Figure 1.2 Zeolites have an anionic framework that requires a balancing cation.
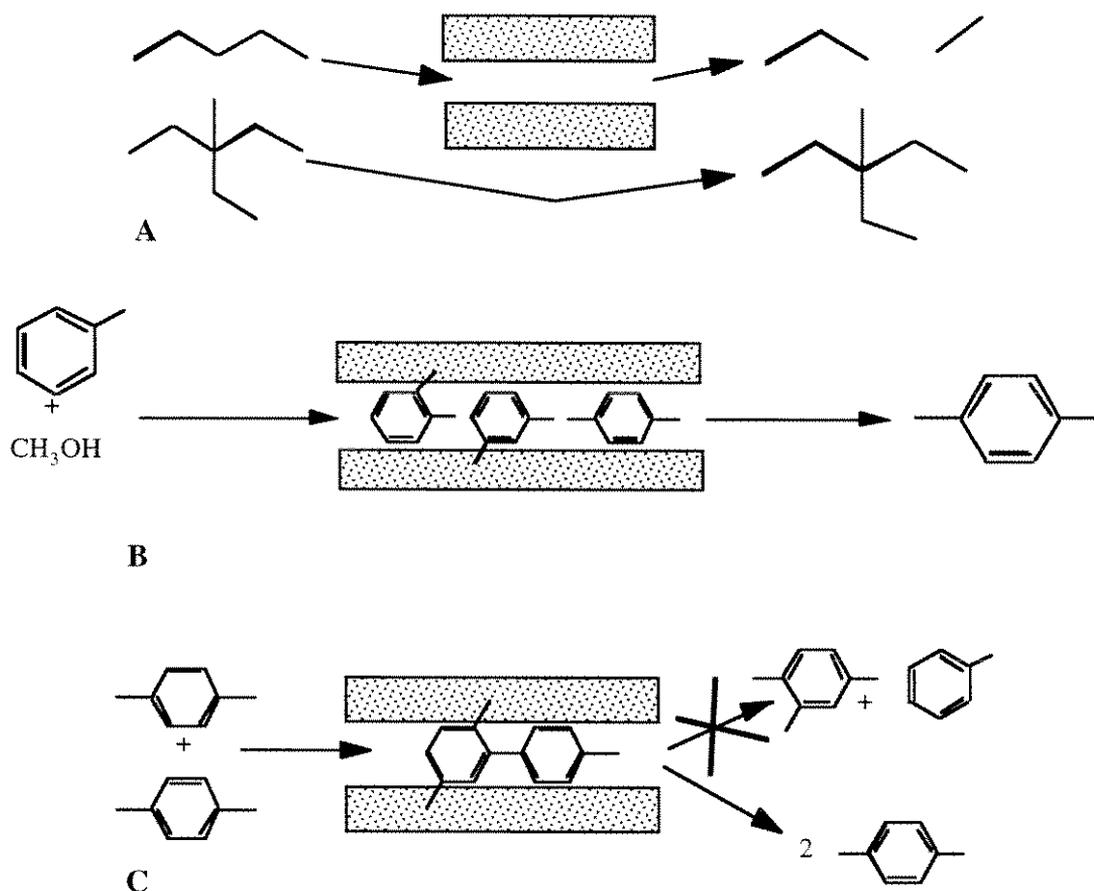
Figure 1.3 Shape-selective catalysis over molecular sieves. Reactant (A), product (B) and transition state (C) shape-selectivity. Adapted from [18].
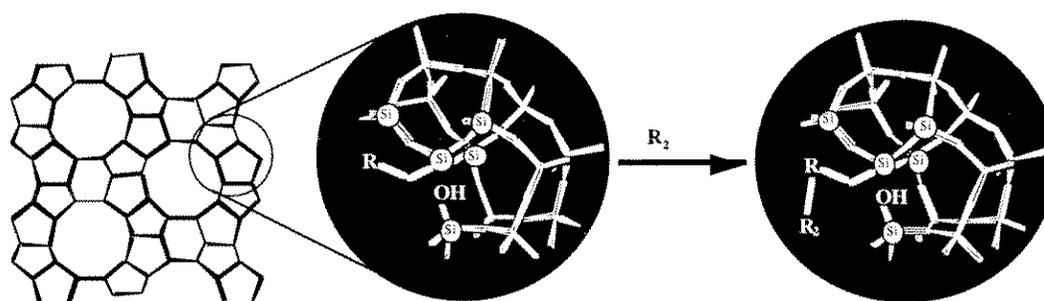
Figure 1.4   OFMS active site.   Incorporation of an organic species

followed by alteration of the species using organic chemical

techniques.   Addition of R_2 makes the organic moiety a

catalytically active species.

16
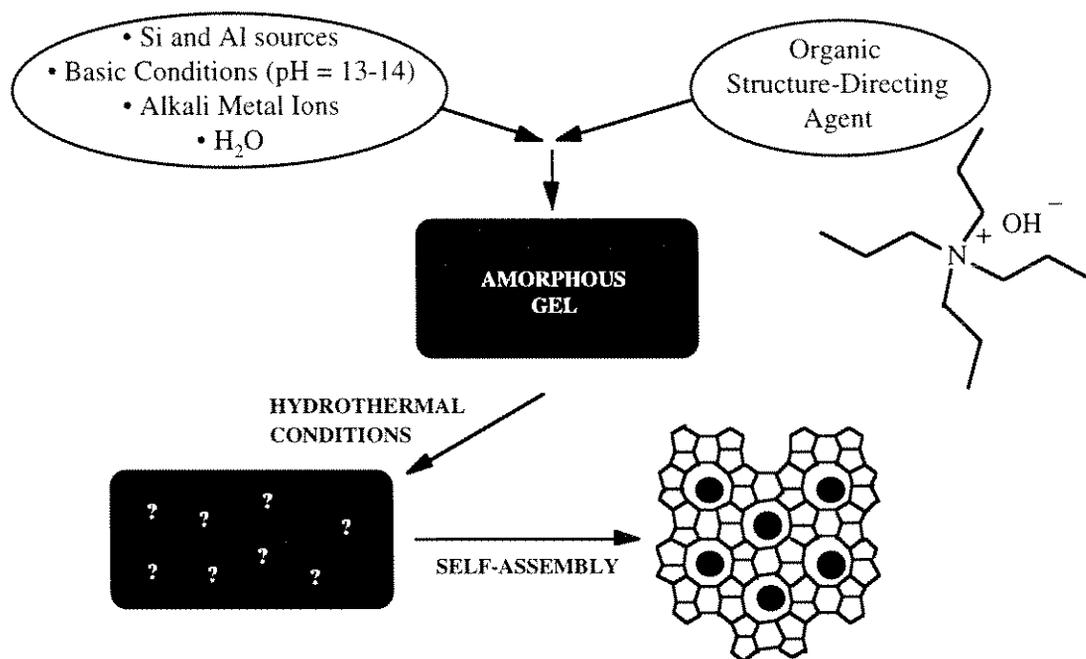
Figure 1.5 General molecular sieve synthesis scheme.

CHAPTER TWO

Investigations into the Synthesis of OFMS's from Hydrophilic, Organic SDA-free Gels

Abstract

The potential to synthesize OFMS's from organic SDA-free zeolite synthesis gels is evaluated. The zeolites NaY and ZSM-5 are synthesized in the presence of various organosilanes and the resulting materials are characterized by X-ray diffraction (XRD), thermogravimetric analysis (TGA), scanning electron microscopy (SEM), nitrogen physisorption, fourier-transform infrared (FTIR) spectroscopy and solid state ^{29}Si and ^{13}C nuclear magnetic resonance (NMR) spectroscopy. XRD results indicate that NaY is the only crystalline phase formed in all cases. TGA results suggest that only some of the organosilanes incorporate into the solid product during NaY synthesis. Additionally, in all cases where an organic group is residing in the final solid, nitrogen adsorption results indicate that the vast majority of the organic groups are likely not contained within the zeolite micropores, but rather on the surface of the zeolite crystals or in a separate, amorphous, organic-rich phase. For ZSM-5 synthesis, the solid product contains the intended organic functionality but multiple solid phases are always synthesized. In some cases, phase separation of the organosilane from the aqueous synthesis gel is observed. The lack of miscibility of the organosilane with the zeolite synthesis gel appears to hamper this approach to the synthesis of OFMS's. Thus, the potential to prepare OFMS's using hydrophilic zeolites appears to be limited.

2.1 Introduction

As described in Chapter 1, the development of OFMS's by grafting organic species onto pre-formed zeolites does not appear to be a viable approach. Using this synthesis strategy, the majority of the organic functional groups are attached to the external surface of the molecular sieve crystals [1,2]. An alternative approach is to synthesize OFMS's directly such that a inorganic-organic (silicon-carbon) linkage is in place in the as-synthesized material. However, developing a rational route to OFMS's by direct synthesis requires a judicious choice of the synthetic procedure.

There are over 120 different molecular sieve structures currently known [3]. In addition, the number of routes available for synthesizing these various molecular sieves far exceeds the number of structures. In order to synthesize a molecular sieve with intracrystalline organic moieties, a viable host structure must be determined and a feasible synthetic strategy developed.

Zeolites and silicate-based molecular sieves have pores bounded by 14 member rings, that is 14 silicon/aluminum atoms alternating with 14 oxygen atoms, or less. Currently, structures with pores bounded by 6,7,8,9,10, 12 and 14 member rings (MR's) are known. Each unique topology has been assigned a three-letter structure code, for example FAU for the zeolites with the topology of the mineral faujasite, by the International Zeolite Association (IZA) [3]. The various molecular sieve structures can include a single pore size (12 MR's, faujasite, FAU) or multiple pore sizes (8 and 10 MR's, ferrierite, FER). Additionally, the topologies range from unidimensional, with all the pores running parallel in one direction, e.g., CIT-5 (CFI), to two-dimensional, e.g., mazzite (MAZ) and three-dimensional, e.g., faujasite (FAU) structures.

For the development of an OFMS, the molecular sieve pores must be large enough to accommodate the intended organic functionality and they must have sufficient intracrystalline space for the sorption of additional species if these materials

are to be used in catalytic or molecular recognition applications. Multidimensional topologies are best suited for OFMS development because they provide for efficient adsorption and desorption of reactants and products. In addition, the channel intersections create voids that are necessarily larger than the pore-diameter of the material, providing additional internal space.

As described in Chapter 1, most zeolites and molecular sieves are synthesized in the presence of an organic SDA that remains occluded in the pores of the as-synthesized product. Removal of this SDA, which in most cases is done by calcination in air, is required to generate porosity. Unfortunately, calcination also would remove the intended organic functionality.

Several zeolites can be synthesized in the absence of an organic SDA. These zeolites, such as faujasite analogues (FAU), mordenite (MOR), and ZSM-5 (MFI), are therefore good candidates for development of OFMS's because no calcination step is needed to generate porosity. Timely introduction of an inorganic-organic linking species such as an organosilane into the synthesis gel of one of these zeolites may be a viable pathway to the development of OFMS's.

This chapter details the investigations into the synthesis of OFMS's from synthesis gels that do not contain any organic SDA's. Faujasite (FAU), which is a three-dimensional, 12 MR zeolite with pores 7.4 Å in diameter, and ZSM-5 (MFI), a three-dimensional, 10 MR zeolite with 5.1 - 5.5 Å pores, were chosen as host structures for OFMS development for the reasons denoted above.

2.2 Experimental

2.2.1 Synthesis

NaY (FAU) zeolites were synthesized from a gel with the following composition:

$$(1-X) \ Si \ / \ 0.86 \ Na \ / \ 0.36 \ Al \ / \ 22.6 \ H2O \ / \ X \ R-Si,$$
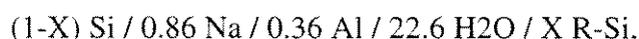
where R-Si was an organosilane containing the desired organic functionality and

$$0.09 \geq X \geq 0.$$

First, sodium aluminate (Pfaltz and Bauer) was dissolved in a sodium hydroxide solution. In a separate container, the organosilane (Gelest) was added dropwise with stirring to a solution of the silica source (Ludox HS-30 colloidal silica, DuPont) and water. After 60 minutes, the two solutions were combined by adding the aluminum solution dropwise to the silica solution under stirring. The resulting gel was allowed to stir vigorously for 5-7 hours and was then aged statically at room temperature for 18-24 hours. The gel was subsequently added to a Teflon-lined autoclave and the autoclave was heated statically in an oven at 110°C. After the 24 hours, the autoclave was rapidly cooled in a water bath. The contents were washed thoroughly with water and acetone, recovered by filtration, and then dried in an oven at ~75°C for 6 hours or more.

ZSM-5 (MFI) zeolites were synthesized by adapting a MFI synthesis from reference 4 such that it was amenable to the inclusion of organosilanes. Additionally, the acetone used in the synthesis described in reference 4 has been omitted in favor of t-butanol. A synthesis gel with the composition:

1 Si / 0.02 Al / 0.3 Na / 0.7 t-butanol / 45 H2O / 0-0.09 R-Si
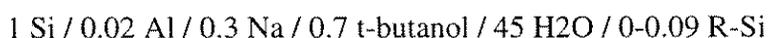
was used (Si- Ludox HS-30; Al- aluminum hydroxide, Reheis; Na- sodium hydroxide, EM Science). The synthesis, like the NaY synthesis described above, involved stirring the silica, organosiloxane and some water together, stirring the Al, Na and the remaining water together, and then combining the two solutions. This combined solution was mixed for 1-4 hours and then the tert-butanol was added, with continued stirring for 15 minutes. The final solution was added to a Teflon-lined Parr autoclave with ZSM-5 seeds (0.36% by weight). The autoclave was then heated at 150°C for up to 10 days while rotating at ~120 rpm in an oven. The autoclave was removed from the oven and quenched in a water bath. The products were recovered by filtration, washed with water and acetone and then dried in an oven at ~75°C for at least 6 hours.

2.2.2 Analytical Procedures

X-ray diffraction (XRD) was carried out using a Scintag XDS 2000 powder diffractometer equipped with a liquid-nitrogen-cooled detector using Cu-Kα radiation. Nitrogen physical adsorption experiments were conducted on an Omnisorp 100 apparatus in static mode using fixed dosing at 77K. Samples were dehydrated under vacuum to 200°C prior to analysis. Thermogravimetric analyses (TGA) were carried out on a DuPont 951 thermogravimetric analyzer by heating in air to 800°C at 10°C/minute. Scanning electron microscopy (SEM) images were obtained on a Camscan Series 2-LV microscope using an accelerating voltage of 15 kV. Solid-state nuclear magnetic resonance (NMR) spectroscopy was performed on Bruker AM 300 spectrometer equipped with a cross-polarization (CP) magic angle spinning (MAS) accessory. ^{29}Si (59.63 MHz) spectra were obtained at a spinning speed of 4 KHz and externally referenced to tetramethylsilane. ^{13}C (75.60 MHz) spectra were obtained at a spinning speed of 4 KHz and externally referenced to adamantane. Fourier-transform infrared (FTIR) spectra were obtained on a Nicolet System 800 Spectrophotometer with 3M brand Polytetrafluoroethylene Type 62 and Polyethylene Type 61 windows. Fluorolube (Spectra Tech 0026-111) and Nujol (Spectra Tech 0026-110) were used as mulls.

2.3   Results and Discussion

2.3.1 Zeolite synthesis

NaY samples were synthesized in the presence of a wide variety of organosilanes, some of which are described in Table 2.1 and Figure 2.1. In all cases described in Table 2.1, crystalline NaY resulted, as powder XRD patterns were in all cases indicative of the faujasite (FAU) structure. No differences were notable between samples synthesized in the presence or absence of organosilanes, as illustrated in Figure 2.2.

ZSM-5 samples were synthesized in the absence of any organosilanes and in the presence of [2-(3-cyclohexenyl)ethyl]trimethoxysilane (CHE). In the absence of CHE, the crystallization of ZSM-5 was very rapid, requiring less than one day in the oven. With CHE in the synthesis gel, crystallization requires a significantly increased time in the oven. Table 2.2 enumerates the results of several ZSM-5 syntheses. When CHE is included in the gel, MFI is formed with some additional impurity phases as described in Table 2.2. XRD results indicate that the impurity phases are most likely layered and amorphous phases. Figure 2.3 shows the XRD patterns for several of the ZSM-5 samples. Significantly increasing the crystallization time in an effort to reduce the amount of the layered material resulted in formation of dense phases at the expense of MFI.

2.3.2 Thermogravimetric Analysis

TGA data for NaY-1 (Figure 2.4a) indicate that there is only one significant weight loss. This weight loss occurs at a relatively low temperature and can be attributed to desorption of physisorbed water. The TGA results for several samples synthesized in the presence of organosilanes look similar to that of NaY-1, indicating that inclusion of an organosilane in the NaY synthesis gel does not necessarily cause incorporation of an organic species in the solid product. However, in some cases, there is clearly a weight loss at elevated temperatures (>300°C) that is not present in NaY-1 that is attributable to organic species combusting in air. Data in Table 2.1 indicate which organosilanes appear to incorporate into the solid phase. Figure 2.4b shows the TGA result for NaY/CHE-1.

There is a notable trend in which organosilanes incorporate into the final product. Organosilanes with short, non-polar, non-hydrolyzable organic residues such as a vinyl or allyl group are not incorporated into the resulting solid material. However, longer organic chains on the organosilane allow for incorporation of

combustible organic species in the solid. Phenethyltrimethoxysilane, which visibly phase separates in the aqueous synthesis mixture, is not incorporated. Attempts to increase the reactivity and polarity around the aromatic ring by tethering an additional silicon with hydrolyzable groups onto the ring (see Figure 2.1, BEB) allows for incorporation of the organic in the final solid material. Several relatively polar organosilanes such as aminopropyltrimethoxysilane and n-(trimethoxysilylpropyl)-ethylenediamine-triacetic acid-trisodium salt were used in NaY syntheses. In all cases with polar organosilanes, the organic group did not incorporate when NaY was formed.

Varying the hydrolyzable groups around a single organosilane indicates that both alkoxy (CHE) and chloro (CHCL) silanes can be condensed into the solid material. However, substitution of one chloro species for a methyl species (CHCLM) prevents the incorporation of an organic in the final product. If an organosilane were to incorporate into the zeolite framework, substitution of a methyl group for a hydrolyzable methoxy or chloro group should prevent incorporation of the organosilane into the sample. Indeed, this is observed, indicating that CHE may be substituting into the NaY framework.

In the case of ZSM-5, all samples with CHE in the gel have organic species in the solid product as indicated in Table 2.2.

2.3.3 Scanning Electron Microscopy

While powder XRD is useful for indicating which crystalline phases are present, it is not as useful for identifying small amounts of non-crystalline phases that may be present in samples. SEM images can give information on small amounts of non-crystalline phases in addition to crystal size and morphology.

SEM images for most NaY samples look essentially identical. Samples appear highly crystalline with numerous submicron, uniform crystals. SEM micrographs of

all samples appear similar (unless otherwise noted) to NaY/CHE-1, which is shown in Figure 2.5. The only visible non-crystalline phases are minute amounts of spherical particles of unreacted Ludox silica. NaY/BEB is an exception. In this case, an amorphous phase is clearly evident. The sample appears to be made of crystals encased in an outer amorphous shell, as illustrated in the SEM image shown in Figure 2.6.

Multiple phases are evident in all ZSM-5 samples synthesized in the presence of CHE. Images of the highly crystalline ZSM-5-1 and the multiple phase ZSM-5/CHE-4 are shown in Figure 2.7. ZSM-5/CHE-4 appeared to be highly crystalline by XRD, but SEM indicates that there is an additional, non-crystalline phase in addition to MFI in this sample.

2.3.4 Nitrogen Physisorption

While TGA results are useful for indicating whether an organic species exists in as-synthesized solid, it does not give information concerning the location of the organic species. For shape-selective applications, the organic groups must be situated largely within the micropores of the zeolite. A significant amount of organic species in a non-crystalline phase or on the external surface of the zeolite crystals significantly reduces the utility of these materials for shape-selective applications.

NaY-1 had a nitrogen uptake of 0.29 - 0.30 cc/g zeolite, indicative of a highly crystalline sample as previously noted by SEM and XRD. Samples that were synthesized in the presence of an organosilane that did not incorporate, such as NaY-ALY-1, also had a similar nitrogen capacity. The samples that contained an organic species (as determined by TGA), with one exception, had nitrogen capacities of 0.28 - 0.29 cc/g zeolite. When the samples were calcined to remove the organic species, a significant increase in microporosity was not observed. The nitrogen adsorption uptake was essentially unchanged. This indicates that the organic species in these materials are residing in locations other than the micropores of the zeolite. For example,

NaY/HEXA-2 contains approximately 5% wt. organic (dry basis) as determined by TGA. If the density of the hexane group is approximated as the density of liquid n-hexane, the organic can be expected to occupy 0.033 cc/g. Hence, if all of the hexane groups were localized within the zeolite micropores, a 0.033 cc/g difference in nitrogen capacity between the as-synthesized and calcined samples would be expected. Since no differences exist in the nitrogen capacity of the as-synthesized and calcined materials, it is clear that the organic groups are likely not within the micropores.

Calcined NaY/CHE-1 has a larger nitrogen adsorption uptake than the as-synthesized material. NaY/CHE-1 contained 12.8% wt. organic (dry basis), which translates to 0.10 cc/g pore space that should be occupied by the cyclohexenylethyl groups if they were localized within the zeolite micropores. However, the difference in nitrogen capacity of the calcined and as-synthesized materials was only 0.016 cc/g (0.267 cc/g as-synthesized; 0.283 cc/g calcined). Hence, in the case of this organosilane, a fraction of the functional groups could be located within the zeolite micropores. Another possibility is that a small amount of the CHE is in a non-zeolitic phase.

2.3.5 Solid State NMR Spectroscopy

Figure 2.8 illustrates the ^{29}Si MAS NMR spectrum of NaY/CHE-1. The resonances were assigned as follows:

-103 ppm	$Si(OSi)_4$
-99 ppm	$Si(OSi)_3(OAl)$
-94 ppm	$Si(OSi)_2(OAl)_2$
-89 ppm	$Si(OSi)(OAl)_3$
-84 ppm	$Si(OAl)_4$
-68 ppm	$Si(R)(OSi)_3$,

with the first five resonances present in all NaY samples and the last resonance, which is indicative of a covalent silicon carbon bond, present in organic-containing samples such as NaY/CHE. The assignment of the -68 ppm resonance to a Si-C species fully bonded to other silicon atoms through oxygen bridges is consistent with the results of others [5,6]. It is noteworthy that there is no signal for organosilicon species bonded to an adjacent aluminum atom through oxygen bridges, such as $Si(R)(OSi)_x(OAl)_{3-x}$, as this would give a downfield shift of at least 5 ppm. This indicates that any organosilane, such as CHE, that may be included in the zeolite framework is confined to a small fraction of the available tetrahedral sites in the sample, as the population of $Si(OSi)_4$ sites is very low in these materials (see Figure 2.8). It is noteworthy that this resonance is also present in samples that contain organic in regions that are clearly outside the zeolite micropores. Hence, these results are consistent with the nitrogen adsorption observation that the majority of the organic species were incorporated in a separate, organosilane-rich phase, or on the external surface of the zeolite crystals. When NaY/CHE-1 is dehydrated and analyzed by ^{29}Si CPMAS NMR spectroscopy, only the resonance at -68 ppm is apparent. There is no cross-polarization between the organic group and the zeolite framework silicons, consistent with the presence of the majority of the organic species in areas outside the zeolite micropores.

The observed results indicate that it may be unfavorable for the organosilane to have an aluminum atom as a second nearest neighbor as described in Figure 2.9b. In all samples analyzed here, ^{29}Si NMR results indicate that the organosilane silicon is surrounded by other silicon atoms through oxygen bridges as shown in Figure 2.9a. Because CHCLM did not incorporate in the solid materials, it appears that organosilanes with only two hydrolyzable moieties can not be incorporated into the solid product, as described in Figure 2.9c.

The ^{13}C CPMAS NMR spectrum of NaY/CHE-1 indicates that the intended organic functionality is intact in the as-synthesized material. There are 5 resonances assignable to the CHE group as shown in Figure 2.10.

2.3.6 FTIR Spectroscopy

The structure of the organic moieties in these materials can be easily identified by FTIR spectroscopy. Figure 2.11 shows the FTIR spectra for NaY-1 and NaY-CHE-1. It is clear that an organic species is present in the sample and that the double bond is intact. The spectrum of NaY/CHE-1 contains absorptions at 3020 cm^{-1}, 2914 cm^{-1}, 2850 cm^{-1}, and 2835 cm^{-1} in the C-H stretching region, while the NaY-1 spectrum contains no such peaks. All of the absorptions noted are assigned to saturated C-H stretching modes except the peak at 3020 cm^{-1}, which is due to a C-H stretch on an unsaturated carbon. All assignments are from reference 7.

The reactivity of the olefinic species was probed by reaction with thiolacetic acid. Thiolacetic acid reacts with olefins to give anti-Markovnikov products in high yields as illustrated in Scheme 2.1 below:
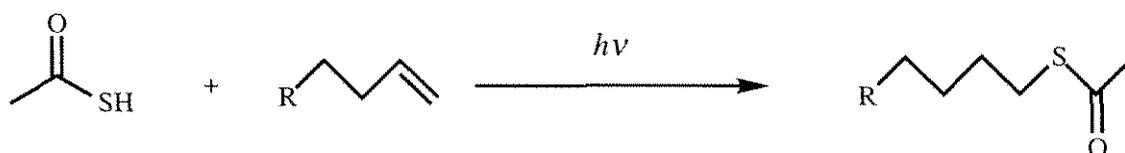
Scheme 2.1

A portion of the NaY/CHE-1 sample was immersed in thiolacetic acid and irradiated with 450 W *uv* light for 24 hours under stirring. The FTIR spectrum of the thiolacetate-treated material in Figure 2.11 indicates that nearly complete formation of the thiolacetate occurred, with a disappearance of the unsaturated C-H stretch and the

formation of a thiolacetate stretch at 1692 cm^{-1}. This result indicates that the organic functional groups are accessible in the NaY/CHE-1 material.

2.4 Summary

The results presented when taken in total indicate that attempts to synthesize OFMS's using the organic SDA-free synthetic strategies described here do not produce useful OFMS materials. In the case of NaY derived materials, solids that appeared to be a single phase by XRD and SEM are produced in almost every case. However, only some organosilanes can be incorporated into the solid product and adsorption results indicate that these species are generally not within the zeolite micropores. NaY functionalized with cyclohexenylethyl groups may be an exception, as it may contain a fraction of the functionalities in the micropores. However, all the results for NaY/CHE-1 are consistent with the presence of CHE either on the external surface of the zeolite crystals or in a separate, silicon-rich, phase. To be widely useful in catalytic or molecular recognition applications where shape-selectivity is desired, the vast majority of the organic functional groups need to be within the micropores.

In the case of ZSM-5 derived materials, all samples contained multiple solid phases. This limits the possible uses of these materials.

The synthesis of OFMS's from a starting gel that does not contain an organic SDA appears to be hampered by several difficulties. The zeolite precursors are highly charged species in an aqueous environment, while the organosilane is generally quite hydrophobic. This leads to a strong driving force for phase separation of the components in the synthesis gel and phase separation was visibly noted in some cases. Phase separation of the synthetic components can account for the principal results observed here: formation of multiple phases and segregation of the organic components outside the zeolite crystals.

2.5 References

[1] A. Cauvel, D. Brunel, F. DiRenzo, P. Moreau, and F. Fajula in *Studies in Surface Science and Catalysis 94* (H. K. Beyer, et al., Eds.) Elsevier, Amsterdam, 1995

[2] W. R. Ahmad and M. E. Davis, unpublished results.

[3] W. M. Meier, D.H. Olson, and Ch. Baerlocher, *Atlas of Zeolite Structure Types*, 4th Edition, International Zeolite Association, 1996; International Zeolite Association Web Site.

[4] E. Narita, K. Sato and T. Okabe *Chem. Lett.* 7 (1984) 1055-1058.

[5] H. X. Li, M. A. Camblor, and M. E. Davis *Microporous Mater.* 3 (1994) 117-121.

[6] E. J. R. Sudholter, R. Huis, G. R. Hays, and N. C. M. Alma *J. Coll. I. Sci.* 103 (1985) 554-560.

[7] N. B Colthup, L. H. Daly, and S. E. Weberley *Introduction to Infrared and Raman Spectroscopy*, Academic Press, NY 1975; H. Baranska, A. Labudzinska, and J. Terpinski *Laser Raman Spectrometry, Analytical Applications*, Ellis Horwood Limited, Chichester 1987.

[8] C.W. Jones, K. Tsuji, and M. E. Davis in *Proceedings of the 12th International Zeolite Conference*, Materials Research Society (1999) 1479-1486.

Table 2.1   NaY synthesis results.

Sample	Organic	X, R-Si in gel	TGA
NaY-1	None	0	No Organic
NaY/PE-1	Phenethyltrimethoxysilane	0.09	No Organic
NaY/PE-2	Phenethyltrimethoxysilane	0.07	No Organic
NaY/PE-3	Phenethyltrimethoxysilane	0.05	No Organic
NaY/BEB	1,4-bis(trimethoxysilylethyl)-benzene	0.09	Organic Present
NaY-CHE-1	[2-(3-cyclohexenyl)-ethyl]trimethoxysilane	0.09	Organic Present
NaY-CHE-2	[2-(3-cyclohexenyl)-ethyl]trimethoxysilane	0.07	Organic Present
NaY-CHE-3	[2-(3-cyclohexenyl)-ethyl]trimethoxysilane	0.05	Organic Present
NaY-ALY-1	allyltriethoxysilane	0.09	No Organic
NaY-ALY-2	allyltriethoxysilane	0.05	No Organic
NaY-VIN-1	vinyltrimethoxysilane	0.09	No Organic
NaY-VIN-2	vinyltrimethoxysilane	0.05	No Organic
NaY-BUT-1	3-butenyltriethoxysilane	0.09	No Organic
NaY-BUT-2	3-butenyltriethoxysilane	0.05	No Organic
NaY-PBR	3-bromopropyltrichlorosilane	0.09	No Organic
NaY-PYR	2-(trimethoxysilylethyl)-pyridine	0.09	No Organic
NaY-HEXE	5-hexenyltrichlorosilane	0.05	Organic Present
NaY-OCTE	7-octenyltrimethoxysilane	0.05	Organic Present
NaY-HEXA	hexyltrimethoxysilane	0.05	Organic Present
NaY-OCTA	octyltrimethoxysilane	0.05	Organic Present
NaY-UBR	bromoundecyltrimethoxysilane	0.05	Organic Present
NaY-CHCL	[2-(3-cyclohexenyl)-ethyl]trichlorosilane	0.05	Organic Present
NaY-CHMCL	[2-(3-cyclohexenyl)-ethyl]methyldichlorosilane	0.05	No Organic

Table 2.2   ZSM-5 synthesis results.

Sample	Heating Time	X, R-Si in gel	XRD	TGA
ZSM-5-1	16 hours	0	MFI	No Organic
ZSM-5/CHE-1	6 days	0.09	MFI, layered, amorphous	Organic Present
ZSM-5/CHE-2	6 days	0.06	MFI, layered, amorphous	Organic Present
ZSM-5/CHE-3	4 days	0.08	MFI, layered, amorphous	Organic Present
ZSM-5/CHE-4	8 days	0.08	MFI	Organic Present
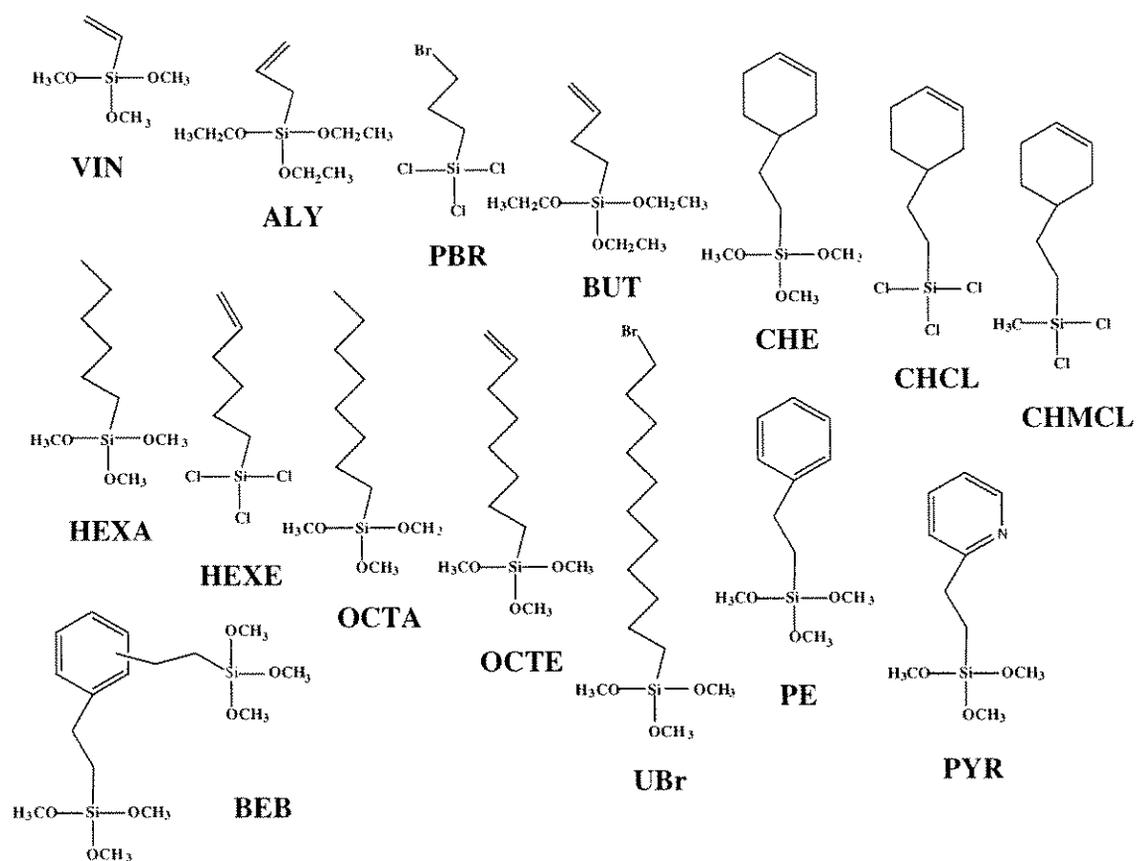
Figure 2.1 Organosilanes used in NaY syntheses.
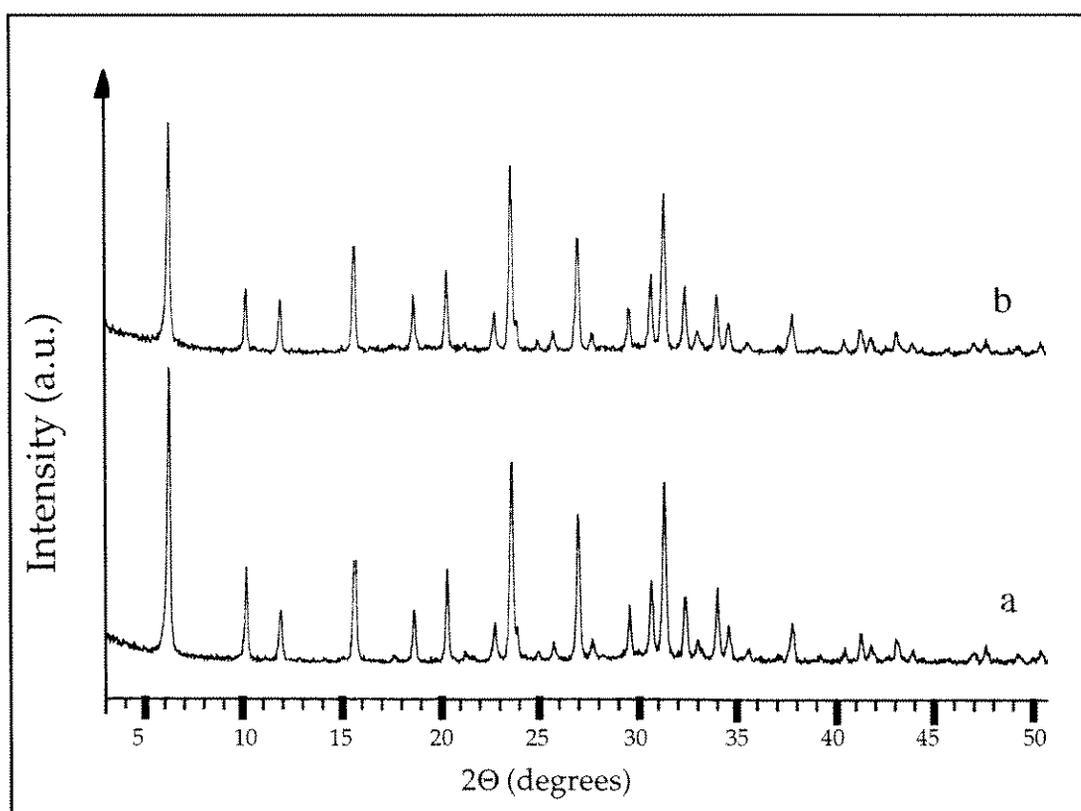
Figure 2.2 XRD patterns of NaY-1 (a) and NaY/CHE-1 (b).
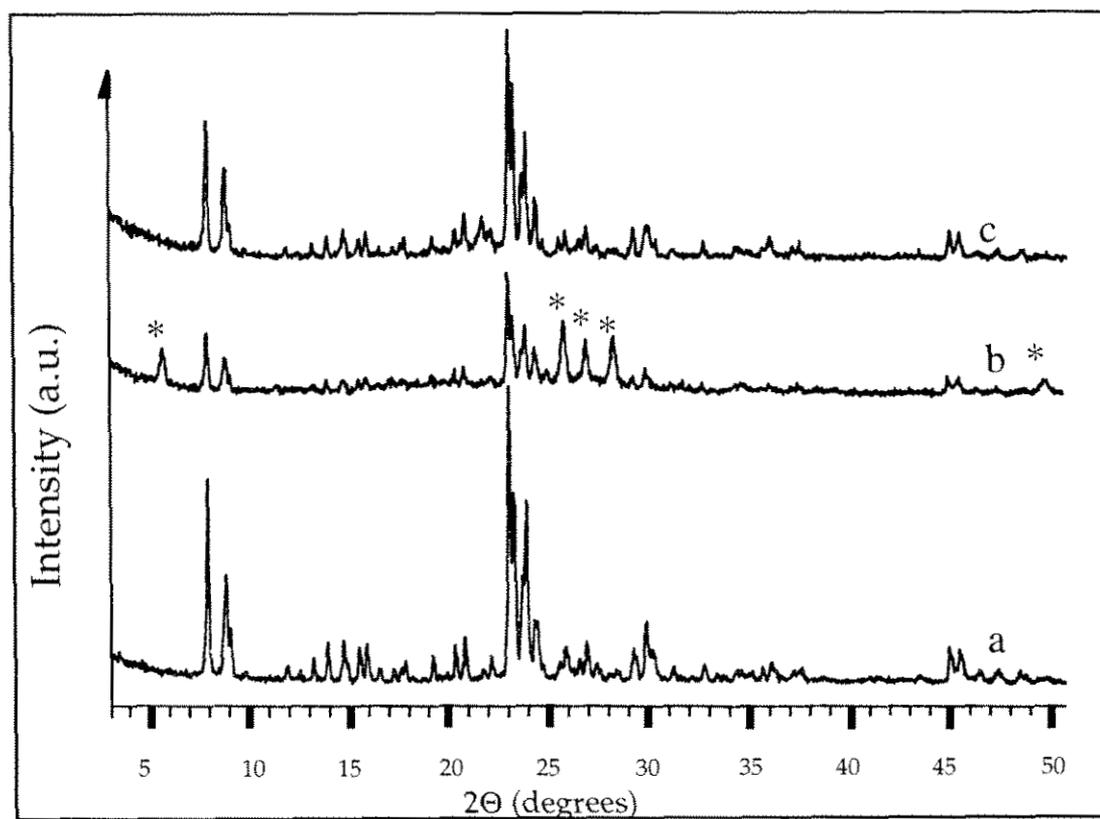
Figure 2.3 **XRD patterns for ZSM-5-1 (a), ZSM-5/CHE-3 (b) and ZSM-5/CHE-4 (c). Intensities due to a layered material are marked *.**
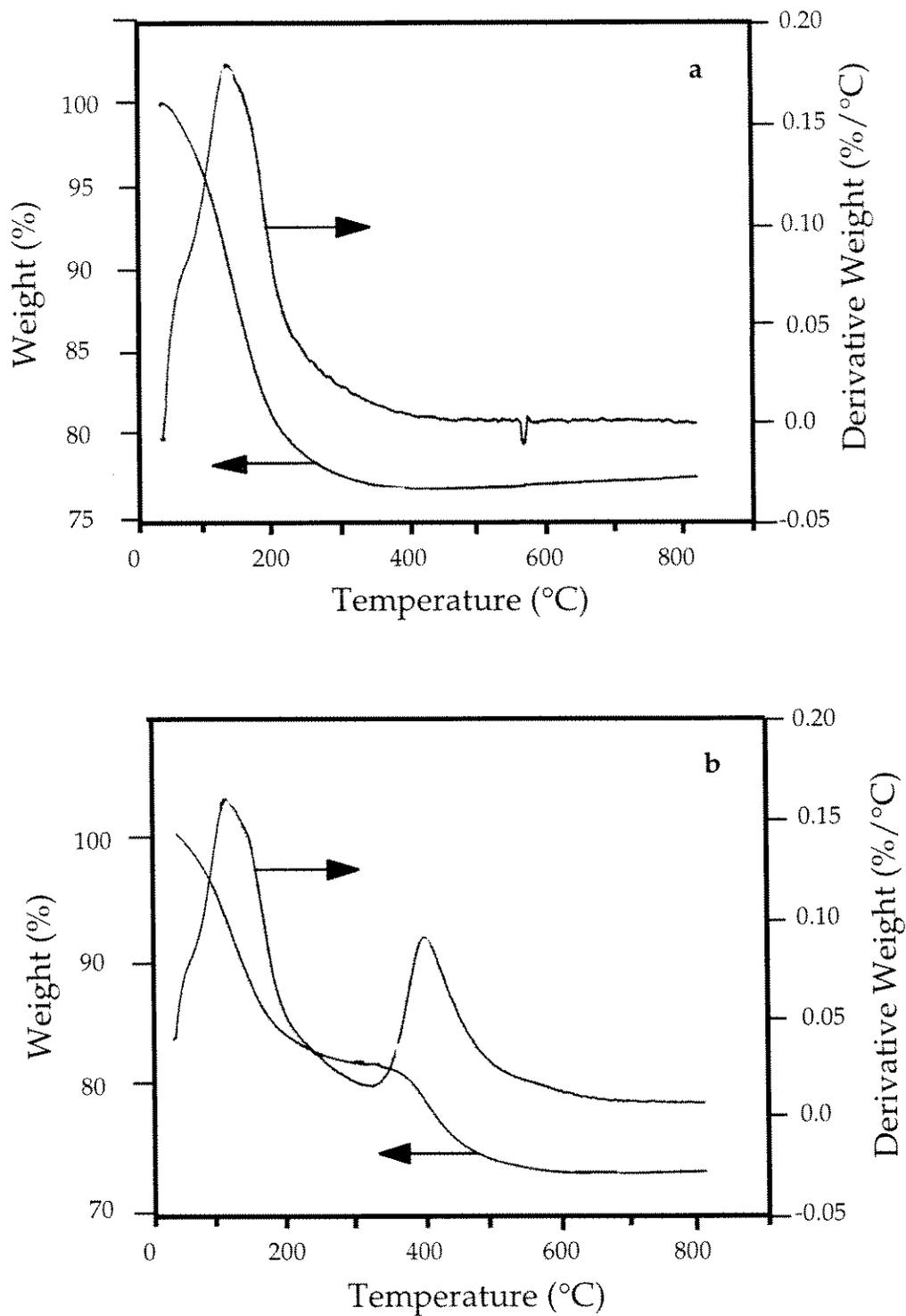
Figure 2.4   TGA results for NaY-1 (a) and NaY/CHE-1 (b).
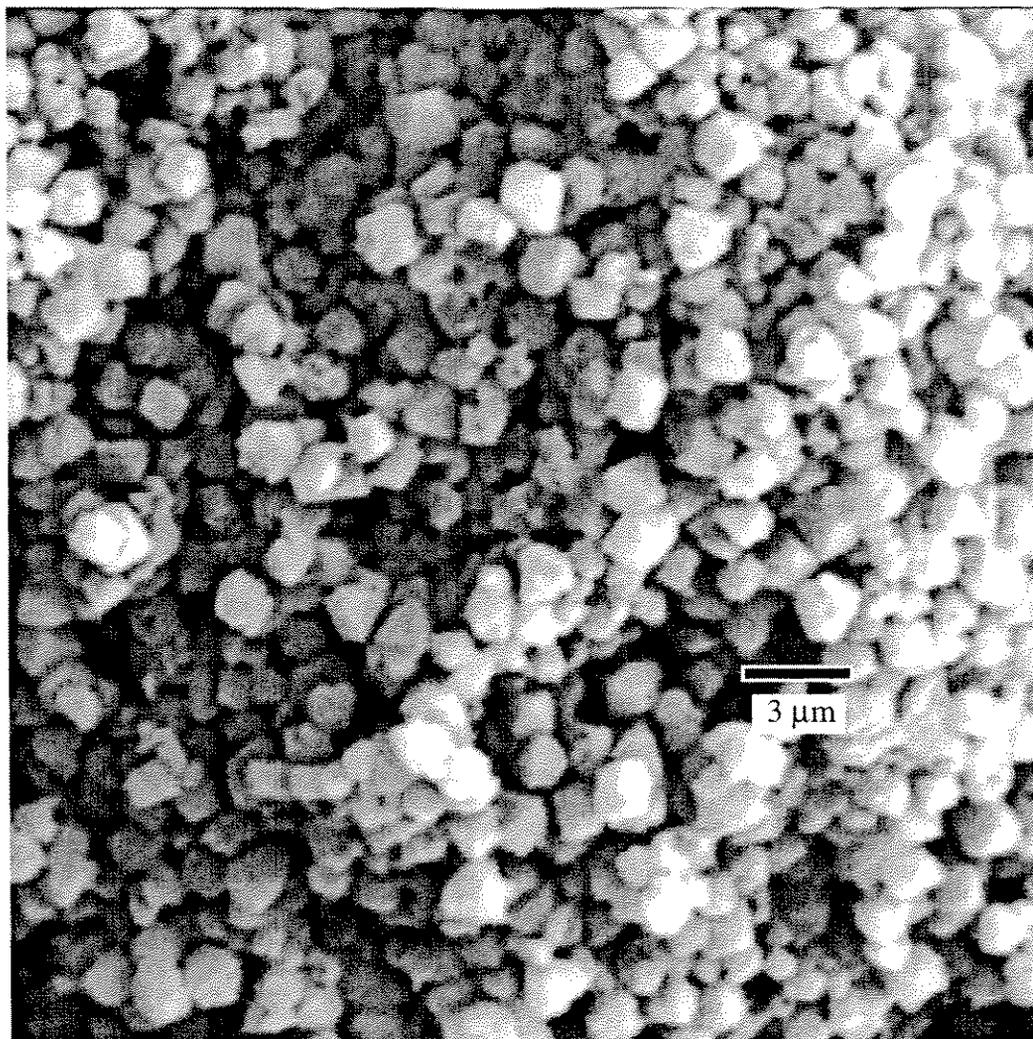
Figure 2.5 SEM image of NaY/CHE-1.
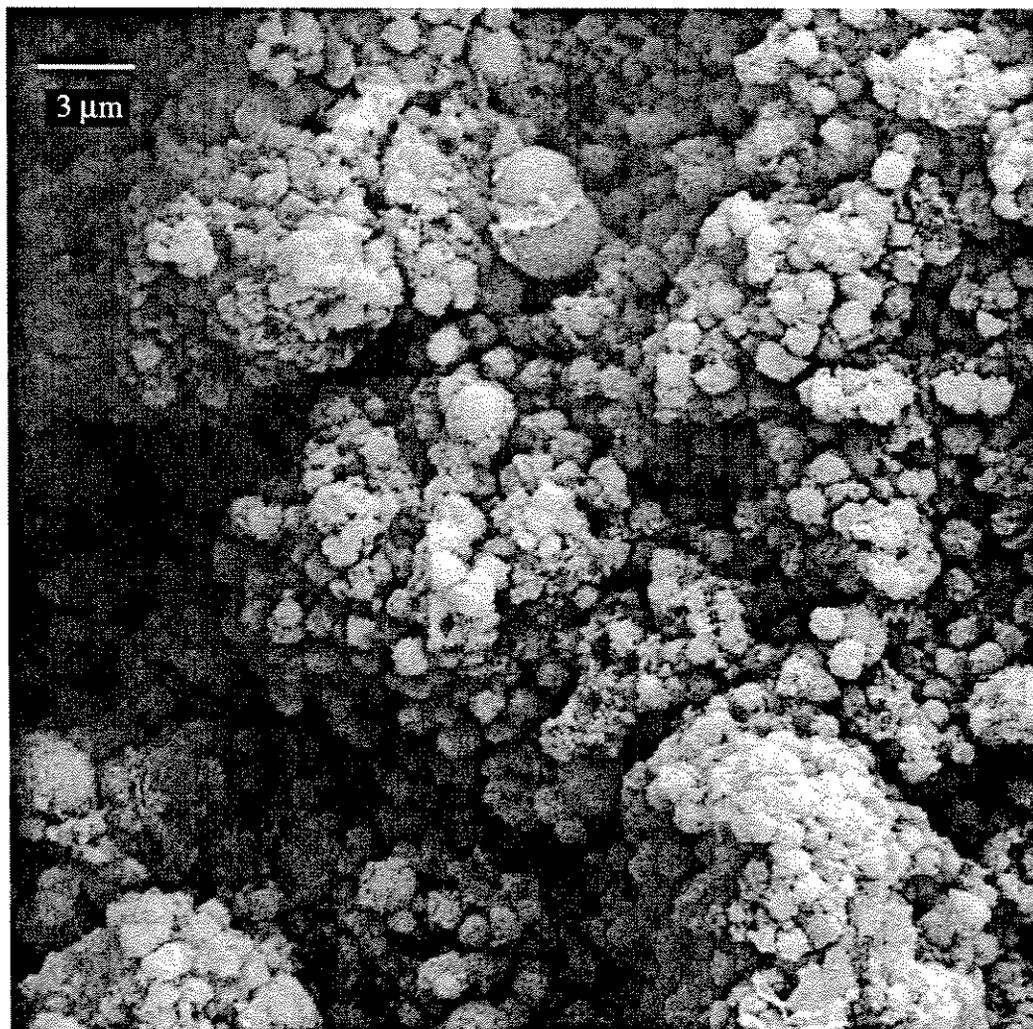
Figure 2.6 SEM image of NaY/BEB-1.
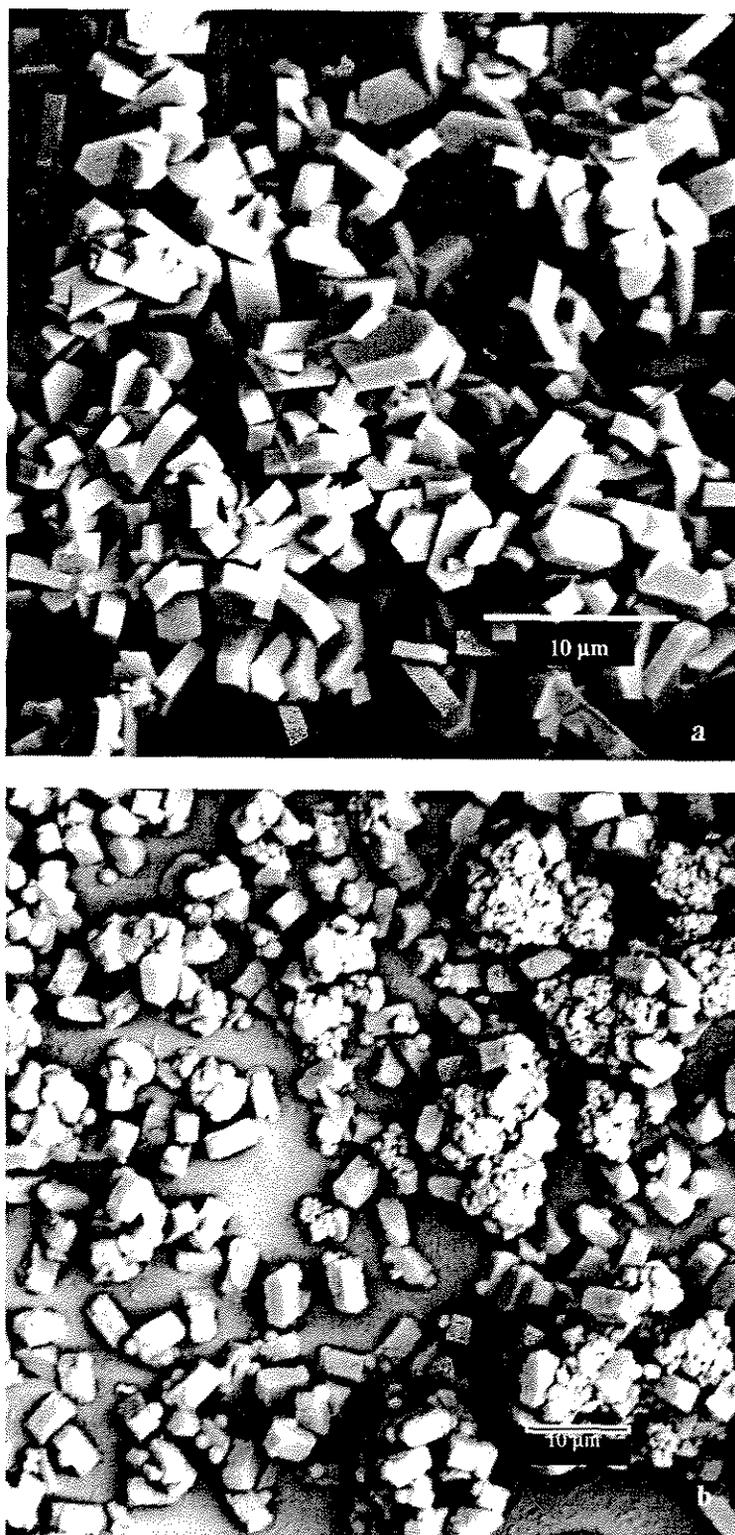
Figure 2.7 SEM images of ZSM-5-1 (a) and ZSM-5/CHE-3 (b).
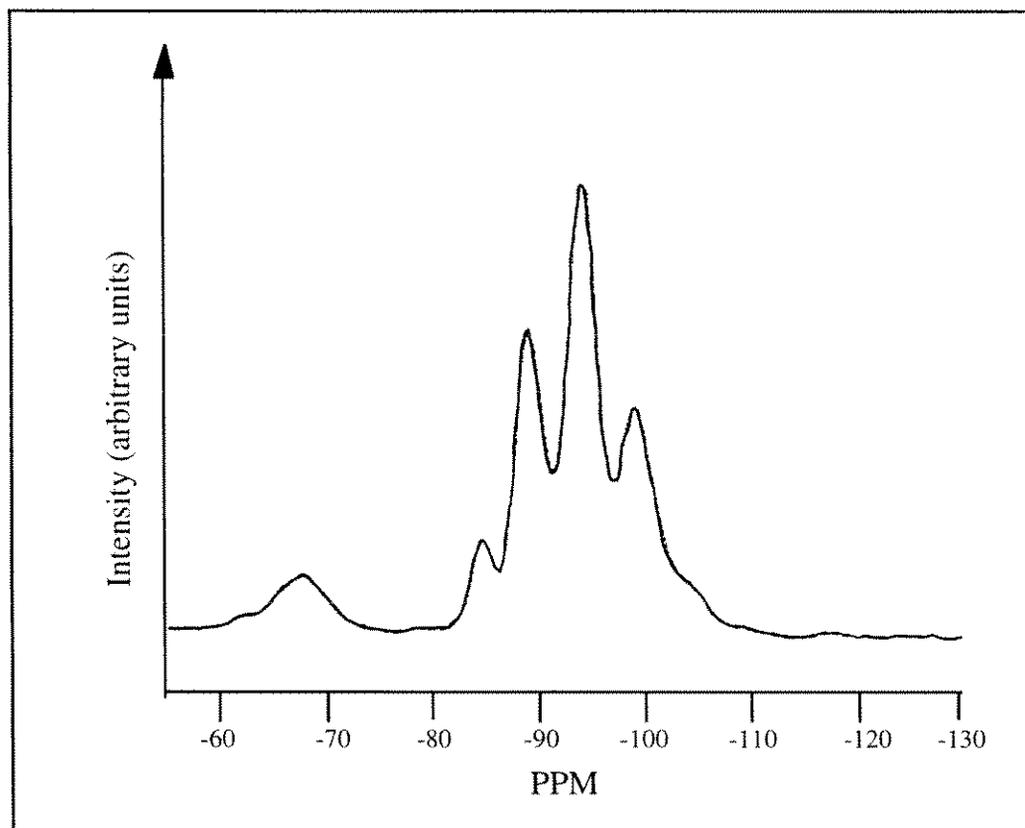
Figure 2.8 ^{29}Si MAS NMR spectrum of NaY/CHE-1.

Adapted from [8].
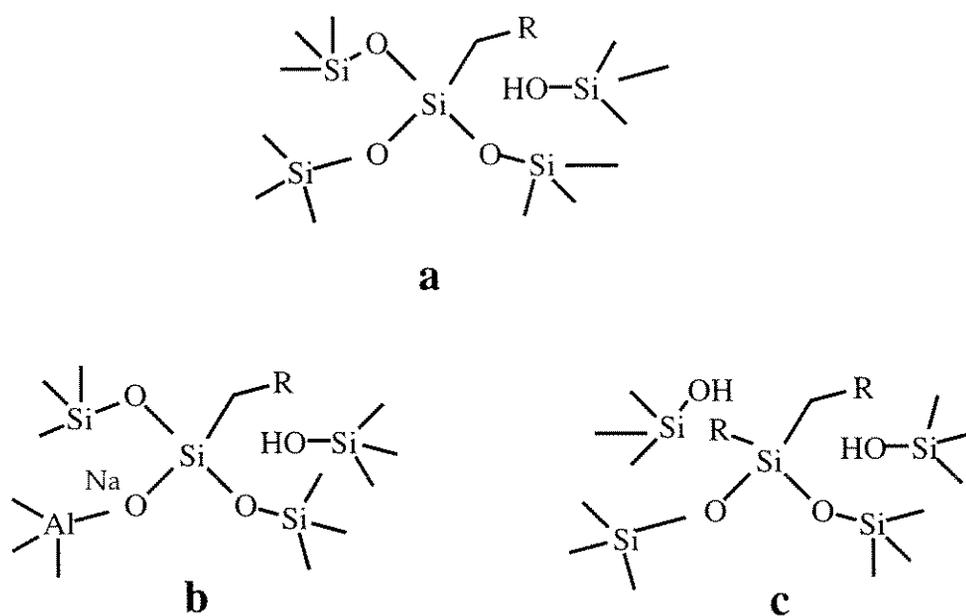
Figure 2.9 Organosilane environments in products derived from NaY gels. State of the organosilane as observed by ^{29}Si MAS NMR (a), and unfavorable, unobserved species (b, c).

1) 11.5 ppm

2)   27 ppm

3,4) 30 ppm

5)   37 ppm

6)   127 ppm
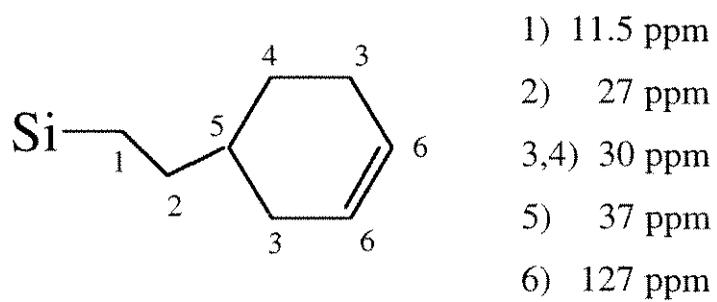
Figure 2.10 ^{13}**C CPMAS NMR assignments for NaY/CHE-1.**
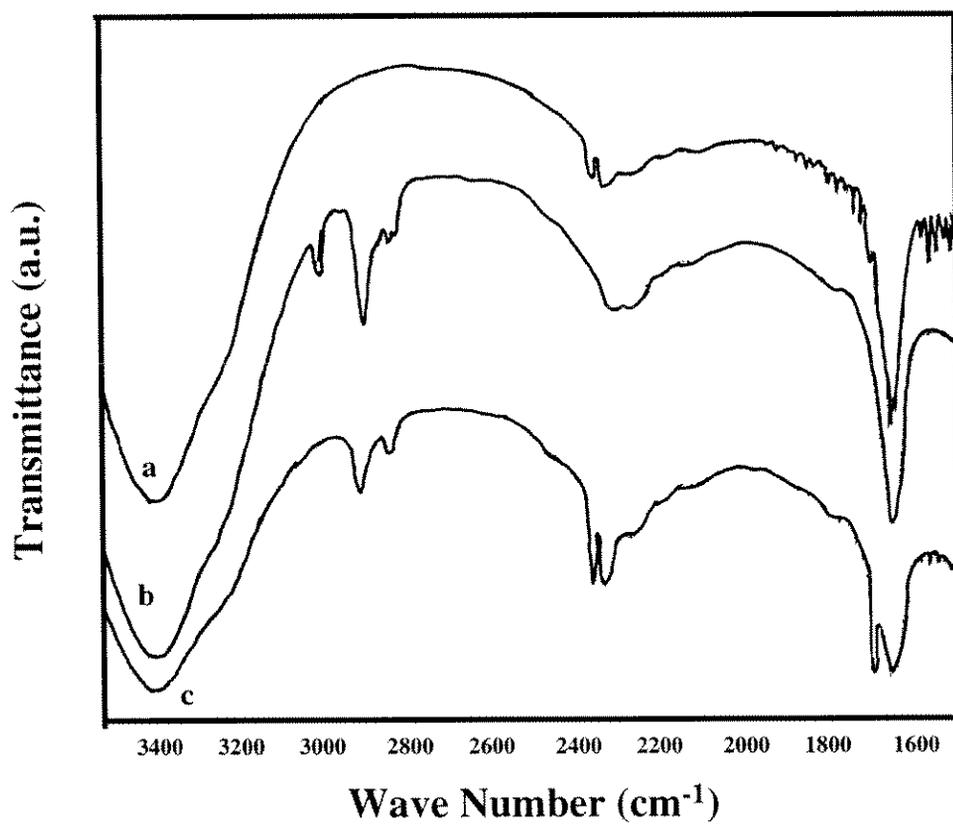
Figure 2.11 FTIR spectra of NaY-1 (a), NaY/CHE-1 (b), and NaY/CHE-1 reacted with thiolacetic acid (c).

CHAPTER THREE

Organic-Functionalized Molecular Sieves (OFMS's) as Shape-Selective Catalysts

Organic-Functionalized Molecular Sieves as Shape-Selective Catalysts

by

Christopher W. Jones, Katsuyuki Tsuji and Mark E. Davis

Chemical Engineering
California Institute of Technology
Pasadena, CA 91125, USA

Zeolites and related molecular sieves are effective catalysts for performing shape-selective reactions. In order to expand the range of active sites and the types of shape-selective reactions that can be accomplished, a new class of molecular sieve-based catalysts is prepared. Unlike the successful functionalization of mesoporous materials with organosilanes (grafting [1-3], direct synthesis [4-7]), attempts at grafting organic functionalities into the void spaces of pre-formed zeolites leave a large fraction of organic groups on the exterior surface of the zeolite crystals, mitigating their ability to perform as shape-selective catalysts [8]. Zeolites and molecular sieves have previously been synthesized using organosilanes as structure-directing agents (SDA's) [9,10]. However, creation of porosity requires Si-C bond cleavage and complete loss of all organic moieties. Here, we report a new methodology for the synthesis of organic-functionalized molecular sieves (OFMS) and show that these materials contain organic functionalities within the micropores. We prepared pure-silica zeolite beta containing intracrystalline phenethyl groups covalently tethered to framework silicon atoms by direct synthesis using a reaction mixture containing phenethyltrimethoxysilane (PETMS) and tetraethylammonium fluoride (TEAF) as a SDA. Subsequent removal of

external surface-bound functionalities by a caustic wash, removal of TEAF by extraction to create microporosity followed by sulfonation of the phenyl rings produces intrazeolitic sulfonic acid sites. The resulting organic-inorganic hybrid material is shown to perform shape-selective catalysis.

3.1 Introduction

Zeolites and related crystalline molecular sieves possess uniformly sized and shaped intracrystalline void spaces that can be used to control the nature of the products obtained from chemical reactions occurring within the crystals. Since most of these materials contain acid sites, it is not surprising that shape-selective, acid-mediated reactions, e.g., formation of para-xylene, dimethylamine, and para-ethyltoluene, are accomplished on a commercial scale with zeolites [11]. Additionally, there are a limited number of laboratory-scale results showing that other classes of catalysis, e.g., oxidation with TS-1, can occur in a shape-selective manner [12]. It is clear that the type of active sites available in zeolites is rather restrictive when compared to antibody, enzyme, and homogeneous catalysts. To expand the classes of shape-selective, catalytic chemistries possible using zeolites and crystalline molecular sieves, we have prepared a new family of shape-selective catalysts, namely, organic-functionalized molecular sieves. These materials provide the means to create a broad range of active site types and thus open new opportunities for shape-selective catalysis.

3.1 Results and Discussion

A major key to success in synthesizing OFMS's is the identification of a molecular sieve that can be prepared in the absence of an organic SDA, e.g., NaY, or where the SDA can be removed by extraction. We have synthesized organic-functionalized molecular sieves via both routes, e.g., NaY (no organic SDA) or pure-silica zeolite beta using TEAF. We prefer the use of high-silica materials because they provide a hydrophobic void space in which to conduct chemical reactions. An example of the synthetic methodology is illustrated by the synthesis of pure-silica zeolite beta using TEAF as the SDA in the presence of PETMS. Following the procedure of Camblor et al. [13] for the synthesis of pure-silica zeolite beta using TEAF as the SDA,

we crystallized the hybrid material with 5 atom% or less (2.8 atom% for the sample described here) of the silicon substituted by PETMS. The X-ray diffraction pattern of the hybrid material clearly identifies it as crystalline zeolite beta (Figure 3.1). Figure 3.2 shows the ^{29}Si cross-polarization magic angle spinning (CPMAS) NMR spectra for the as-synthesized, pure-silica zeolite beta and the organic-functionalized beta. It is clear from the spectrum of the hybrid material that the phenethyl group is covalently linked to a framework silicon atom (peak at -68 ppm: C-Si-OSi$_3$ [9,14]). This resonance indicates that the linking silicon atom is fully condensed in the framework [15]. Organic functionalities on the exterior surface of the beta crystals can be removed by reacting the as-synthesized material with concentrated sodium hydroxide solutions (~8 M NaOH, 5% methanol, 25°C, 1 hour). Subsequently, extraction of TEAF from the hybrid material is possible by repeated exposures to acetic acid/water mixtures at 140°C. Essentially complete removal of TEAF is accomplished for the sample described here (>99% removed as determined by thermogravimetric analysis and ^{13}C MAS NMR). The extracted organic-functionalized molecular sieve is sulfonated by contact with vapor from 30% SO$_3$/H$_2$SO$_4$ at room temperature after heating at ~100 °C under less than 10^{-6} Torr vacuum overnight. Following sulfonation, the sample is washed with water and then dioxane to remove residual sulfuric acid resulting from the sulfonation procedure. Scanning electron microscopy (SEM) images of this fully modified material do not appear different from the images of the as-made materials. Prior to use as a catalyst, the solid is dehydrated at ~100°C for at least 6 hours under less than 10^{-6} Torr vacuum. Verification of sulfonic acid formation is obtained by Raman spectroscopy and elemental analysis. Nitrogen adsorption isotherms indicated that the extraction procedure creates significant microporosity (Figure 3.3). Figure 3.4 systematically illustrates this synthetic procedure.

The reaction of a cyclic ketone with ethylene glycol is used to illustrate the catalytic activity and shape-selectivity of the sulfonated, extracted phenethyl-

functionalized beta (Beta/PETMS/SO$_3$H) as described in Scheme 3.1. The

Beta/PETMS/SO$_3$H is an active catalyst for the formation of 2,2-pentamethylene-1,3-

dioxolane (cyclic ketal) from ethylene glycol and cyclohexanone (HEX). This activity

is due to the phenyl-sulfonic acid groups covalently linked to the zeolite framework.

The data in Table 3.1 show that para-toluenesulfonic acid monohydrate, phenyl-

sulfonic acid anchored to controlled-pore-glass (CPG-240, mean pore diameter 240 Å),

and Beta/PETMS/SO$_3$H are active catalysts for this transformation. All the OFMS

synthesis intermediates and the non-functionalized, pure-silica materials are not active

catalysts. The results clearly indicate that on Beta/PETMS/SO$_3$H the phenyl-sulfonic

acid site is the active center.

HEX   **PYC**
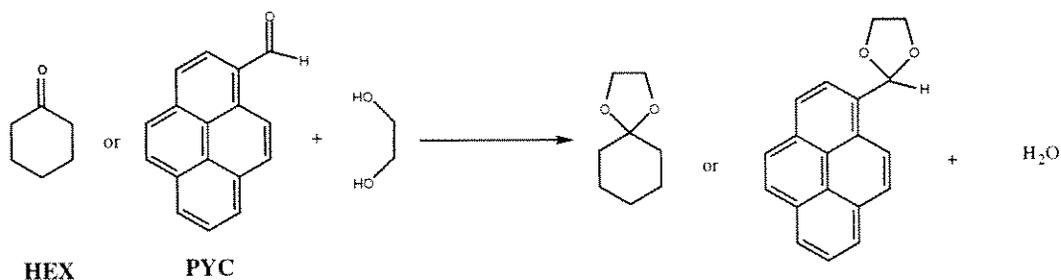
Scheme 3.1

To illustrate shape selectivity, 1-pyrenecarboxaldehyde (PYC), which is too

large to enter the pore system of beta, is reacted with ethylene glycol. Both HEX and

PYC react with ethylene glycol over para-toluenesulfonic acid monohydrate to form a

ketal or acetal (see Table 3.1). These two reactions are used to elucidate the location of

the phenyl-sulfonic acid moieties in the Beta/PETMS/SO$_3$H material. Figure 3.5

illustrates the conversion of PYC or HEX as a function of time using

Beta/PETMS/SO$_3$H as catalyst. The acetal of PYC is undetectable over the initial 3.5

hours of contact. This is due to the lack of a sufficient quantity of surface catalytic sites

that would be required to react the bulky PYC within this time frame. In contrast, HEX

is readily converted to its ketal. Upon the addition of di(2-naphthyl)-2-pyrrolidinemethanol (NPM: a bulky poison that can not access the beta pore system) after 1.15 hours of reaction, the conversion of HEX proceeds, thus indicating that the active sites are intrazeolitic. Addition of a small poison that can enter the molecular sieve pores, triethylamine (Et_3N), stops all reaction at 0.5 hours, as indicated by the data in Figure 3.5.

As a further control, phenethyl sulfonic acid sites are prepared on the surface of CPG-240. This material has a uniform pore diameter of 240 Å and can not be a shape-selective catalyst. Over this catalyst, both HEX and PYC are converted, as denoted in Table 3.1. However, if NPM is added at the outset neither HEX or PYC is reacted. Thus, the shape-selectivity of the OFMS catalyst is demonstrated by the fact that NPM poisons all active sites in CPG-240/PETMS/SO_3H, but has little affect on Beta/PETMS/SO_3H.

A commercial zeolite beta (PQ, Si/Al=25) is able to catalyze the reaction demonstrated here. However, in the absence of the surface poison, NPM, there is significant conversion of PYC by this catalyst (initial rates: HEX/PYC = 16, same conditions as those for experiments described in Figure 3.3). Thus, the aluminosilicate is not as shape-selective due to the reactivity of the external crystal surface. Also, there are no proven examples of shape-selective catalysis with organic-functionalized mesoporous solids. The pores of the mesoporous MCM-41-type materials can be constricted into the micropore range by silanation treatments. However, these modifications will not likely result in a single, fixed diameter pore opening as found in crystalline silicate molecular sieves. Instead, a distribution of pore sizes would be expected. In addition, the crystalline OFMS are physically and chemically more robust than amorphous, mesoporous materials.

The organic-functionalized materials of the type described here provide new opportunities for shape-selective catalysis. In principle, any functional group that

catalyzes homogeneous reactions can be "tailor-made" into an intrazeolitic organic moiety. Thus far, we have prepared OFMS using zeolite beta (TEAF as SDA), ZSM-5 (hexamethylenediamine as SDA) and NaY and have placed numerous functional groups into their structures, e.g., phenethyl, cyclohexenyl, aminopropyl (information regarding zeolite NaY with tethered cyclohexenylethyl groups is included in Supplementary Information). Additionally, we have demonstrated not only acid catalysis, but base-catalyzed conversions. Finally, the organic moieties may perform functions other than catalysis, e.g., synthesis of vicinal diols via oxidation of tethered cyclohexenyl groups could be employed as a chelating site for adsorbing metal ions from solution. We believe that this synthetic method is general for high-silica molecular sieve syntheses, and particularly F mediated syntheses, so long as the SDA is extractable and there exists sufficient intracrystalline space for both the organic functional group and the SDA. Thus, organic-functionalized molecular sieves should provide for new applications of shape-selectivity.

3.3 Methods

3.3.1 Catalytic Reactions

Table 3.1; Reactions were conducted in magnetically stirred glass reactors at 70°C for 24 hours. The reactor was charged with 9 g toluene, 10 mmole of each reactant, and approximately 10 mg catalyst. Products were identified by gas chromotography using authentic samples.

Figure 3.5; Reactions were conducted in magnetically stirred glass reactors at 70°C. The reactor was charged with 10 g toluene, 10 mmole of reactants in the case of HEX or 3 mmole in the case of PYC, and 13 mg catalyst. Samples were taken periodically and analyzed by GC/MS spectroscopy. Acid content of catalyst: ~0.14 mmol H^+/g cat.

3.2.2 Active Site Density

0.21 g of Beta/PETMS/SO$_3$H were washed with 15 ml of saturated NaCl solution at room temperature. The OFMS was removed by filtration. Several drops of phenolphthalein solution were added to the filtrate and then this solution was titrated with 0.001 M NaOH to neutrality. The active site density obtained from this method agreed well with the total mass of organic material as determined by TGA, and elemental analysis for sodium.

3.4 References

[1]   A. Corma, M. Iglesias, C. del Pino, and F. Sanchez *J. C. S. Chem. Commun.*, (1991) 1253-1255.

[2]   D. Brunel, A. Cauvel, F. Fajula, and F. DiRenzo in *Studies in Surface Science and Catalysis 97* (L. Bonneviot, et al., Eds.) Elsevier, Amsterdam, 1995.

[3]   J. J. Diaz, K. J. Balkus Jr., F. Bedioui, V. Kurshev, and L. Kevan *Chem. Mater.* 9 (1997) 61-67.

[4]   S. L. Burkett, S. D. Sims, and S. Mann *Chem. Commun.* (1996) 1367-1368

[5]   M. H. Lim, C. F. Blanford, and A. Stein *J. Am. Chem. Soc.* 119 (1997) 4090-4091.

[6]   C. E. Fowler, S. L. Burkett, and S. Mann *Chem. Commun.* (1997) 1769-1770.

[7]   D. J. Macquarrie *Chem Commun.* (1996) 1961-1962.

[8]   A. Cauvel, D. Brunel, F. DiRenzo, P. Moreau, and F. Fajula in *Studies in Surface Science and Catalysis 94* (H.K. Beyer, et al., Eds.) Elsevier, Amsterdam, 1995.

[9]   H. X. Li, M. A. Camblor, and M. E.Davis *Microporous Mater.* 3 (1994) 117-121.

[10]   D. C. Calabro, U.S. Patent 5,194,410, 1993.

[11]   P. B. Venuto *Microporous Mater.* 2 (1994) 297-411.

[12]   T. Tatsumi, K. Yanagisawa, K. Asano, M. Nakamura, and H. Tominaga in *Studies in Surface Science and Catalysis 83* (eds. Hattori, T. et al.) Elsevier, Amsterdam, 1994.

[13]   M. A. Camblor, A. Corma, and S. Valencia *Chem. Commun,* (1996) 2365-2366.

[14]   E. J. R. Sudholter, R. Huis, G. R. Hays, and N. C. M. Alma *J. Coll. I. Sci.* 103 (1985) 554-560.

[15]   T. Bein, R. F. Carver, R. D. Farlee, and G. D. Stucky *J. Am. Chem. Soc.* 110 (1988) 4546-4553.

Table 3.1   **Ketal or acetal formation with cyclohexanone or 1-pyrenecarboxaldehyde and ethylene glycol.**

Catalyst	Conversion (%) of HEX
None	<2
CPG-240	<2
CPG-240/PETMS	<2
CPG-240/PETMS/SO$_3$H* [#]	71.0
Si-Beta, as made	<2
Si-Beta, extracted	<2
Si-Beta, sulfonated	<2
Si-Beta/PETMS, as-made	<2
Si-Beta/PETMS, as-made sulfonated	<2
Si-Beta/PETMS, extracted	<2
Si-Beta/PETMS, extracted, SO$_3$H[†][#]	72.0
Para-toluenesulfonic acid [#]	70.0
Para-toluenesulfonic acid, NPM[‡]	0
Para-toluenesulfonic acid[§][#]	40.0
CPG-240/PETMS/SO$_3$H, NPM[‡]	0
CPG-240/PETMS/SO$_3$H[§][#]	40.0

*CPG-240/PETMS/SO$_3$H: ~0.13 mmol H$^+$/g cat.

[†] Si-Beta/PETMS, extracted, SO$_3$H: ~0.14 mmol H$^+$/g cat.

[‡] No conversion for both HEX and PYC. NPM poisons all active sites in CPG-240 and Para-toluenesulfonic acid, unlike Beta.

[§] Conversion of PYC.

[#] Conversions are limited by equilibrium.
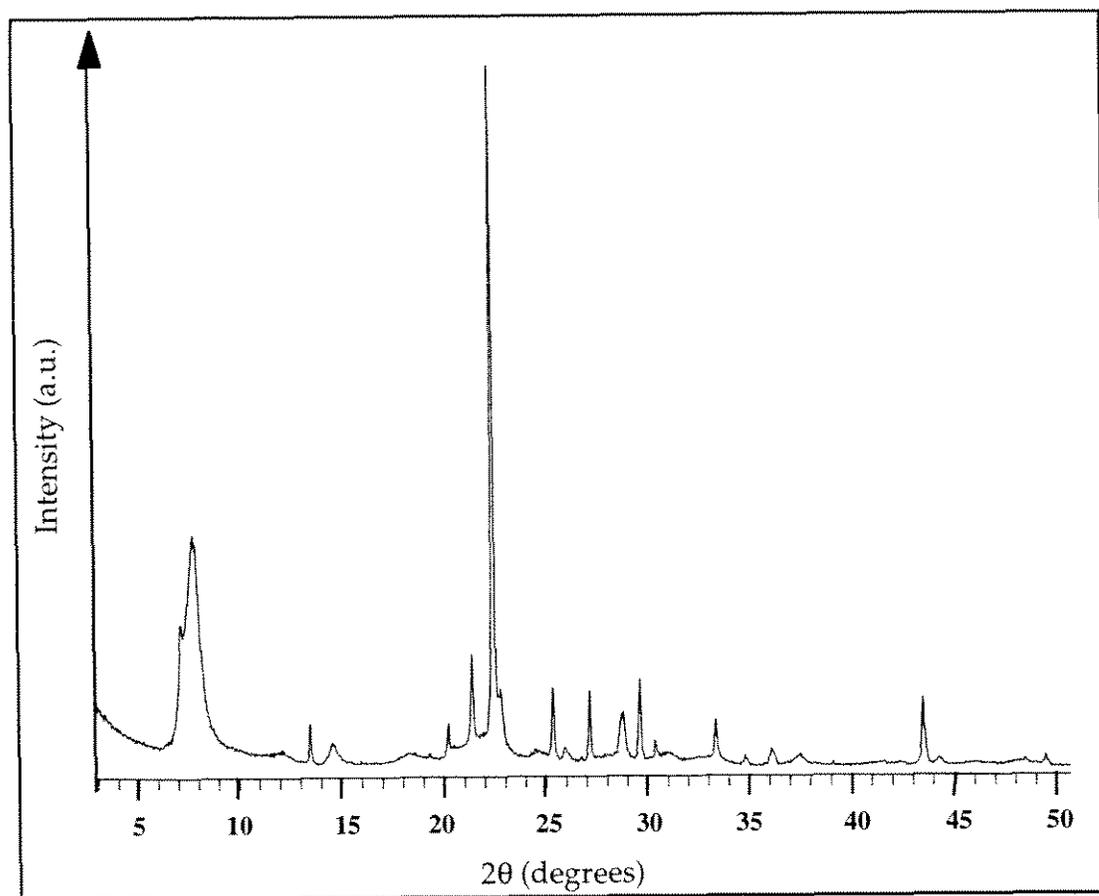
Figure 3.1   XRD pattern of extracted, phenethyl-functionalized Beta.
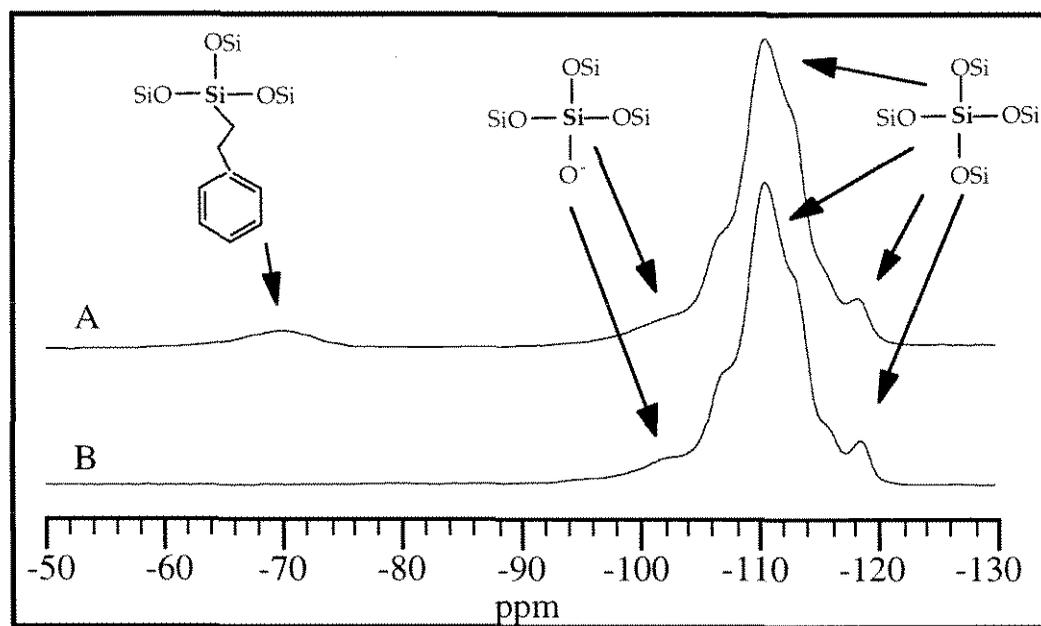
Figure 3.2 ²⁹Si CPMAS NMR spectra of a) organic-functionalized beta and b) pure-silica beta. Spectra are from as-synthesized materials and are referenced to TMS.
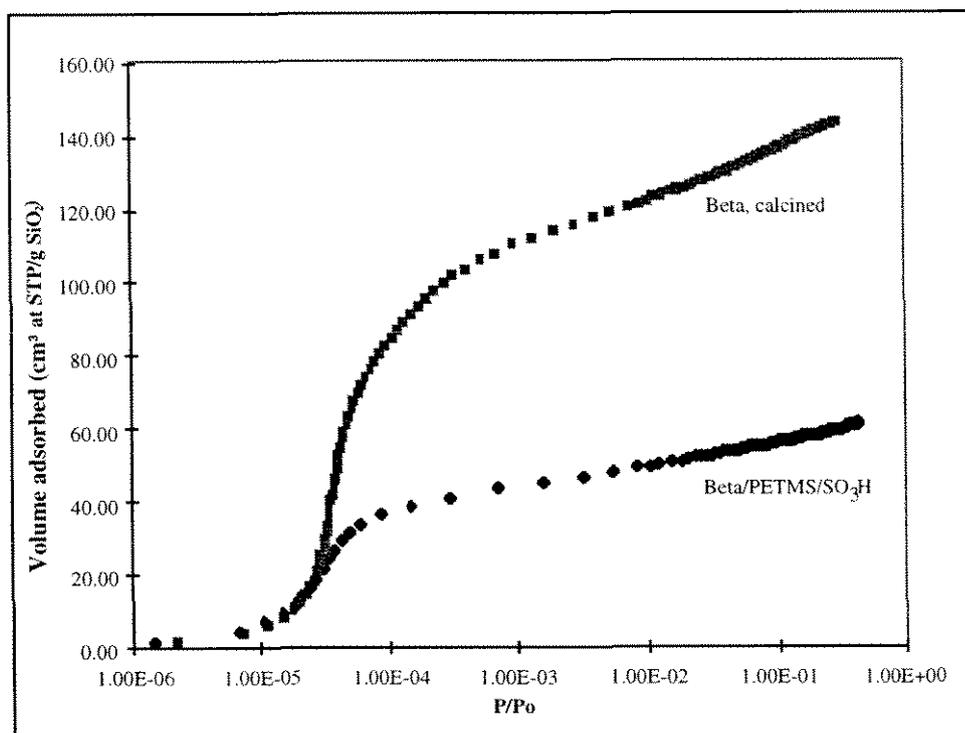
Figure 3.3 Nitrogen adsorption at 77K of the extracted, sulfonated phenethyl-functionalized Beta and the calcined Beta after pre-treatment under vacuum at 100°C overnight.
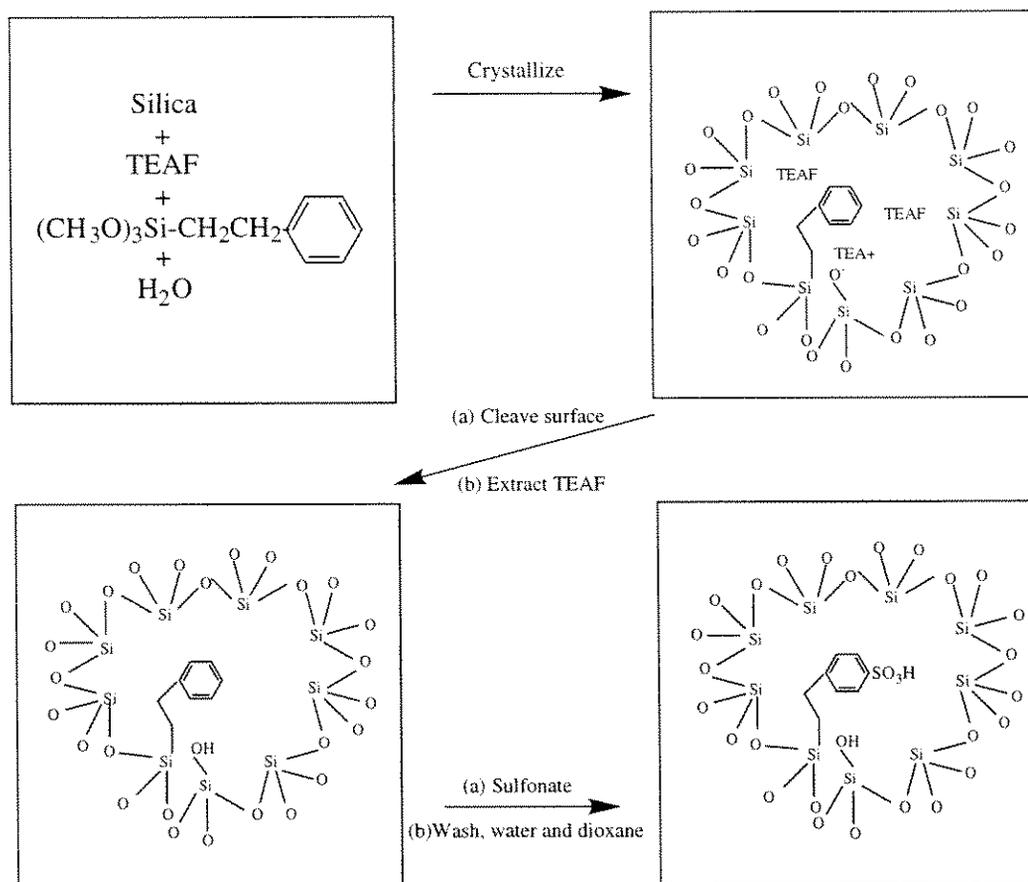
Figure 3.4 Schematic illustration of the preparation procedures used to create a sulfonic acid-functionalized molecular sieve.
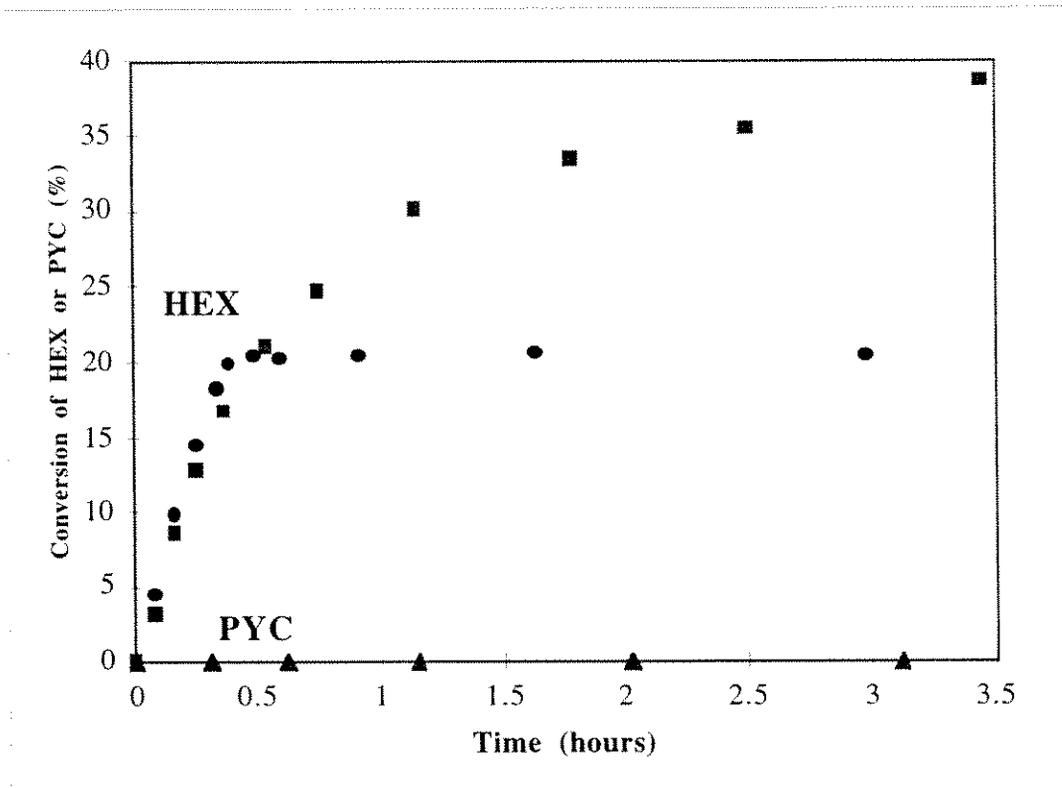
Figure 3.5 Shape-selective catalysis over organic-functionalized beta. Reactions of PYC (▲) and HEX (■, ●). 27.5 mg NPM added at 1.15 hours for the experiment denoted by (■) and 100 mg Et_3N added at 0.5 hours for the experiment denoted by (●). Acid content of catalyst: ~0.14 mmol H^+/g cat.

CHAPTER FOUR

Organic-Functionalized Molecular Sieves (OFMS's): I. Synthesis and Characterization of OFMS's with Polar Functional Groups

Organic-functionalized Molecular Sieves (OFMS's): I. Synthesis and Characterization of OFMS's with Polar Functional Groups

by

Katsuyuki Tsuji, Christopher W. Jones and Mark E. Davis

Chemical Engineering
California Institute of Technology
Pasadena, CA 91125, USA

Organic-functionalized molecular sieves that contain polar functional groups are synthesized and characterized. Small, uniform-sized crystals with the BEA topology are obtained when tetraethylammonium fluoride is used as a structure-directing agent (SDA) and added at the initiation of tetraethylorthosilicate / organosilane hydrolysis. An aminopropyl functionalized material with the BEA topology is prepared and characterized by X-ray diffraction (XRD), solid-state nuclear magnetic resonance (NMR) spectroscopy, Raman spectroscopy and diffuse reflectance ultra violet - visible (DR UV-VIS) spectroscopy. The results indicate that the aminopropyl group is located within the intracrystalline void space and that it can be reacted with aldehydes to form occluded imines.

4.1 Introduction

Organic functionalities have been incorporated onto and into amorphous silica and other solid phases for chromatographic and catalytic purposes for many years. The discovery of the periodic, mesoporous structures such as the MCM-41/MCM-48 type materials [1] added a higher degree of regularity to materials that could be functionalized by organic moieties. Organic functionality has been incorporated into these materials via two routes. First, organosilanes can be grafted onto preformed materials [2]. The second route to functionalized mesoporous materials is to synthesize the material with an organosilane to the synthesis gel. This approach, pioneered by Burkett, Mann and coworkers [3] has subsequently been used by a number of research groups. Several recent reviews discuss these materials [4-6].

In contrast, there has been little success in the functionalization of microporous materials with organosilanes. Corma and coworkers first functionalized zeolites with organic species by grafting organic groups into the mesoporous region of USY (ultra-stable Y) zeolites [7]. The grafted silanes were then used as ligands for the heterogenization of metal complex catalysts. Cauvel et al. also investigated the grafting of organosilanes onto a series of Y zeolites with varying mesopore content (mesopores introduced via steaming) [8]. They found that the grafting efficiency increased with the mesopore (and hence silanol) content. This result indicates that the majority of functionalization occurs on the external surface or in the mesopores, not in the micropores. Similar results have been obtained in our laboratory [9].

Organic-functionalized, microporous aluminophosphonates have been synthesized by Maeda et al. [10]. The organic functionality is introduced by using methylphosphonic acid in the synthesis. Unlike the inorganic/organic hybrid materials described above, that have a Si-C inorganic/organic linkage, the aluminophosphonates have a P-C inorganic/organic linkage. In addition, the only organic group reported is a

methyl group, which can not act as a catalytically active site, nor can it be further functionalized to behave as one.

Recently, we reported the first synthesis of a shape-selective OFMS [11]. In that initial study, an OFMS with the BEA topology that contained a tethered sulfophenethyl group was prepared. Here, we report the syntheses and characterizations of OFMS; and detail the case for a polar functional group; namely, an aminopropyl-functionalized, pure-silica beta molecular sieve.

4.2 Experimental

4.2.1 Synthesis of OFMS's

The materials that have the BEA topology were synthesized by modifying the method reported by Camblor et al. [12]. The gel composition of the reaction mixture was: x R-Si/ 1 SiO_2/ 0.54(1+x) TEAF/ $7H_2O$, where R-Si denotes an organosilane, TEAF is tetraethylammonium fluoride and 0<x<0.1. A typical synthesis procedure is as follows for the case of aminopropyl-tethered BEA. Aminopropyltrimethoxysilane (APTMS) (0.162g, 0.9 mmol, Gelest) was added to a 100ml flask that contained tetraethylorthosilicate (TEOS) (6.38g, 30 mmol, 98% Aldrich) and a stir bar. A solution of tetraethylammonium fluoride (TEAF) (3.04g, 16.5 mmol, % Aldrich) in water (15 ml) was added to the APTMS/ TEOS mixture with stirring. The reaction contents were agitated overnight to obtain a white slurry. The generated ethanol and excess water were removed by evaporation at 50°C. Water was added to the resultant wet solid to adjust the water content. The final gel composition was:

0.03 Aminopropylsilaneoxide/ 1 SiO_2/ 0.56 TEAF/ $7H_2O$.
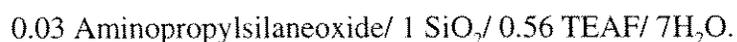
The whole was transferred to a Teflon-lined autoclave and heated at 140°C with rotation (about 60 rpm). The product was recovered by filtration and washed with water and acetone and dried at room temperature.

4.2.2 Extraction of TEAF and pretreatment of aminopropyl-tethered BEA

As-synthesized, aminopropyl-tethered beta (0.5 g) was heated at 80°C with

gentle stirring in a mixture of pyridine (30 ml) and 1N HCl aq (50 ml) for 24hr. The

solid was recovered by filtration, washed with water and acetone. The whole

extraction procedure was repeated again to obtain a completely extracted material

(confirmed by Thermogravimetric analyses (TGA)). The resultant solid was added to a

mixture of 28% NH_3 aq (5 ml) and methanol (15 ml) and aged for 12 hr. Filtration and

washing with water and acetone gave a white solid. That was dried under vacuum at

150°C for 12 hr.

4.2.3 Preparation of imines from aminopropyl groups

Condensation reactions of aminopropyl-functionalized materials (aminopropyl-

functionalized beta and aminopropyl-functionalized silica (Aldrich)) with aldehydes

were carried out to form imines. At least a five times excess 4-(dimethylamino)-

benzaldehyde (Aldrich, designated as DMBA) and 4-dimethylamino-1-naphthaldehyde

(Aldrich, designated as DMNA) were used relative to the amount of amino groups in

the materials. For the case of the reaction of aminopropyl-tethered beta with DMBA,

the specific procedure is provided below.

An aminopropyl-functionalized beta (0.1 g) and DMBA (0.1 g) were added to a

vial that contained molecular sieve 3A beads (EM Science, 8-12 mesh, 8 g). 10 ml of

methanol was added and the whole was shaken for 12 hr. The beads were removed by

sieving and the remaining solid was recovered by filtration, washed with 300 ml of

methanol and dried under vacuum at room temperature for 8 hr.

4.2.4 Analytical procedures

X-ray powder diffraction (XRD) patterns were collected on a Scintag XDS

2000 diffractometer equipped with a liquid-nitrogen cooled Ge detector using Cu-Kα

radiation. Thermogravimetric analyses (TGA) were carried out on a Du Pont 951

thermogravimetric analyzer. The samples were heated in air and the temperature ramp

was 10°C/min. Solid-state NMR spectroscopy was performed on a Bruker AM 300

spectrometer equipped with a high power assembly for solids. Samples were packed

into 7 mm ZrO_2 rotors and spun in air. ^{1}H-^{29}Si CP/MAS NMR spectra were measured

with ^{1}H decoupling at magic angle spinning (MAS) of 4.0 kHz using a 7 μs ^{1}H pulse

(^{1}H 90°), ^{29}Si contact times of 2.5 ms, and recycle times of 5 s.

Tetrakis(trimethylsilyl)silane was used as the reference material for ^{29}Si NMR chemical

shift determinations, and all chemical shifts are reported in ppm relative to external

TMS. Scanning electron microscopy (SEM) images were recorded on a Camscan 2-LV

scanning electron microscope operating with an accelerating voltage of 15 kV. UV-VIS

spectra were acquired on Varian Cary 3G UV-Visible spectrophotometer equipped with

diffuse reflectance accessory. Nitrogen adsorption isotherms were collected at liquid

nitrogen temperature (77K) on a Omnisorp 100 analyzer. The cyclohexane adsorption

amounts were analyzed using McBain-Bakr balance at 24 mm Hg at room temperature.

The samples were dehydrated under vacuum at 150°C for 4 hr before dosing

cyclohexane.

4.3   Results and discussion

4.3.1 Synthesis of OFMS's

Figure 4.1 shows SEM images of the pure-silica molecular sieves with the BEA

topology obtained with tetraethylammonium fluoride (TEAF) as SDA (top) and with

tetraethylammonium hydroxide (TEAOH) and hydrofluoric acid (HF) (bottom). The
dispersion in the crystal sizes is large (1~30μm) when using TEAOH+HF while the
use of TEAF alone from the beginning of the hydrolysis yields product that has
relatively, uniform-sized crystals (1~5 μm). This is probably due to the increased
homogeneity of the reaction components in the synthesis gel when using TEAF. When
using TEAOH+HF, addition of about half of the required amount of HF to the solution
of silica and TEAOH in water forms a solid and it becomes impossible to magnetically
stir the whole mixture. Thus, it is necessary to stir by hand after the mixture becomes
solid and the resultant gel appears to be not very homogeneous. Therefore, it is
advantageous to use TEAF instead of TEAOH+HF in order to obtain uniform-sized
crystals. Also, the use of TEAF enables the hydrolysis reaction to occur at neutral pH.
This feature is also preferred, as the organosilane and TEOS tend to hydrolyze at
distinctly different rates in alkaline media [13]. Thus, unless otherwise noted, TEAF is
used in the synthesis studies of organic-functionalized molecular sieves reported below.

Table 4.1 shows the results of pure-silica beta syntheses using various organic
trimethyoxysilanes. The ratio of organosilane to TEOS in these experiments was R-
Si/Si=0.02. Well-crystallized beta materials are obtained in all the cases (from XRD
analysis) and the crystals are similar to the pure-silica beta obtained without
organosilanes (Figure 4.1, top). It is observed that longer crystallization times are
required with the bulkier functional groups.

4.3.2 Extraction of SDA from as-synthesized molecular sieves

In order to use an organic-functionalized molecular sieve as a catalyst or for
separations, it is necessary to remove the structure-directing agent (SDA) that fills the
pores of the as-synthesized material. Several methods were examined for the extraction
of the TEAF from as-synthesized, pure-silica beta (not functionalized with organic

groups). The results are summarized in Table 4.2. The best extraction is obtained

using a mixture of acetic acid and water at 120°C. However, if the temperature is

increased to 140°C, a loss in the degree of crystallinity is observed by XRD for the

cases of acetic acid/water, methanol/water and acetonitrile/water mixtures. This is

likely caused by acidity originating from either the solvent or the HF generated during

extraction. Extracting solvents such as a mixture of methanol/ water become acidic

after the extraction. However, this is not the case for a basic solvent (the degree of

crystallinity is similar to the as-synthesized material). The addition of small amount of

HCl accelerates the extraction without loss of crystallinity. Thus, a mixture of pyridine

and 1N-HCl aq is the best solvent system for the general extraction among the

conditions employed here. All extractions on the OFMS materials were performed by

the pyridine/ HCl aq solvent as described in the Experimental Section.

4.3.3 Characterization

Figure 4.2 shows the XRD patterns of as-synthesized and extracted beta that

contain the aminopropyl functionality. In the pattern of extracted BEA, two peaks at

13.5 and 14.6° are intensified when compared to the as-synthesized material. This is

also a characteristic feature of the calcined beta and suggests that the SDA is removed

from the material. The ^{29}Si CP-MAS NMR spectrum of the extracted aminopropyl-

tethered beta is shown in Figure 4.3. There is a resonance at -68 ppm that corresponds

to the Si atom covalently bonded to carbon and three framework oxygens [14]. This

result confirms that the Si-C bond exists in the extracted material and this bond is stable

under the synthesis and extraction conditions. There is a broad shoulder around -100

ppm that corresponds to $Si(OSi)_3$-X (Q_3). Thus, it is likely that one framework Si-O-Si

linkage in the pure-silica beta is substituted by two Q_3 silicon, one attached to the

carbon of the organic moiety and the other yielding a silanol group. The results of

TGA analyses of the as-synthesized and the extracted aminopropyl-beta materials are given in Figure 4.4 with the results of calcined pure-silica beta. The TGA curve of as-synthesized aminopropyl-beta (Figure 4.4-a) is very similar to the as-synthesized beta without any organic functional groups (not shown). There is a large weight loss from 200 to 400°C and this is the typical temperature region for the combustion of the SDA. However, almost no weight loss is observed from 150 to 300°C for extracted aminopropyl-beta and there is a loss due to the adsorbed water at under 150°C (Figure 4.4b). The 2.4% weight loss observed in the range of 300-700°C can be attributed to the loss of aminopropyl groups from the material as there is almost no loss in the calcined pure-silica beta over this same temperature range (Figure 4.4c). The amount of aminopropyl groups calculated from this weight loss data is $R-Si/SiO_2 = 0.027$ and compares well to the amount in the starting gel (0.03). Elemental analyses of the extracted aminopropyl-beta (C:1.3%, N: 0.2% and Si: 42%) agree reasonably well with the TGA results ($R-Si/SiO_2$ calculated from carbon to silicone ratio is 0.024).

It is clear that the organic moieties exist in OFMS but the integrity of the functional groups and their locations need to be determined. In order to address these points, an extracted sample is used to demonstrate the existence of amino groups and to obtain information concerning their locations. Attempts to identify the small number densities of amines in these materials by infra red (IR) and Raman spectroscopies proved inconclusive. Therefore, the sample was reacted with aldehydes to transform the amino groups to imines so that their intensity in Raman spectroscopy is increased. 4-(Dimethylamino)benzaldehyde (DMBA) and 4-dimethylamino-1-naphthaldehyde (DMNA) were used for these reactions. While DMBA is small enough to migrate into the pores of the BEA structure, DMNA is not. Therefore, the reactions with these aldehydes can be used to determine whether the amino groups are located inside the

pore structure or outer surface of the material, as illustrated in Scheme 4.1 below.

Figure 4.5 shows the Raman spectra of aminopropyl-grafted silica purchased from

Aldrich (aminopropyl-silica) before and after reaction with DMBA and DMNA. In the

spectrum of pure aminopropyl-silica (bottom), a small peak indicative of the amino

group is observed at 3310 cm^{-1} (ν_{N-H}) and there are also several bands from CH_2 groups

at 2830-3000 cm^{-1} (ν_{CH2}). These bands are good indications of the aminopropyl group.

Once this material is contacted with aldehydes, the peak at 3310 cm^{-1} disappears and

new bands appear. The most important peak to note is that of imine that
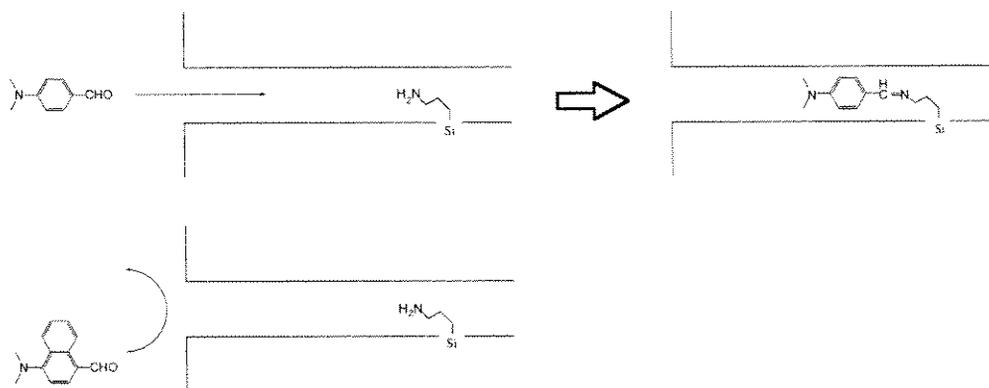
Scheme 4.1

appears at 1640 cm^{-1} ($\nu_{C=N}$). Although aromatic aldehydes also have an absorption at

1650-1670 cm^{-1} ($\nu_{C=O}$), these peaks are distinguishable from the imine band (the

shoulders at 1680cm^{-1} in Figure 4.5-middle and top are likely due to the unreacted

(adsorbed) aldehydes). The band at 1640 cm^{-1} is observed in samples contacted either

DMBA or DMNA. These results indicate that the amorphous silica material containing

aminopropyl group forms imines with both DMBA and DMNA (since both aldehydes

can access the amino group). Figure 4.6 shows the Raman spectra of aminopropyl-

tethered beta (aminopropyl-beta). The sample of aminopropyl-beta is treated with

ammonia and dried at 150°C under vacuum before contacting the aldehydes in order to make sure that the tethered amine are not protonated. From the bottom, the spectra are shown for the aminopropyl-beta before the contact, after the contact with DMNA and after the contact with DMBA, respectively. Since there are bands around 2830-3000 cm^{-1} in the spectrum before contact with aldehydes, it is apparent that this material has CH_2 groups. The peak at 3310 cm^{-1} exists although it is very weak. Thus, the aminopropyl group is verified by Raman spectroscopy. Unlike the case of aminopropyl-silica, a difference in the reactivity of the aldehydes is observed with the aminopropyl-beta. The spectrum of the aminopropyl-beta contacted with DMBA (Figure 4.6-top) has an intense band at 1640 cm^{-1} whereas this peak is hardly observed after the contact with DMNA (Figure 4.6 middle). There also may exist a difference in the region for v_{N-H}. The band at 3310 cm^{-1} disappears from the spectrum of the beta contacted with DMBA while a small "hump" is observed in the spectrum of the sample exposed to DMNA. Therefore, the aminopropyl groups in the beta appear to be accessible to DMBA and not to DMNA. The obvious location at the aminopropyl groups is inside the pore of the BEA structure. If such is the case, a loss in micropore volume should be observed. Indeed, a loss of N_2 uptake is observed as is shown in Figure 4.7. The N_2 uptake of aminopropyl-beta is less than that of calcined aminopropyl-beta (calcined at 600°C). This is the case of cyclohexane adsorption; the amount adsorbed on aminopropyl-beta is 0.226 ml/g sample whereas calcined aminopropyl-beta adsorbs 0.261 ml/g-sample. If the density of aminopropyl group is assumed to be similar to 1-propylamine (0.719 g/ml), the amount of aminopropyl groups within the aminopropyl-beta material calculated from these data is R-Si/SiO_2=0.025 that agrees very well with the results of TGA (0.027) and elemental analyses (0.024).

The imines produced by the reaction of the aminopropyl group and aldehydes are relatively stable Schiff bases and DMBA has been used to detect trace amounts of nitrogen compounds since the resultant imines usually are colored [15]. This is the case for aminopropyl-tethered silicate materials. Both aminopropyl-silica and aminopropyl-beta turn yellow (from white) after exposure to DMBA. For contact with DMNA, aminopropyl-silica becomes yellow while aminopropyl-beta becomes very weakly colored. Such a slight color change is observed on the calcined pure-silica beta after contact with DMNA since DMNA itself is yellow. The UV-VIS spectra of these materials are shown in Figures 4.8 and 4.9. The aminopropyl-silica contacted with DMBA and DMNA have intense absorptions below 500 nm (Figure 4.8-c and Figure 4.9-c) as expected. This intense peak is also observed in the spectrum of aminopropyl-beta contacted with DMBA (Figure 4.8-b, λ_{max} is around 350 nm). However,

aminopropyl-beta does not have such an intense absorption after contact with DMNA, but rather small absorptions at 250 and 380 nm with a shoulder at 470 nm (Figure 4.9-b). Since the former two bands are also observed in the pure-silica beta contacted with DMNA (Figure 4.9-a), they are probably due to the DMNA adsorbed on the surface of beta that makes these materials slightly yellow. However, there is an additional shoulder at 470 nm in the spectrum of the aminopropyl-beta contacted with DMNA that is not seen in calcined beta. This band is also observed in the aminopropyl-silica contacted with DMNA. Thus, a trace amount of imine might be generated by contacting the aminopropyl-beta with DMNA. This imine formation with DMNA could occur if some of the aminopropyl groups are located near the outer surface. This is probably the case because the contact of DMNA to the as-synthesized, aminopropyl-beta does not generate this absorption. The color and the spectrum of the material obtained by the reaction of extracted aminopropyl-beta (without pretreatment with ammonia) with DMBA are similar to those of the ammonia treated aminopropyl-beta (yellow), while the acid treated aminopropyl-silica gives a red product that has a

different UV-VIS spectrum (Figure 4.8-d). Since it is reported previously that

protonation of imine compounds gives intense absorption bands at long wavelengths

[16], the aminopropyl groups in the extracted material may not be protonated and

ammonia pretreatment may not be necessary.

4.4 Summary

Addition of small amounts of organic species to a zeolite synthesis mixture can

have an extreme influence on the synthesis. Often, a mixture of crystalline phases is

obtained, or no crystalline phase results. In syntheses free of an organic structure-

directing agent, the organosilane often phase separates from the zeolite synthesis gel

and the organic functionality is not incorporated when a zeolite is formed. When

performing syntheses that require an organic SDA, there is an additional requirement

that SDA must be extracted in order to obtain porosity. These severe requirements limit

the scope of synthesizing molecular sieves with organic functionalities. The synthesis

method used to obtain the pure-silica analogue of zeolite beta with TEAF by Camblor et

al. [12] allows the circumvention of these problem. Camblor's synthesis method has

desirable features that allow it to be adapted to the synthesis of OFMS's. The reaction

gel appears to be sufficiently hydrophobic so that an organosilane does not phase-

separate from the other components and the TEAF that is used as the SDA is small

enough compared to the pore opening of the BEA structure to be extracted. As we

previously reported [11], this system successfully prepares beta with organic

functionalities such as phenethyl groups. The phenethyl-functionalized material

contains intracrystalline phenethyl groups as revealed by catalytic tests [11]. The

success of this synthesis can be attributed to the hydrophobic nature of the phenethyl

group that prevents disruption of the beta synthesis. We hypothesized that polar

functional groups may behave similarly to SDAs and disturb the formation of zeolites.

However, this is not the case as demonstrated here. Well-crystallized beta is obtained

with a variety of polar organosilanes. Although details proving organic incorporation are not provided for all cases, the aminopropyl group is used as a model to demonstrate that it is so. The aminopropyl groups are shown to be intrazeolitic by noting the difference in the reactivity of the aminopropyl group with large and small aldehydes. Additionally, the aminopropyl group is able to be transformed to other functional groups such as an imine by common organic synthetic methods (in the previous reports, the phenethyl group was reacted to sulfophenethyl by SO_3) [11]. Thus, the methodologies illustrated here are useful for synthesizing organic-functionalized beta that has functional groups inside the pore system independent of whether the organic functional groups are polar or not. Finally, it is notable that the use of TEAF as an SDA leads to the formation of the product with relatively small, uniform-sized crystals, since it is often advantageous to have smaller crystals for the catalysis or separation applications.

4.5   References

[1]   C.T. Kresge, M.E. Leonowicz, W.J. Roth, J.C. Vartuli, and J.S. Beck *Nature* 359 (1992) 710.

[2]   J.S. Beck, J.C. Varfuli, W.j. Roth, M.E. Leonowicz, C.T. Kresge, K.D. Schmitt, C.T.-W. Chu, D.H. Olson, E.W. Sheppard, S.B. McCullen, J.O. Higgins, and J.L. Schlenker *J. Am. Chem. Soc.* 114 (1992) 10834; D. Brunel, A. Cauvel, F. Fajula, and F. Di Renzo in *Studies in Surface Science and Catalysis 97* (L. Bonneviot et al., Eds.) Elsevier, Amsterdam, 1995.

[3]   S.L. Burkett, D.D. Sims, and S. Mann *Chem. Commun.* (1996) 1367; C.E. Fowler, S.L. Burkett, and S. Mann *Chem. Commun.* (1997) 1769.

[4]   J.H. Clark and D.J. Macquarrie *Chem. Commun.* (1998) 853.

[5]   K. Moller and T. Bein, *Chem. Mater.* 10 (1998) 2950-2963.

[6]   J. Liu, X. Feng, G. Fryxell, L.Q. Wang, A.Y. Kim, and M. Gong *Advan. Mater.* 10 (1998) 161.

[7]   A. Corma, M. Iglesias, C. del Pino, and F. Sanchez *J. Chem. Soc. Chem. Commun.* (1991) 1253; F. Sanchez, M. Iglesias, A. Corma, and C. del Pino *J. Mol. Catal.* 70 (1991) 369; A. Corma, M. Iglesias, M.V. Martin, J. Rubio, and F. Sanchez *Tett. Asym.* 3 (1992) 845; A. Carmona, A. Corma, M. Iglesias, A. San Jose, and F. Sanchez *J. Organomettalic Chem.* 492 (1995) 11.

[8]   A. Cauvel, D. Brunel, F. DiRenzo, P. Moreau, and F. Fajula in *Studies in Surface Science and Catalysis 94* (H. K. Beyer, et al., Eds.) Elsevier, Amsterdam, 1995.

[9]   W.R. Ahmad and M.E. Davis, unpublished results.

[10] K. Maeda, Y. Kiyozumi, and F. Mizukami *Angew. Chem. Int. Ed. Engl.* 33 (1994) 2335; K. Maeda, J. Akimoto, Y. Kiyozumi, and F. Mizukami *J. Chem. Soc. Chem. Commun.* (1995) 1033; K. Maeda, J. Akimoto, Y. Kiyozumi, and F. Mizukami *Angew. Chem. Int. Ed. Engl.* 34 (1995) 1199; K. Maeda, A. Sasaki, K. Watanabe, Y. Kiyozumi, and F. Mizukami *Chem. Lett.* (1997) 879.

[11] C.W. Jones, K. Tsuji, and M.E. Davis *Nature* 393 (1998) 52.

[12] M.A. Camblor, A. Corma, and S. Valencia *Chem. Commum.* (1996) 2365.

[13] C.J. Brinker and G.W. Scherer, *Sol-Gel Science: The Physics and Chemistry of Sol-Gel Processing*, Academic Press, San Diego, CA, 1990.

[14] H.X. Li, M.A. Camblor, and M.E. Davis *Microporous Mater.* 3 (1994) 117.

[15] C. Menzie *Anal. Chem.* 28 (1956) 1321.

[16] D. Gargiulo, N. Lkemoto, J. Odingo, N. Bozhkova, T. Iwashita, N. Berova, and K. Nakanishi *J. Am. Chem. Soc.* 116 (1994) 3760.

Table 4.1 **Results of BEA syntheses using various organic silanes.**

Organosilane	Time /days
None (pure-silica)	5
2-Cyanoethyltrimethoxysilane	15
3-Iodopropyltrimethoxysilane	15
Allyltrimethoxysilane	17
3-Bromopropyltrimethoxysilane	17
3-Aminopropyltrimethoxysilane	18
N,N-Dimethyl-3-aminopropyltrimethoxysilane	21
Phenethyltrimethoxysilane	27
2-(4-Chlorosulfonylphenyl)ethyltrimethoxysilane	28
3-Mercaptopropyltrimethoxysilane	47

Table 4.2 **Extraction of TEAF from as-synthesized pure-silica BEA*.**

Solvent	Temp./°C	Time/h	Efficiency**/%
H_2O	120	24	36
CH_3OH/ H_2O (1:1)	120	24	34
CH_3CN/ H_2O (1:1)	120	24	42
CH_3COOH/ H_2O (1:1)	120	24	90
Pyridine/ H_2O (1:1)	120	24	43
Pyridine/ 1N-Hclaq (1:1)	120	24	72
under vacuum	200	12	48

* 0.05g of sample were treated in 3ml of solvent.
** Percentage of TEAF removed.
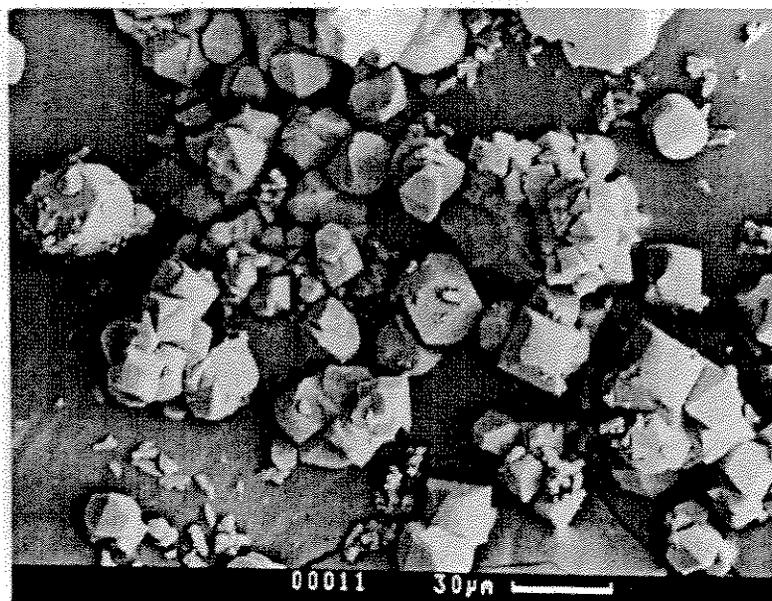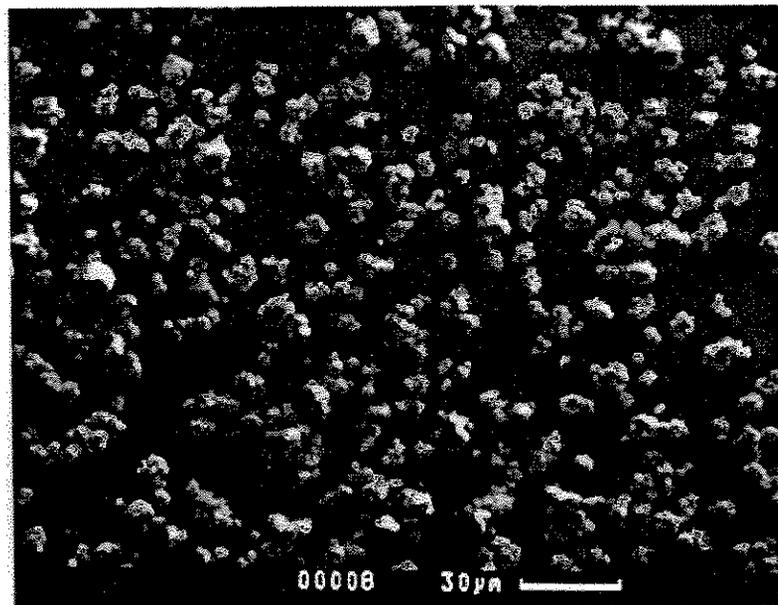
Figure 4.1   SEM images of as-synthesized, pure-silica beta. Top: synthesized using TEAF, Bottom: synthesized using TEAOH+HF.
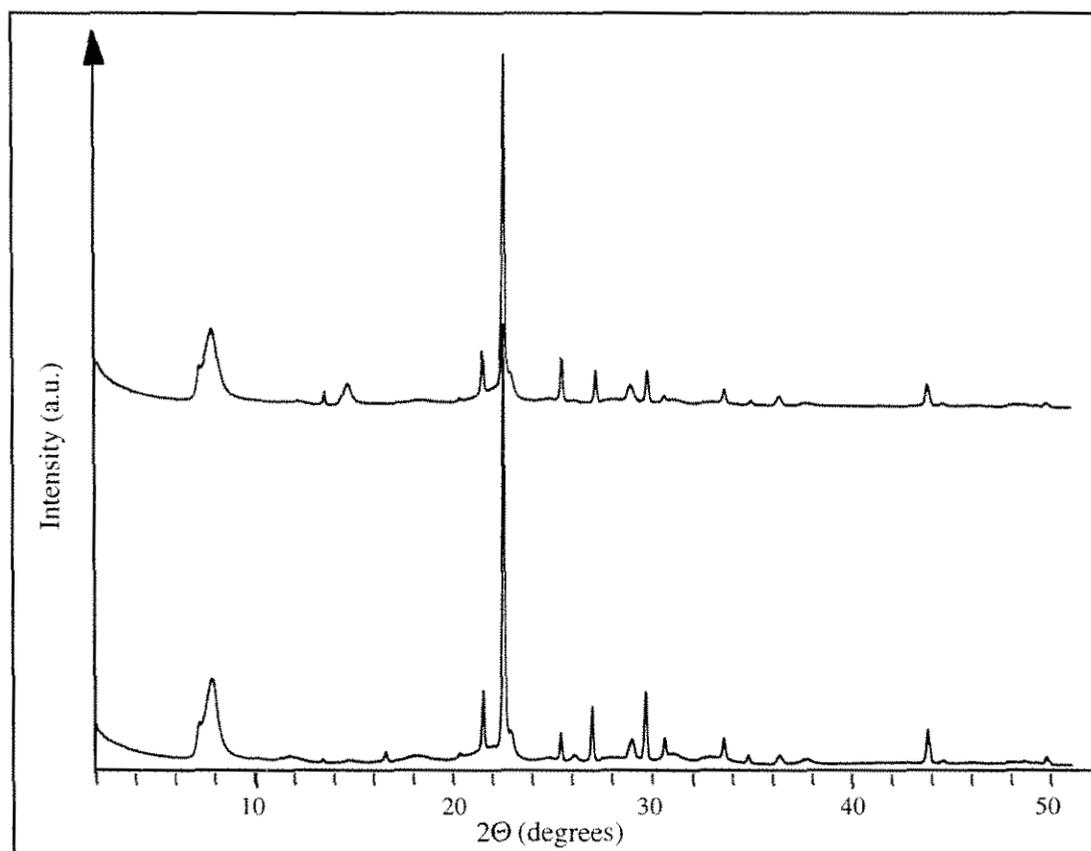
Figure 4.2 XRD patterns of aminopropyl-beta. Top: the extracted, Bottom: as-synthesized.
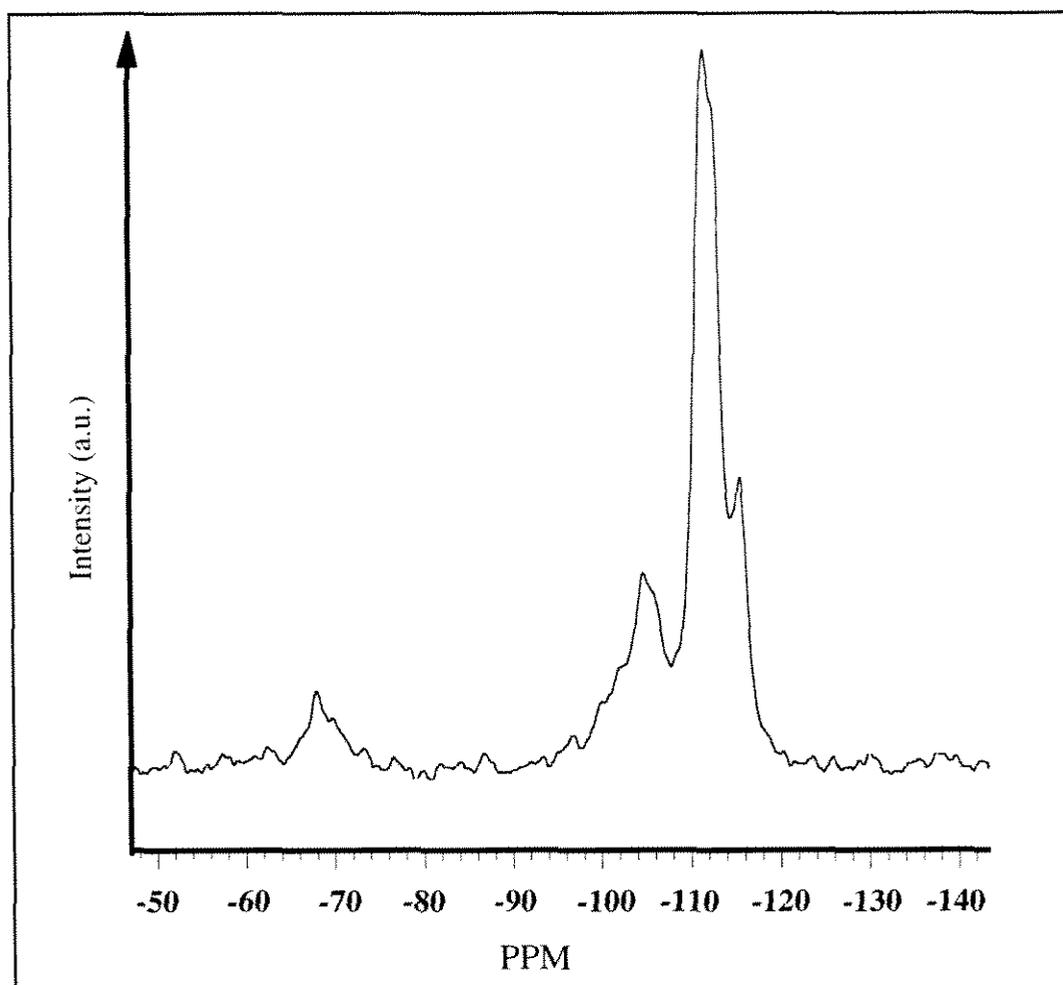
Figure 4.3 ^{29}Si CP-MAS NMR spectrum of aminopropyl-beta.
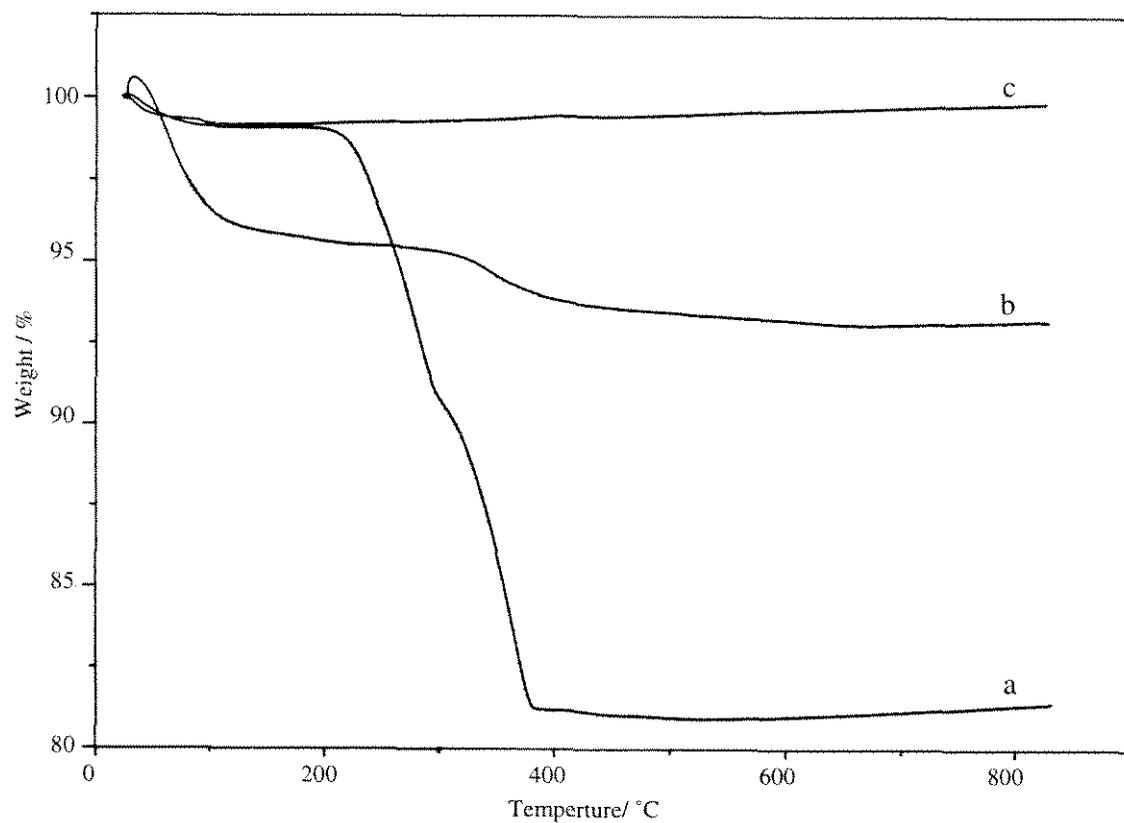
Figure 4.4 TG curve of the aminopropyl-beta. a: As-synthesized
aminopropyl-beta, b: Extracted aminopropyl-beta,
c: Calcined beta. (Slight weight gain illustrated is from
improper buoyancy corrections in the TGA.)
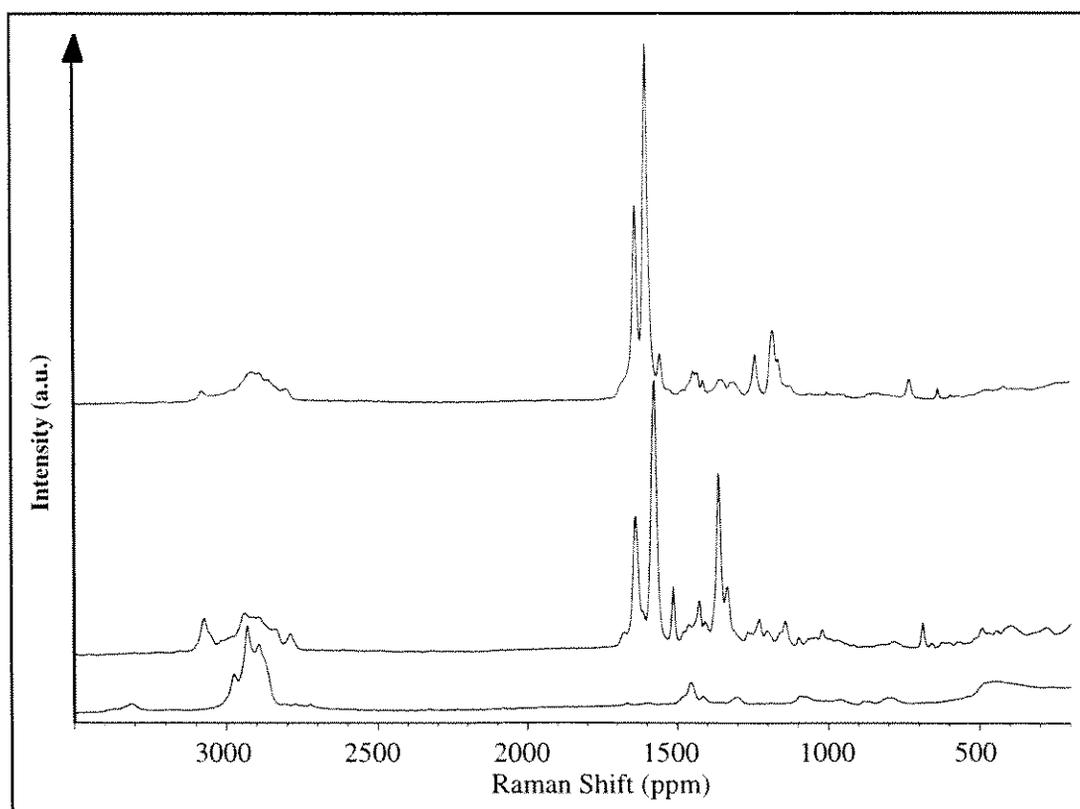
Figure 4.5 **Raman spectra of aminopropyl-silica (Aldrich). From the bottom: before the reaction, after the contact with DMNA and after the contact with DMBA.**
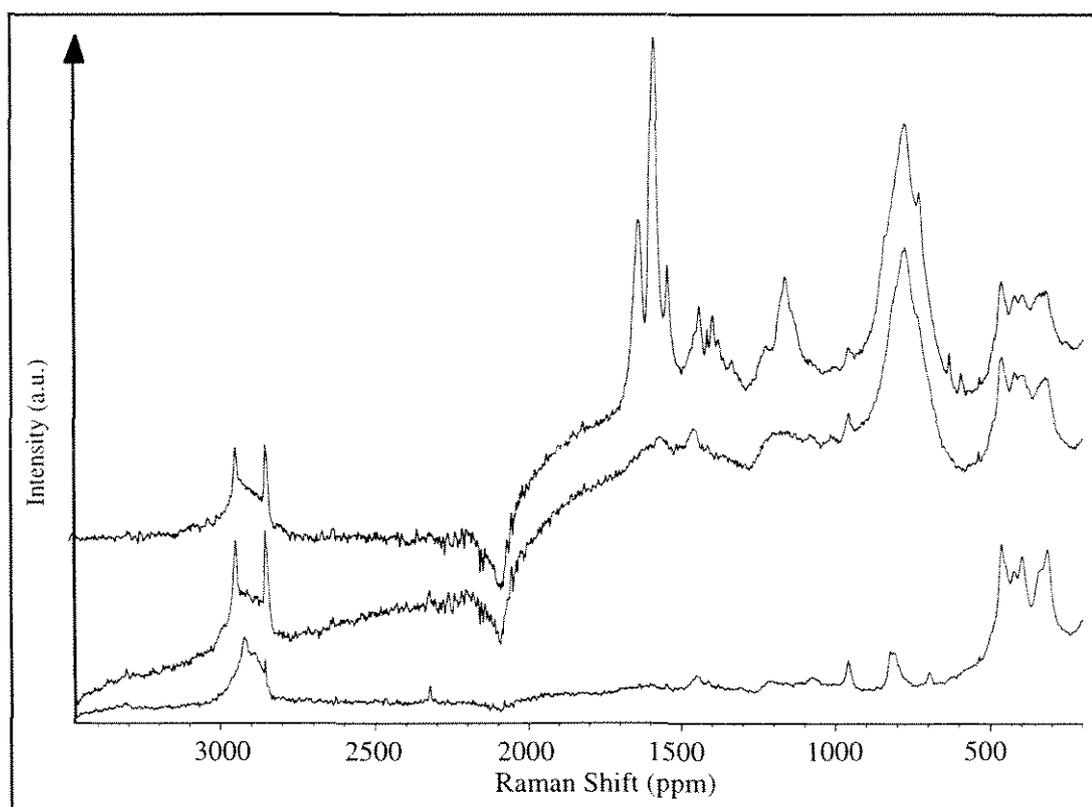
Figure 4.6 **Raman spectra of aminopropyl-beta. From the bottom: before the reaction, after the contact with DMNA and after the contact with DMBA.**
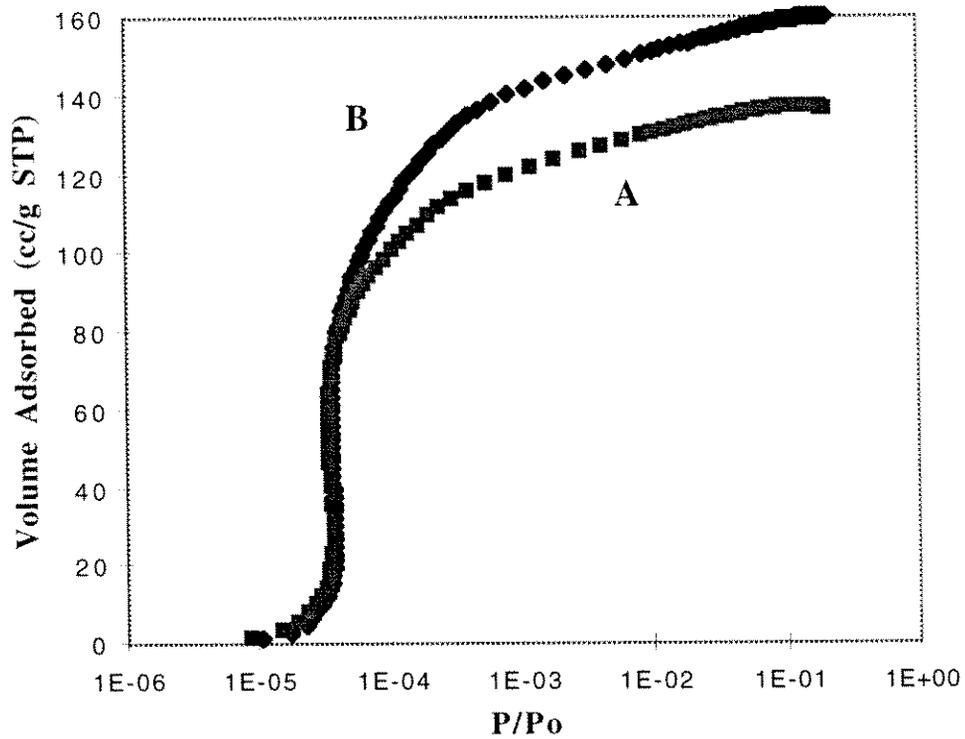
Figure 4.7 **Nitrogen adsorption isotherm at 77K for aminopropyl-beta.**
A: Extracted aminopropyl-beta, B: Calcined aminopropyl-
beta.
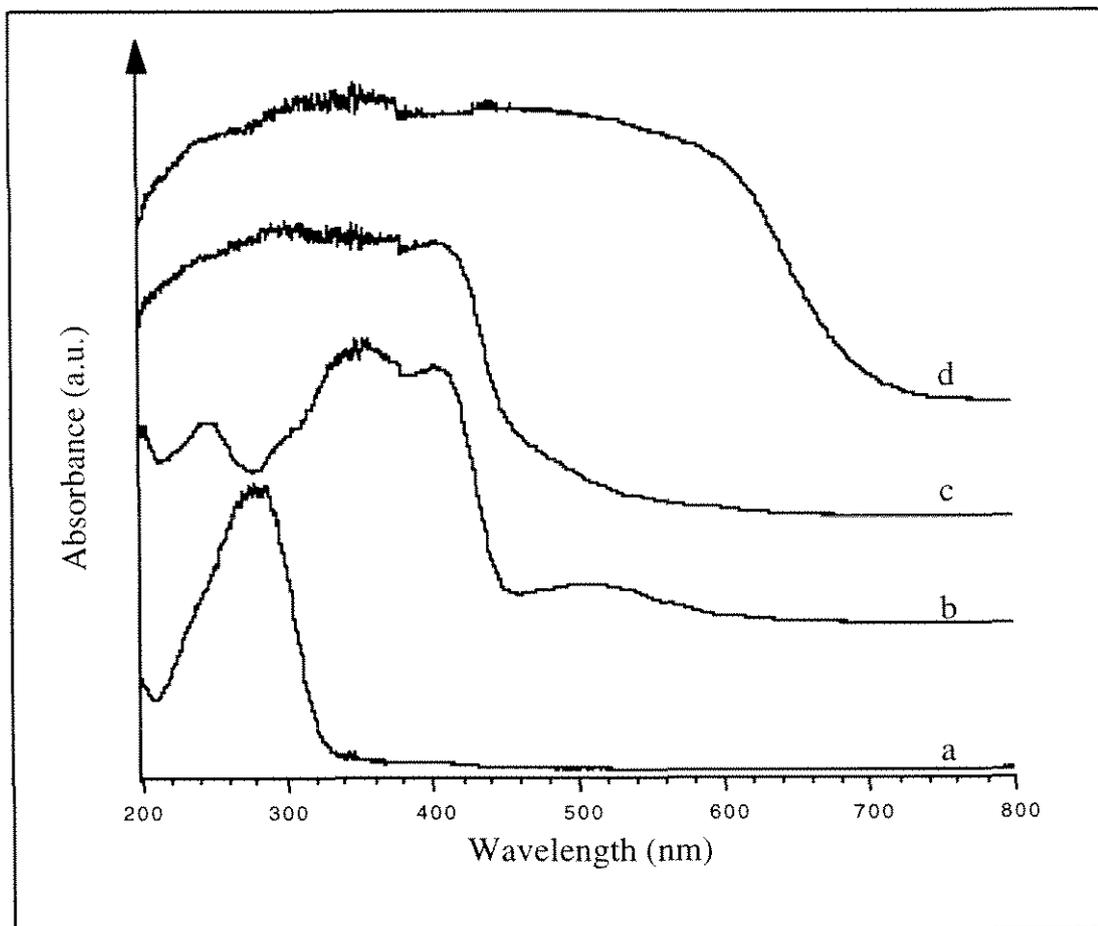
Figure 4.8 UV-VIS spectra of materials contacted with DMBA. a:
calcined pure-silica beta, b: aminopropyl-beta,
c: aminopropyl-silica, d: acid treated aminopropyl-silica
contacted with DMBA.
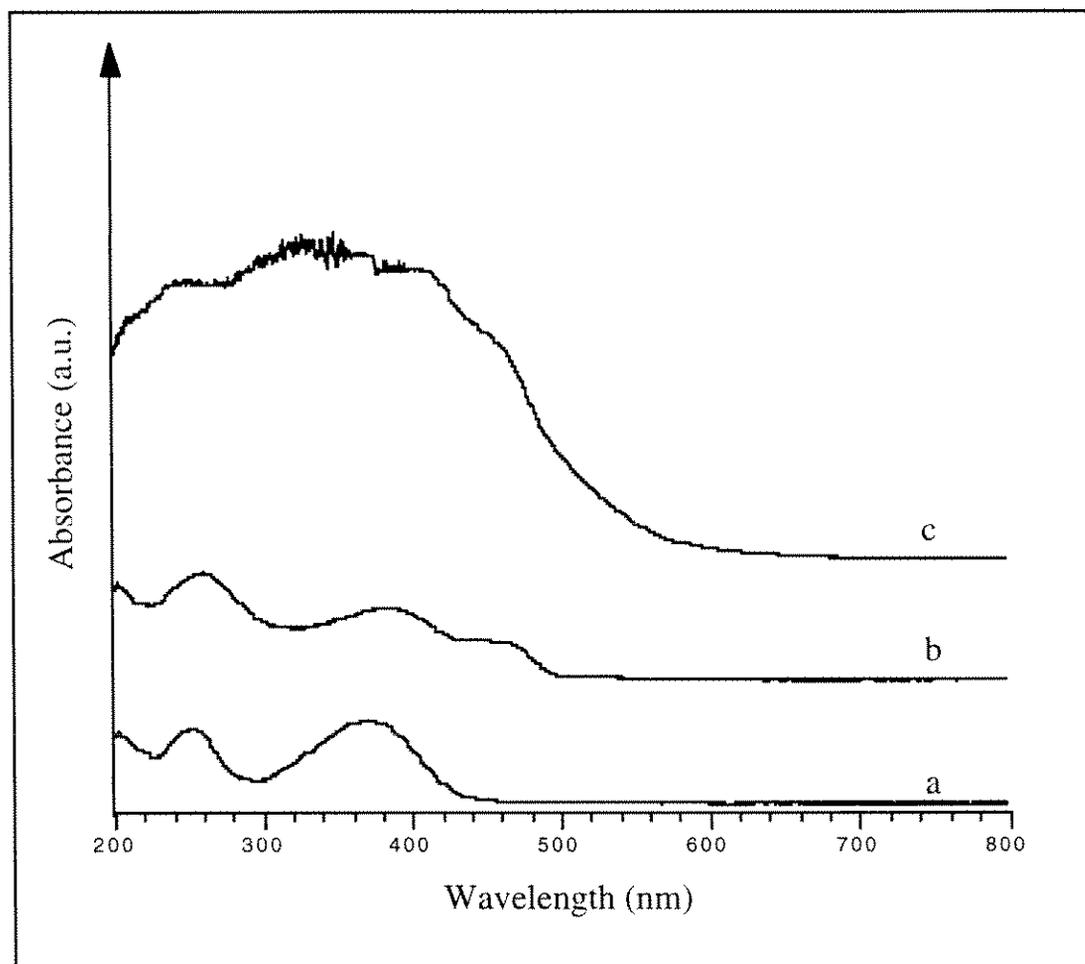
Figure 4.9 UV-VIS spectra of materials contacted DMNA. a: calcined pure-silica beta, b: aminopropyl-beta, c: aminopropyl-silica contacted with DMNA.

CHAPTER FIVE

Organic-Functionalized Molecular Sieves (OFMS's): II. Synthesis, Characterization and the Transformation of OFMS's containing Non-Polar Functional Groups into Solid Acids

Organic-Functionalized Molecular Sieves (OFMS's): II Synthesis, Characterization and the Transformation of OFMS's containing Non-Polar Functional Groups into Solid Acids

by

Christopher W. Jones, Katsuyuki Tsuji and Mark E. Davis

Chemical Engineering
California Institute of Technology
Pasadena, CA 91125, USA

Organic-functionalized molecular sieves (OFMS's) with a beta-type structure (*BEA) containing intracrystalline phenethyl (PE) groups are synthesized and characterized by X-ray diffraction (XRD), thermogravimetric analysis (TGA), FT-Raman spectroscopy, ^{29}Si, ^{13}C and ^{27}Al solid-state nuclear magnetic resonance (NMR) spectroscopy, X-ray photoelectron spectroscopy (XPS), bulk elemental analysis, scanning electron microscopy (SEM) and physisorption techniques. The OFMS's are synthesized from monomeric silicon sources such as tetraethylorthosilicate (TEOS) and phenethyltrimethoxysilane and via the solid-state conversion of extracted, PE-functionalized MCM-41. Occluded structure-directing agent (tetraethylammonium fluoride; TEAF) is removed by solvent extraction techniques. By varying the extraction conditions, OFMS's with varying hydrophobicity and porosity are synthesized. Bulk and surface elemental analysis indicate that there is an even distribution of organic functionalities throughout the material at levels of PE incorporation below 5% (silicon basis). The phenethyl groups are sulfonated using SO_3 vapor to produce a microporous solid containing intracrystalline sulfonic acids.

5.1 Introduction

Recently, we reported the first synthesis of crystalline, microporous silicates with organic functionalities covalently tethered within the micropores [1]. These materials (denoted organic-functionalized molecular sieves (OFMS's)) were shown to be amenable to the design of shape-selective catalysts based on organic active sites. Subsequently, we reported that polar organic-functionalities, such as an aminopropyl group can be incorporated into the OFMS materials in addition to the non-polar phenethyl group incorporated in reference 1 [2]. In both cases it was demonstrated that the vast majority of both the aminopropyl [2] and phenethyl [1] groups were located within the micropores.

In general, the organic functionalities in these molecular sieves can be further altered after molecular sieve synthesis using standard organic synthesis techniques. Hence, a variety of organic groups can be included within the micropores by design (aromatic, sulfonic acid [1]; amine, imine [2]). These materials show promise for use in low temperature, liquid phase catalytic and molecular recognition applications, as the active sites can be tailored to meet the needs of the reaction of interest.

Here, we now report a detailed investigation of the synthesis of the phenethyl-containing *BEA OFMS and the detailed characterization of this material. In addition to the original synthesis method, we report here another route to OFMS's. OFMS's are obtained through the solid-phase transformation of an amorphous silicate to an OFMS with the *BEA topology. Additionally, the synthesis of *BEA containing several other organic groups is provided to further demonstrate the breadth of this approach.

5.2 Experimental

5.2.1 Synthesis

OFMS materials were prepared with several non-polar organic groups. Two different routes to OFMS's with the *BEA topology are described below. The synthetic strategies are illustrated in Scheme 5.1.
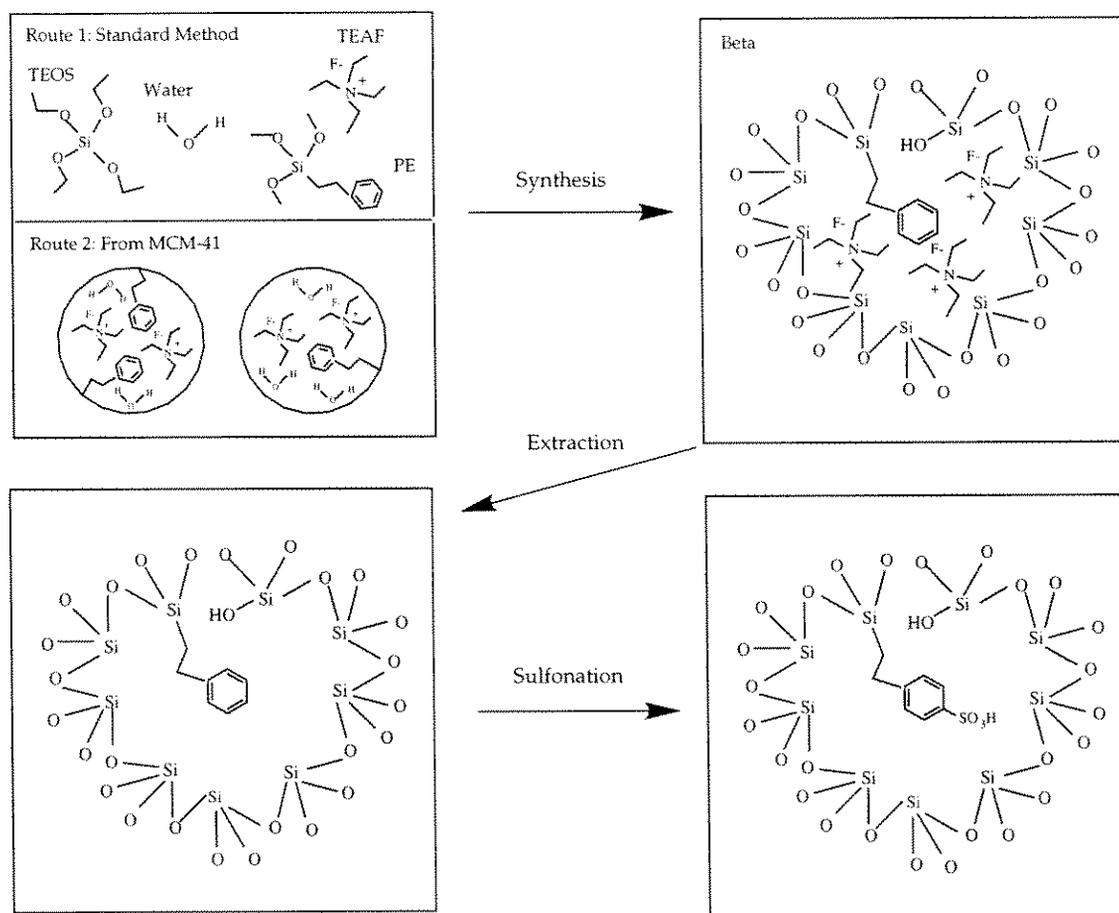
Scheme 5.1

<u>Route 1</u>:

In a typical synthesis, 6.25 g of TEAF (Aldrich or Fluka) were dissolved in 7.75 g water. To this solution, a mixture of 12.65 g of tetraethylorthosilicate (TEOS, Aldrich) and 0.30 g of phenethyltrimethoxysilane (PETMS, Gelest) were added dropwise. The flask containing this solution was covered loosely with parafilm and the

solution was allowed to stir for 18-24 hours. Next, the alcohols generated by the hydrolysis of the silanes and some water were removed by rotary evaporation. Additional water was added and the evaporation procedure was then repeated. The thick mixture was then added to a Teflon liner and water was added to make the final gel composition:

$$1 \text{ SiO}_2 \text{ / } 0.55 \text{ TEAF / } 0.025 \text{ PhenethylSiO}_{1.5} \text{ / } 7.25 \text{ H}_2\text{O}.$$
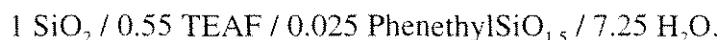
The Teflon liner was placed into an autoclave and the autoclave was heated in a oven with rotation (~60 rpm) for 42 days at 140°C. The autoclave was quenched in a water bath and the products were washed with water and acetone and recovered by filtration. The product material is denoted Beta/PE. In this work, this procedure is sometime referred to as the standard synthetic method.

Variations on the Route 1 synthetic strategy were made. The effects of using as-synthesized Beta/PE as seed, added aluminum (aluminum nitrate nonahydrate, Baker) or boron (boric acid, Baker), and variation of the silica source were also investigated. When silica sources other than TEOS were used, the addition of the silica source and the organosilane was performed in separate steps. First, the silica source was added under agitation and the mixture was allowed to stir for 2 hours. Next, the organosilane was added slowly and dropwise with stirring.

Route 2:

PE-functionalized MCM-41 (PE/MCM-41) was synthesized by adapting slightly the procedure first described by Burkett and coworkers [3]. TEOS, PE, sodium hydroxide, cetyltrimethyammonium bromide (CTAB, Fluka) and water were combined in ratio: 1.0 Si / 0.02 PE/ 0.12 CTAB/ 0.5 Na/ 130 H$_2$O and mixed at room temperature for 24 hours. The product was recovered by filtration and extracted by refluxing in acidified methanol as described by Stein and coworkers [4].

The extracted PE/MCM-41 was then transformed into a solid having the *BEA topology by hydrothermal treatment in a manner similar the method described in

reference 5. In a typical synthesis, 720 mg of extracted PE/MCM-41 were added to a Teflon-lined Parr autoclave. A solution of TEAF in water was then added to give a total composition of 1 Si/0.55 TEAF/ 7.25 H_2O. The autoclave was then heated in an oven under rotation at 140°C for 4 weeks. The autoclave was then quenched in a water bath and the solid product was recovered by filtration. Beta obtained by this method is labeled Beta-2/PE or Beta-2 in the case where the parent MCM-41 does not contain PE.

5.2.2 Extraction of SDA

SDA was extracted from the *BEA OFMS materials using three techniques. Method 1 (Pyr/H_2O): Beta/PE (~0.4 g) was added to a Teflon-lined, 45 ml Parr autoclave along with 35g of extraction solution (50% water, 50% pyridine). The autoclave was heated in an oven with rotation at 120°C. Method 2 (Pyr/HCl): Beta/PE (~0.5g) was added to a flask with 100 ml of extraction solution (50% 1N HCl, 50% pyridine). The flask was heated in an oil bath at 80°C with stirring. Method 3 (Acet/ H_2O): Beta/PE (~0.5g) was added to a flask with 100 ml of extraction solution (50% acetic acid, 50% water). The flask was heated in an oil bath at 80°C with stirring. After 12-24 hours of treatment, the solids were recovered by filtration. Method 3 was also used for extraction at higher temperatures in autoclaves as follows. Beta/PE (~0.4 g) was added to a Teflon-lined, 45ml Parr autoclave along with 35 g of extraction solution (50% water, 50% glacial acetic acid). The autoclave was heated in an oven with rotation at 120°C or 135°C. Following 12-24 hours of treatment, the solid were recovered by filtration. The extraction procedures were repeated until there was no change in the resulting material by TGA analysis.

5.2.3 Modification of Organic Species

The phenethyl groups of Beta/PE were sulfonated by reaction with SO_3 vapor at room temperature. The OFMS (~0.5 g) was added to the sample chamber of the glass

apparatus of a type that is schematically shown in Figure 5.1. With stopcocks A and B open, the sample was dehydrated overnight at 100-150°C. After dehydration, the stopcocks were closed and 2 ml of 30% oleum (30% SO_3 in H_2SO_4, Aldrich) were added to the oleum chamber. The oleum was then degassed with liquid-nitrogen (LN_2) freeze/thaw/vacuum cycles (4x) while maintaining stopcock B closed. Next, with the oleum chamber immersed in LN_2, stopcock B was opened and the entire chamber placed under vacuum for 15 minutes. Stopcock A was then closed and the oleum is allowed to warm to room temperature. SO_3 vaporizes and traveled to the sample through the connecting arm, thus sulfonating the sample. The sample was allowed to react with the vapors for 12-24 hours at room temperature. After the allotted time, the oleum chamber was immersed in LN_2 for 15 minutes. While maintaining the oleum chamber in LN_2, stopcock A was opened and the system was placed under vacuum for 20 minutes. After removing the sample from the apparatus, it was washed liberally with water. The total volume of water used was approximately 2 L.

5.2.4 Elemental Analysis Sample Preparation

All samples for elemental analysis were contacted with a 0.1 M CsCl solution (0.02g sample / g solution) for 45 minutes at room temperature. Samples were recovered by filtration and washed with ~10 ml of 0.0065 M CsCl solution. The filtrate was retained and subsequently titrated with 0.0011 M NaOH to determine the H^+ concentration in solution. The exchanged solid was dried overnight in an oven at ~100°C.

5.2.5 Analytical Methods

X-ray powder diffraction (XRD) patterns were collected on a Scintag XDS 2000 diffractometer using Cu-Kα radiation. Nitrogen adsorption isotherms were obtained at 77K using an Omnisorp 100 sorption apparatus operating in static mode

using fixed dosing. Vapor phase cyclohexane and water adsorption isotherms were obtained on a McBain-Bakr balance. Prior to all adsorption experiments, the samples were degassed under vacuum at 175°C for 3 hours. ^{27}Al, ^{29}Si, ^{13}C NMR spectra were collected on a Bruker AM 300 spectrometer equipped with a cross-polarization MAS accessory. Samples were packed in zirconia rotors and spun in air. The ^{27}Al (78.2 MHz) spectra were obtained at a spinning speed 8 KHz using fully hydrated samples. The spectra were referenced externally to 1M aqueous aluminum nitrate solution. The ^{29}Si (59.63 MHz) NMR spectra were obtained at a spinning speed of 4 KHz and externally referenced to tetramethylsilane. The ^{13}C (75.60 Mhz) NMR spectra were obtained at a spinning speed of 4 KHz and externally referenced to adamantane. Raman spectra were recorded on a Nicolet Raman 950 stand alone FT-Raman spectrometer using Happ-Genzel Apodization. Thermogravimetric analyses (TGA) were performed on DuPont 951 thermogravimetric analyzer. Samples were heated in air at a rate of 10°C/min. X-ray photoelectron spectroscopy (XPS) experiments were performed on a Kratos AXIS-HS. The X-ray source was monochromatized Al Ka at 1478 eV. Line positions were corrected for the offset caused by the charge neutralization circuit. Scanning electron micrographs (SEM) were recorded on a Camscan Series 2-LV scanning electron microscope. Elemental analyses were performed at Galbraith Laboratories, Inc., Knoxville, Tennessee.

5.3 Results

5.3.1 Synthesis of Beta/PE

OFMS materials were first synthesized by heating the synthesis gel for a long period of time at 140°C under rotation (1). Subsequently, the conditions necessary for crystallization were examined in an effort to optimize the synthesis of these materials. The time required to crystallize OFMS's under various conditions are listed in Table 5.1. Under conditions reported previously [1] (R-Si/Si = 0.02; entry 1, Table 1),

where TEOS is used as the silica source and the autoclave is rotated in an oven (140°C) at ~60 rpm, approximately 19 days are required to obtain highly crystalline Beta/PE. By increasing the temperature, the time required can be decreased significantly. However, at temperatures of 170°C and higher, MFI begins to form in competition with *BEA. Addition of a small amount of Beta/PE seeds to the autoclave decreases the time required to obtain crystalline product. Inclusion of aluminum or boron to the gel results in the formation of the alumino and borosilicate forms of Beta/PE. Beta/PE can be crystallized using silica sources other than TEOS. When Cab-O-Sil M5 and Ludox HS-30 are used as silica sources Beta/PE was obtained after approximately 5 weeks of heating at 140°C. In general, when the autoclave is placed in the oven and heated statically, the time required for crystallization is significantly increased.

A series of samples were synthesized with increasing organosilicon content. These samples all contained a constant total amount of silicon and were prepared from a gel composition of: X TEOS / 0.55 TEAF / 7.25 H2O / (1-X) PE . The gels were formulated as described in the Experimental Section. These samples are denoted Beta/PE-(1-X). For example, the sample synthesized with a ratio of 0.9 TEOS / 0.1 PE is denoted by Beta/PE-0.1.

In addition to the samples described above and in Table 51, three large batches of Beta/PE were synthesized for more detailed characterization. These samples were synthesized using TEOS as the silica source at 140°C with rotation. Beta/PE-NS was synthesized without the addition of seed, Beta/PE-S was made using a seeded synthesis and Beta-S was synthesized from a seeded gel without PE.

Two samples were prepared using synthesis route 2. These samples were made from PE-functionalized silica-MCM-41 (Beta-2/PE) as the silica source. This synthetic approach is related to the vapor-phase transport method, first reported by Xu and coworkers [6] and subsequently investigated by others [5, 7, 8]. In the vapor-phase transport method, the amorphous gel phase, which is separated from the liquid phase,

is crystallized by contact with a vapor phase created upon heating. In this work, the dried, extracted MCM-41 is physically mixed with a aqueous TEAF solution and added together to a Teflon-lined autoclave. In both cases, an amorphous gel is transformed into a crystalline molecular sieve. It is observed here that use of a porous, amorphous solid such as MCM-41 is beneficial. If MCM-41 that has lost order during extraction, i.e. there are no low 2Θ XRD peaks, is used as a silica source, an increased heating time is required to synthesize *BEA. Additionally, in some cases, an amorphous phase impurity remains with the product *BEA when a collapsed MCM-41 sample is used as the silicate source.

5.3.2 Characterization

5.3.2.1 X-ray diffraction

All samples were characterized by XRD. Unless otherwise noted, all samples gave similar XRD patterns. Figure 5.2 illustrates the XRD patterns for as-synthesized Beta/PE-S (a), as-synthesized Beta-S (b), Beta/PE-S that has been extracted by Method 2 (c), and Beta-S that has been extracted by Method 2 (d). The XRD patterns of the as-synthesized materials are identical for the samples synthesized in the presence and the absence of PE. After extraction, the patterns for both materials are slightly altered in the $2\Theta = 12\text{-}18$ region, compared to the as-synthesized case. The changes in the XRD patterns for the extracted materials are consistent with those of the calcined materials (not shown), indicating that the changes in the above noted 2Θ positions likely indicate the presence of porosity in the extracted samples.

The XRD patterns of the samples synthesized with a variable amount of PE are shown in Figure 5.3. As the amount of PE in the gel is increased, a broad intensity begins to appear in the XRD pattern at approximately $2\Theta = 5$. For the samples

Beta/PE-0.02, Beta/PE-0.05, and Beta/PE-0.075, there are no visible peaks in this region of the XRD patterns as illustrated in Figure 5.3.

5.3.2.2 Scanning electron microscopy

SEM showed that there are variations in crystal size depending on the synthetic procedure. Pure-silica samples synthesized with rotation at 140°C such as Beta/PE-1, Beta/PE-NS, Beta/PE-S, and Beta-S have a distribution of crystal sizes, with crystals ranging from submicron to approximately 4 microns in size. Figure 5.4 illustrates SEM images for Beta/PE-NS, Beta/PE-S, and Beta-S. It is evident that samples synthesized with or without PE, in the presence or in the absence of seeds, have the same crystal morphology and size distribution. The same gel, when heated statically in an oven, produces crystals up to an order-of-magnitude larger [2]. No amorphous phases are evident in these images.

Introduction of aluminum into the synthesis gel results in a product with smaller crystals and a more uniform crystal size distribution. This result is similar to those of Camblor and coworkers [9] in a related system (BEA; TEAOH HF). The addition of boron produces a similar but less pronounced effect. Higher temperatures give slightly larger crystals. Use of Cab-O-Sil M5 as a silica source results in large crystals (5-20 mm) in polycrystalline aggregates up to several hundred microns in size (Beta/PE-15) as shown in Figure 5.4e. Additionally, a small number of rod-like crystals (likely MFI) are a notable phase impurity. When seeds are used in the same synthesis (Beta/PE-16), well-defined, non-aggregated single crystals of Beta are obtained (3-6 mm) as shown in Figure 5.4f. There is no evidence for any phase impurities. When Ludox HS-30 is used as the silica source (Beta/PE-17), amorphous and MFI phase impurities in addition to large *BEA crystals are notable. Addition of seeds to a Ludox HS-30 derived gel (Beta/PE-18) results in a single *BEA phase with small crystals (submicron-2 mm). It is noteworthy that Beta/PE-15 - Beta/PE-18 all had XRD

patterns indicative of highly crystalline *BEA with no evidence of amorphous or crystalline phase impurities. However, SEM clearly shows that these samples are different. Beta-2/PE samples generally consist of slightly larger crystals, as shown in Figure 5.4d.

It was noted in the previous section that samples containing a large amount of PE (PE $\geq$ 0.1), had a broad XRD intensity (at $2\Theta \sim 5$) that increased with increasing PE content. SEM images of these samples indicate that there is an amorphous phase impurity that begins to be apparent in samples with a PE content of approximately 0.1 or greater. Figure 5.5a shows the SEM image of Beta/PE-0.05. Here, it is evident that the sample is highly crystalline, with no visible evidence of other phases. In contrast, Figure 5.5b depicts an SEM image of Beta/PE-0.20. For this case, the arrows highlight large agglomerations that appear to be amorphous. These are present in addition to the smaller crystals that can be seen in other sections of the image. Figure 5.5c illustrates the second phase at higher magnification. It is noteworthy that the approximate abundance of this impurity as estimated visually by SEM scales with increasing PE content and increasing intensity in the XRD at $2\Theta \sim 5$. Hence, this intensity in the XRD is assigned to the presence of a phase that appears to be amorphous by SEM. It appears that the inclusion of too large a fraction of an organosilane may cause phase separation in the gel and the formation of this extra phase.

5.3.2.3 Thermogravimetric analysis

TGA is a useful tool for characterizing the degree of extraction of the OFMS materials and additionally, the approximate weight percentage of organic functional group in the extracted material. In the TGA pattern of as-synthesized Beta-S (shown in Figure 5.6a), there is a large weight loss in the range of 170-380°C ($\sim$18% wt.) that is

attributable to the loss of the organic SDA (TEAF). There is no significant weight loss at temperatures higher than approximately 400°C. In contrast, Figure 5.6b illustrates the TGA results for Beta/PE-NS. For this sample, there is an additional (~1-2% wt.) mass loss at higher temperatures (380-580°C) that is attributable to the combustion of the PE groups.

After extracting Beta/PE materials using methods 1, 2, and 3 it is apparent that methods 2 and 3 are far superior to method 1. When extracting with aqueous pyridine as in method 1, the efficiency for removing TEAF after one extraction is significantly less than when using method 2 (pyridine and 1N HCl) or method 3 (acetic acid in water) [2]. Approximately 4-5 extraction cycles are required to remove most of the TEAF (>99% removal). Multiple extractions with this basic solvent at high temperatures appear to cause the destruction of the PE groups. At the end of the extraction cycle, nearly all of the PE groups have been removed from the sample, either by hydrolysis of the Si-O-Si bonds at the silicon atom that links the PE to the framework or by cleavage of the Si-C bond. In contrast, methods 2 and 3 remove nearly all the TEAF after only 1 extraction cycle. A second cycle is performed to insure that nearly all the TEAF is expelled from the sample. Figure 5.6d shows the TGA results for Beta/PE-NS that was extracted 2x by method 2.   The loss labeled region 1 is due to adsorbed acetone, pyridine and water, as it can be removed by heating under vacuum. The loss labeled region 2 may be due to strongly bound residual TEA^+ at a defect site. This mass appears to be present in all extracted samples and can not be removed by multiple extractions or ion exchange. This mass is typically quite small, roughly 0.05-0.25% by mass. The loss labeled region 3 is due to combustion of PE. Using methods 2 and 3, there is a new, high temperature labeled region 4 in Figure 56d. This loss is also present in Beta-S extracted by method 2, as shown in Figure 56c. Hence, this loss is not due to PE and it is not attributable to carbonaceous species (carbon mass balance by elemental analysis). Rather, it is likely due to condensation of

silanols. Apparently, extraction methods that contain an acidic component (methods 2 and 3) cause the formation of this high temperature weight loss. This loss is not as prominent when method 1 is used to extract the materials. It is possible that this effect is caused by partial structural degradation due to liberated HF species during extraction. Despite the presence of this new high temperature weight loss, there is no loss in sample crystallinity as measured by XRD. Upon sulfonation, a new weight loss is evident by TGA in the range of 300-415°C (not shown), attributable to the addition of SO_3 to the phenyl rings of PE.

Samples synthesized using PE-functionalized MCM-41 as the silica source, Beta-2/PE, cannot be extracted to the same extent that samples synthesized by the standard route can. TGA analyses of samples synthesized in this manner indicate that there is an increased amount of occluded organic SDA (0.5-1% wt.) relative to samples synthesized in the standard manner, that can not be removed by extraction

5.3.2.4 Solid-state ^{29}Si and ^{27}Al NMR spectroscopy

Figure 5.7 illustrates the ^{29}Si CPMAS NMR spectra of as-synthesized Beta-S (a) and Beta/PE-S (b). It is noteworthy that both spectra are identical except in the -55 to -75 ppm region. Here, the PE-containing sample shows an additional resonance at -69.4 ppm, attributable to the Si-C bond (R-Si(OSi)$_3$) [10, 11]. Resonances at -109.4, -111.4, -114.1 and -117.2 ppm are assigned to Si(OSi)$_4$. The intensity at -101.3 is assigned to Q^3 silicon. The resonance at -105.4 could be assigned to either Q^3 or Q^4 silicon. Figure 5.8 shows the ^{29}Si MAS NMR spectra of extracted beta samples. Beta-S extracted by method 2 (Figure 8a), Beta/PE-S extracted by method 2 (Figure 5.8b) and Beta/PE-S (Figure 5.8c) extracted by method 3 at all temperatures (80°C shown) all lack a resonance in the range of -55 to -75 ppm. For the case of the Beta/PE samples, this is due to the low abundance of the R-Si(OSi)$_3$ species, which makes this moiety undetectable by Bloch decay experiments with the instrumentation used. It is

noteworthy that the Beta/PE-S, when extracted by method 3 (Figure 5.8c), has virtually no Q^3 silicon, with extremely weak resonances in the range of -100 to -106 ppm. In contrast, Beta/PE extracted by method 2 has strong Q^3 silicon resonances around 103.7 ppm. This indicates that extraction with aqueous acetic acid produces a material that is closer to the defect-free ideal structure than extraction with pyridine/HCl mixtures. The spectra of Beta-S and Beta/PE-S extracted by method 2 (Figure 5.8a and 5.8b) appear essentially identical.

The ^{29}Si CPMAS NMR spectra of Beta-S (Figure 5.9a) and Beta/PE-S (Figure 5.9c) extracted by method 2 are not the same. Beta/PE-S extracted by method 2 has an additional peak at -68 ppm assigned to the Si-C bond (R-Si(OSi)$_3$). The ^{29}Si CPMAS NMR spectrum of Beta/PE-S extracted by method 1 (Figure 5.9b) appears very similar to the spectrum of Beta-S extracted by method 2 (Figure 5.9a). The Beta/PE-S extracted by method 1 shows virtually no intensity in the -65 to -75 ppm region indicating that there is very little PE remaining. These data are in agreement with the TGA results that indicated that extraction using method 1 produces a product with little organic weight loss in the TGA pattern. Figure 5.9c illustrates the ^{29}Si CPMAS NMR spectrum of Beta/PE-S extracted by method 3 (80°C). Here it is evident that the Si-C bond is intact (-68 ppm). Additionally, the Q^3 defect site that must be present for the incorporation of PE into the framework is indeed notable as a broad intensity at -103 ppm.

^{27}Al MAS NMR spectroscopy of Beta/PE-3 gives a single resonance at approximately 52.5 ppm that is assignable to tetrahedral aluminum (not shown), in agreement with Camblor et al.'s non-PE containing samples [9].

5.3.2.5 Solid-state ^{13}C NMR spectroscopy

Figure 5.10 illustrates the ^{13}C CPMAS NMR spectroscopy spectrum for

extracted Beta/PE-0.05. It is clear that the integrity of the PE group in this extracted

material is unaltered by the extraction method. There are four strong resonances that

are assigned to the PE group (142.8, 128.1 ppm: aromatic carbons; 28.8, 13.1 ppm :

methylene carbons). In addition, there are 4 resonances that have been assigned to

spinning side-bands associated with the aromatic carbons. A small intensity at 24 ppm

is likely due to a small amount of residual TEAF and a second order spinning side

band. By changing the spinning speed the locations of the spinning side-bands have

been altered. This greatly decreases the intensity of the resonance at 24 ppm but does

not result in the complete disappearance of this peak.

5.3.2.6 FT-Raman spectroscopy

Raman spectroscopy allows for the elucidation of the nature of the organic

species in the OFMS materials. Figure 5.11 illustrates the Raman spectra for TEAF

(a), the pure organosilane liquid phenethyltrimethoxysilane (b), and p-toluenesulfonic

acid monohydrate (c). The Raman spectra of as-synthesized Beta-S (a) and Beta/PE-S

(b) are shown in Figure 5.12. By comparison of Figure 5.12 with Figure 5.11a, it is

apparent that the majority of the bands in the Beta-S spectrum are attributable to TEAF

in the pores of the molecular sieve. The spectrum of Beta/PE-S (Figure 5.12b) has

numerous additional bands that can be assigned to PE (compare to Figure 5.11b).

Several of the important bands are numbered on the figure and are described below

(assignments referenced to [12]).

1) aromatic υ C-H, 3060 cm^{-1} 4) aromatic δ C-H, 1030 cm^{-1}

2) aromatic υ C=C, 1600, 1580 cm^{-1} 5) aromatic ring in-plane bend, 625 cm^{-1}

3) Si-CH$_2$-R, 1205 cm^{-1}

As mentioned above, solvent extraction techniques can remove virtually all of the TEAF from the OFMS materials. Figure 5.13 illustrates the spectra of Beta-S extracted by method 2 (a), Beta/PE-S extracted by method 2 (b) and Beta/PE-S extracted by method 2 and sulfonated (c). It is apparent that most, but not all of the TEAF species have been removed from Beta-S by extraction (Figure 5.13a) in agreement with TGA results. A similar result is seen in Figure 5.13b for the extracted Beta/PE-S. In this spectrum, bands attributable to PE are identifiable, as listed below.

1) aromatic υ C=C, 1600, 1580 cm^{-1} 5) aromatic ring in-plane bend, 625 cm^{-1}
2) Si-CH$_2$-R, 1205 cm^{-1} 6) aromatic υ skeletal, 636 cm^{-1}
3) aromatic δ C-H, 1030 cm^{-1} 7) aromatic C=C sym, 1000 cm^{-1}
4) aromatic υ C=C sym, 1000 cm^{-1} 8) hyd. sulfonic acid SO$_3$ stretch, 1133 cm^{-1}

After sulfonation, the two bands near 1600 and 1580 cm^{-1} coalesce and become one, broader band. Additionally, a new peak, indicative of a para-substituted phenyl rings, appears at 636 cm^{-1}. The hydrated sulfonic acid stretch at 1133 cm^{-1} is further evidence of sulfonation of the phenyl rings. These changes upon sulfonation of the sample are in agreement with the differences observed between the Raman spectra of pure PE (Figure 5.10b) and TsOH (Figure 5.10c).

5.2.2.7 Porosity measurements

The porosities of the various extracted samples were evaluated by physisorption techniques. Table 5.2 summarizes the results of nitrogen adsorption, cyclohexane adsorption and water adsorption experiments performed on Beta-S, Beta/PE-S and Beta/PE-NS samples prepared via a variety of methods. In every case, the nitrogen adsorption capacity and cyclohexane adsorption capacity are in good agreement. This indicates that both a small (nitrogen) and relatively large (cyclohexane) molecule can fill the micropores equally well. Also, noteworthy is that the adsorption capacities of the

all the calcined samples are nearly the same. However, the total capacity is lower than would be expected from the ideal *BEA crystal structure (0.26 cc/g) [13]. The results are in agreement with those described by Camblor et al. for pure-silica Beta samples synthesized using a similar technique (TEAOH + HF as SDA). Pure-silica samples reported had nitrogen capacities of roughly 0.225-0.230 cc/g at P/Po=0.3 [9]. For the sample synthesized without any PE, Beta-S, the extraction by method 2 or method 3 at 80°C results in a material with the same nitrogen/cyclohexane capacity as the calcined sample. This indicates that the small amount of residual TEAF (0.05-0.25% wt.) that sometimes remains in the sample after extraction does not have a large impact on the available pore space. If Beta-S is extracted by method 3 at an elevated temperature (120°C) in an autoclave, the porosity of the sample decreases. This is an indication of a partial loss in crystallinity, although no loss is evident by powder X-ray diffraction.

For the OFMS Beta/PE-NS, extraction at elevated temperatures using method 3 also results in a significantly reduced pore volume compared to the calcined sample, as noted by the data in Table 5.2. However, extraction by method 2 or 3 at 80°C gives materials with a pore capacity that is only slightly reduced. The loss in porosity for these two materials relative to the calcined sample may be attributed to PE occupying space within the micropores. If the density of PE is approximated by the density of liquid ethylbenzene at room temperature, the pore space attributable to PE within the micropores can be estimated (PE content is estimated by elemental analysis and/or TGA). Using this method, a value of roughly 0.017 cc/g is calculated, in good agreement with the difference in porosity between the extracted (~0.225-0.230 cc/g) and calcined (0.245-0.250 cc/g) samples.

The large porosity loss in Beta/PE-NS treated at high temperature with method 3 is likely due to some loss of crystallinity. Figure 5.14 shows the nitrogen adsorption isotherms for Beta/PE-NS extracted by method 3 at 120°C (Figure 5.14a), at 80°C (Figure 5.14b), and for calcined Beta/PE-NS (Figure 5.14c).

Water adsorption data indicate that extraction by method 3 at high temperatures results in a highly hydrophobic sample with a similar water uptake to that of the calcined sample. For samples with good porosity (extraction by method 2 or 3 at 80°C), it is apparent that acetic acid extraction (method 3) results in a more hydrophobic material than pyridine/HCl extraction (method 2). Data from Beta/PE-S are similar to those for Beta/PE-NS. These results agree well with the observation by ^{29}Si MAS NMR that the acetic acid extracted materials have less Q^3 silicon.

Pure-silica beta synthesized from MCM-41 as the silica source (Beta-2) has a significant amount of residual TEAF that can not be removed by extraction relative to beta synthesized using the standard approach, as noted above. Extracted Beta-2 (method 3 at 80°C) has a reduced nitrogen capacity (Table 5.2) relative to the calcined sample. The data indicates that the relatively large amount of residual TEAF decreases the available pore space in samples synthesized by this method. This is not the case for *BEA synthesized in the standard fashion, where the calcined and extracted samples have the same nitrogen capacity.

5.3.2.8 Elemental analysis

Bulk elemental analysis was performed on several samples to determine the cesium, sulfur, carbon and silicon content. Table 5.3 lists the data for both the bulk and surface elemental analysis carried out on several samples. The results are consistent with the addition of a single sulfur atom for every PE moiety, assuming all the carbon in the sample is attributable to PE (traces of TEAF are neglected). Additionally, the data reveal that there is roughly 1 cesium per sulfur atom, indicating near quantitative exchange of sulfonic acid sites with cesium.

Comparison of surface and bulk elemental analyses for the samples indicates that no significant enrichment of cesium exists at the surface or in the bulk. The surface Cs/Si ratio is consistently slightly higher (1.25-3 times) than the bulk Cs/Si ratio, as

shown in the data listed in Table 5.3. However, the external surface Cs/Si ratio for the non-sulfonated Beta/PE sample is also higher (6 times) than the bulk Cs/Si ratio, indicating a probable general over-estimate of surface Cs/Si or underestimate of bulk Cs/Si by the techniques used here. Additional control samples, such as CIT-6 samples exchanged with Cs^+ and subjected to the same analysis, also indicated a similar trend (Cs/Si surface = 0.001; Cs/Si bulk = 0.0004). Titrations of the CsCl solutions with NaOH solutions were carried out to determine the solution H^+ content after ion exchange of the solids. Titration results were in good agreement with elemental analysis. Thus, a uniform distribution of Cs, and hence S and PE, are obtained.

5.3.2.9 Other organic functional groups

Previously, we reported the synthesis of the molecular sieve *BEA in the presence of various organosilanes [2]. However, little experimental evidence of organic-group incorporation was provided. Here we disclose evidence for the incorporation of various organic groups in these OFMS materials and discuss possible uses for these groups.

Table 5.4 summarizes the results of OFMS synthesis with several organosilanes using the standard synthetic approach. Olefins such as a cyclohexenylethyl group and a butenyl group can be incorporated into the OFMS. The functional group can be clearly identified in the materials before and after extraction by Raman spectroscopy. These olefins are useful organic groups because they can easily be transformed into a variety of other functional groups using simple organic chemistry techniques. 3-mercapto-propyltrimethoxysilane was also incorporated into the OFMS. In this case the characteristic thiol Raman band is not evident. However, elemental analysis indicates that carbon and sulfur are present in the sample at the appropriate levels. This result might imply formation of the disulfide in-situ during synthesis.

5.4 Discussion

In the standard synthesis, a white, amorphous gel is formed several hours after mixing the silane solution with the aqueous TEAF solution and is then transferred to an autoclave for heating. The fact that a solid phase is obtained as the molecular sieve precursor indicated that it may be possible to synthesize these materials from other amorphous silica sources where the TEAF can make intimate contact with the internal surface area of the silica. Indeed, we show here that a synthetic strategy employing extracted PE-functionalized MCM-41 is also a potential route to OFMS materials. A more general discussion of this approach to preparing molecular sieves is described elsewhere [5].

The properties of the OFMS's can be tailored by choice of synthetic (crystal size) and extraction method (hydrophobicity, pore volume). As illustrated above, materials with a hydrophobicity similar to calcined samples can be synthesized by extraction with aqueous acetic acid at high temperatures (120-135°C). The high hydrophobicity of the calcined samples is due to the defect-free nature of the material (all Q^4 silicon). The Q^3 silicon centers present in the as-synthesized material are annealed upon calcination. The high hydrophobicity of the materials extracted at high temperatures is likely due to the healing of defect silanols during extraction with aqueous acetic acid. This hypothesis is supported by the ^{29}Si MAS NMR evidence that shows essentially no Q^3 silicon in materials extracted by this method. However, there is the drawback that there is a significant loss in crystallinity when using this approach. By lowering the temperature in the extraction step to 80°C, a material can be produced with good porosity and intermediate hydrophobicity relative to (i) the calcined materials and (ii) the hydrophilic pyridine/1N HCl extracted material.

Results from the SDA extraction techniques have implications for molecular sieves other than OFMS's. In the case of a pure-silica, beta zeolite synthesized using TEAF as a SDA and without any organosilane, we show here that an extremely

hydrophobic material can be made without combustion of the SDA. Recovery of the TEAF from the relatively simple three component mixture (acetic acid, water, TEAF) and reuse of the TEAF could significantly reduce the cost of producing hydrophobic large pore molecular sieves for adsorptive and other applications.

XRD patterns are similar for all materials, regardless of extraction method. In contrast, the nitrogen and cyclohexane adsorption data support some loss in crystallinity (up to 1/3) associated with extraction with acetic acid at high temperatures. Thus, as expected, the adsorption methods are more sensitive than XRD when assessing small changes in crystallinity.

Similarities between bulk elemental analysis and surface analysis (XPS) support a uniform distribution of organic functional groups throughout the materials. Thus, there appears to be no zoning of the phenethyl groups. This evidence, coupled with the adsorption results showing a loss of micropore volume attributable to the PE groups is indicative of an even distribution of the organic groups within the micropores at low PE loadings.

As the amount of the PE in the synthesis is increased, there is evidence for the formation of an additional, amorphous phase. In this case (loadings of PE -> 0.075), the difference in porosity between the extracted and calcined samples can not be attributed to PE solely in the micropores of *BEA. For example, for Beta/PE-0.2, the calcined sample has a nitrogen capacity of 0.228 cc/g and the extracted sample (method 3, 80°C) has a capacity of 0.148 cc/g. Based on the PE content as determined by TGA, the PE should occupy 0.14 cc/g. This volume is not consistent with PE only in the micropores, and hence a significant amount of the PE is likely contained in the amorphous phase.

Clearly, OFMS's have significant potential for use as shape-selective catalysts, particularly in low temperature liquid phase conversions [1]. Sulfonation of the as-synthesized material results in the generation of no sulfonic acids, indicating that

essentially all PE groups are located within the SDA-occluded pores of the as-synthesized material. Nitrogen adsorption and bulk/surface elemental analysis data also support this view. However, catalysis with extracted, sulfonated materials can give results that are less shape-selective than one would expect from an ideal crystalline material, i.e., species that would not be expected to enter the OFMS micropores can be converted over these materials. This may be due to some loss in crystallinity or generation of mesoporosity upon extraction, although no visible difference exists between the as-synthesized, extracted, and sulfonated materials by SEM. Catalysts with nearly perfect shape-selective behavior can be generated by surface passivation of the as-made materials with highly caustic solutions [1], although this harsh treatment is not reliable. While ideal shape-selectivity can be obtained (we have shown this in reference 1), the reproducibility of the techniques used to generate this shape-selectivity require further evaluation. Methods for improving reproducibility in the shape-selectivity of OFMS catalytic materials will be reported at a later date [14].

5.5 Summary

OFMS's with the *BEA structure can be synthesized over a large temperature range (140-170°C) with numerous organic functional groups, in the presence or absence of non-silicon (Al, B) atoms. The OFMS's can also be prepared using extracted, PE-functionalized MCM-41 as the silica/PE source via a solid state transformation. The extraction techniques used to remove the TEAF from the micropores have a strong influence on the concentration of defect sites (Q^3 silicon) and hence on the hydrophobicity of the structure. Additionally, the porosity of the materials is controlled to a degree by the extraction technique. Bulk elemental and surface analysis coupled with nitrogen and cyclohexane adsorption results give evidence that the organic functional groups are distributed evenly throughout the micropores of the

material at low PE loadings. The organic PE group is intact after extraction of the SDA and this group can be easily transformed into a solid acid.

5.6 References

[1] C. W. Jones, K. Tsuji, and M. E. Davis *Nature* 393 (1998) 52.

[2] K. Tsuji, C. W. Jones, and M. E. Davis *Microporous Mesoporous Mater.* in press.

[3] S. L. Burkett, D. D. Sims, and S. Mann *Chem. Commun.* (1996) 1367

[4] M. H. Lim, C. F. Blanford, and A. Stein *J. Am. Chem. Soc.* 119 (1997) 4090.

[5] T. Takewaki, S. J. Hwang, H. Yamashita, and M. E. Davis *Microporous Mesoporous Mater.* submitted.

[6] W. Xu, J. Dong, J. Li, and F. Wu *J. Chem. Soc. Chem. Commun.* (1992) 755.

[7] M. H. Kim, H. X. Li, and M. E. Davis *Microporous Mater.* 1 (1993) 191.

[8] M. Matsukata, N. Nishiyama, and K. Ueyama *Microporous Mater.* 1 (1993) 219.

[9] M. A. Camblor, A. Corma, and S. Valencia *J. Mater. Chem.* 8 (1998) 2137

[10] H. X. Li, M. A. Camblor, and M. E. Davis *Microporous Mater.* 3 (1994) 117-121.

[11] E. J. R. Sudholter, R. Huis, G. R. Hays, and N. C. M. Alma *J. Coll. I. Sci.* 103 (1985) 554-560.

[12] N. B Colthup, L. H. Daly, and S. E. Weberley *Introduction to Infrared and Raman Spectroscopy*, Academic Press, NY 1975; H. Baranska, A. Labudzinska, and J. Terpinski *Laser Raman Spectrometry, Analytical Applications*, Ellis Horwood Limited, Chichester 1987.

[13]   Y. Nakagawa, G. S. Lee, T. V. Harris, L. T. Yuen, and S. I. Zones

Microporous Mesoporous Mater. 22 (1998) 69-85; International Zeolite

Association Web Site.

[14]   C. W. Jones and M. E. Davis, manuscript in preparation.

Table 5.1 Synthetic results for Beta/PE system.

Sample	Silica Source	Non-Silicon atom **	Seed	Temperature	Time (days)
Beta/PE - 1	TEOS	None	No	140°C	19
Beta/PE - 2	TEOS	None	Yes	140°C	9
Beta/PE - 3	TEOS	Al	No	140°C	31
Beta/PE - 4	TEOS	Al	Yes	140°C	10
Beta/PE - 5	TEOS	B	No	140°C	31 (amorphous)
Beta/PE - 6	TEOS	B	Yes	140°C	10
Beta/PE - 7	TEOS	None	No	160°C	6
Beta/PE - 8	TEOS	None	Yes	160°C	4
Beta/PE - 9	TEOS	Al	Yes	160°C	6
Beta/PE - 10	TEOS	B	Yes	160°C	6
Beta/PE - 11	TEOS	None	No	170°C	4 (BEA + MFI)
Beta/PE - 12	TEOS	None	Yes	170°C	3
Beta/PE - 13	TEOS	Al	Yes	170°C	4
Beta/PE - 14	TEOS	B	Yes	170°C	4
Beta/PE - 15	Cab-O-Sil M5	None	No	140°C	38
Beta/PE - 16	Cab-O-Sil M5	None	Yes	140°C	34
Beta/PE - 17	Ludox HS-30	None	No	140°C	38
Beta/PE - 18	Ludox HS-30	None	Yes	140°C	34

* All synthesis with rotation of the autoclave and R-Si/Si=0.02

** When added, non-silicon atom/Si = 0.02

Table 5.2   Physical adsorption results *.

Sample	Nitrogen Capacity [1]	Cyclohexane Capacity [2]	Water Capacity [2]
Beta-S			
ext. method 2	0.235	0.235	ND
ext. method 3 (80°C)	0.235	0.235	ND
ext. method 3 (120°C)	0.160	0.160	ND
calcined	0.235	0.235	ND
Beta/PE-NS			
ext. method 2	0.225	0.230	0.035
ext. method 3 (80°C)	0.230	0.225	0.015
ext. method 3 (120°C)	0.160	0.160	<0.01
ext. method 3 (135°C)	0.195	0.195	<0.01
calcined	0.245	0.245	<0.01
Beta/PE-S			
ext. method 2	0.220	0.230	0.055
calcined	0.245	0.245	<0.01
Beta-2			
ext. method 3 (80°C)	0.210	ND	ND
calcined	0.230	ND	ND

1   from nitrogen adsorption isotherm at 77K
2   from McBain-Bakr balance at 296K
*   all data points at P/Po=0.2

Table 5.3   Elemental analysis results.

Sample	Surface Cs/Si [1]	Bulk Cs/Si [2]	Bulk Cs/S [2]	Bulk PE/S [2]
Beta/PE-S				
ext. method 2	0.006	0.001	ND	ND
ext. method 2 sulfonated	0.03	0.01	0.79	1.1
ext. method 3 sulfonated	0.02	0.015	0.93	0.95
Beta/PE-NS				
ext. method 3 sulfonated	0.025	0.0125	0.90	1.02

1 from XPS
2 from elemental analysis

Table 5.4   Organic functional groups in beta OFMS's.

Organosilane	Combustion in TGA	Raman Fingerprint	Potential Applications	Notes
2-(3-cyclohexenylethyl)trimethoxysilane	320 - 460°C	1653 cm-1 C=C	Olefin is versatile precursor species	--------
3-butenyltriethoxysilane	310 - 430°C	1642 cm-1 C=C	Olefin is versatile precursor species	--------
3-mercaptopropyltrimethoxysilane	250 - 430°C	None; possible disulfide formation	Oxidation to sulfonic acid	Carbon and sulfur by elemental analysis
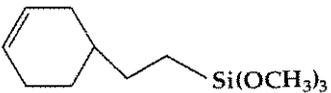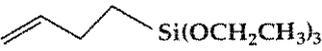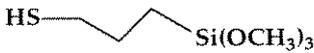
To Vacuum

B

A

Quartz
Frit

Viton O-Rings

Sample
Chamber

Oleum
Chamber
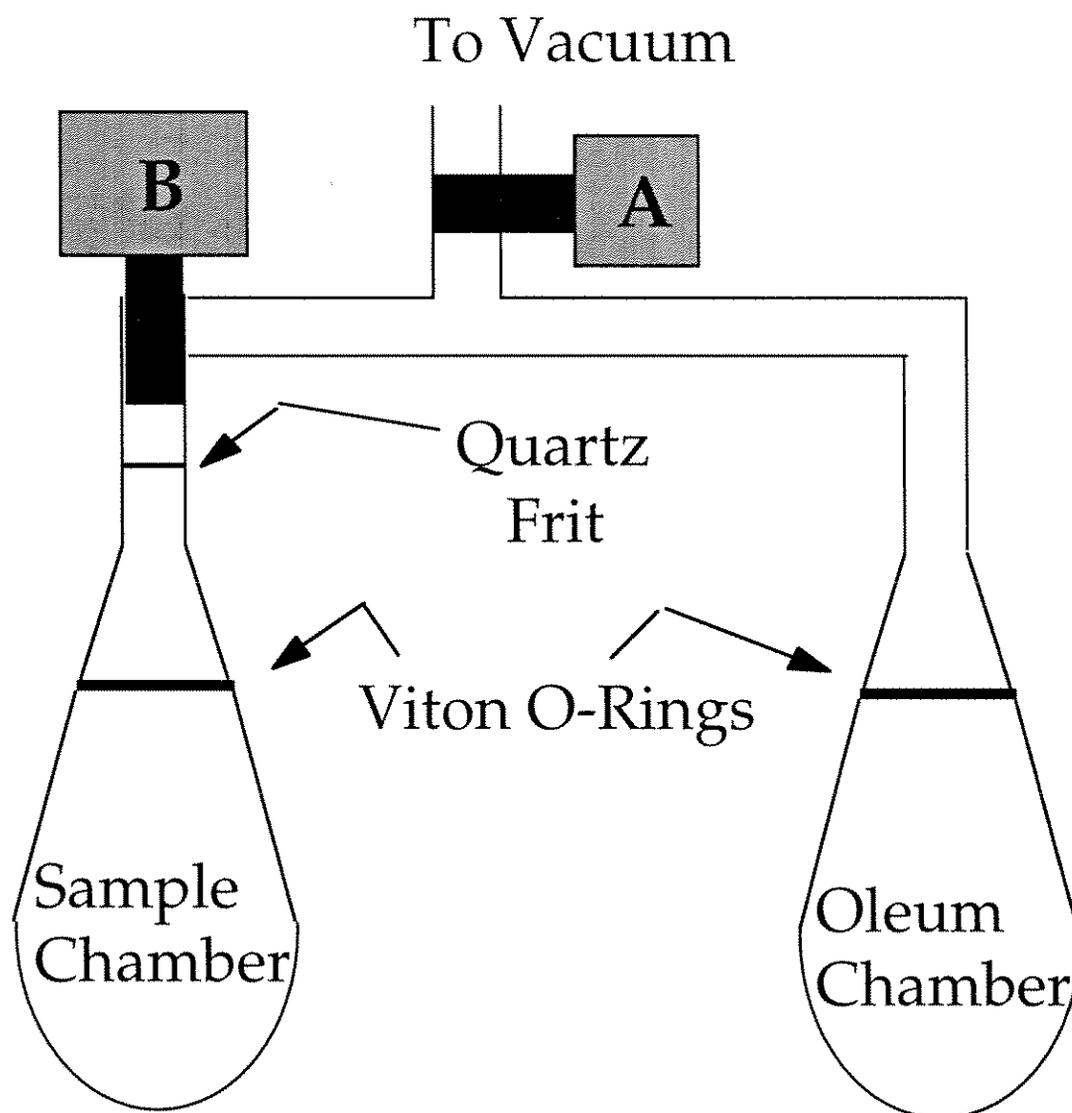
Figure 5.1 Manifold used for sulfonation of phenethyl-functionalized OFMS.
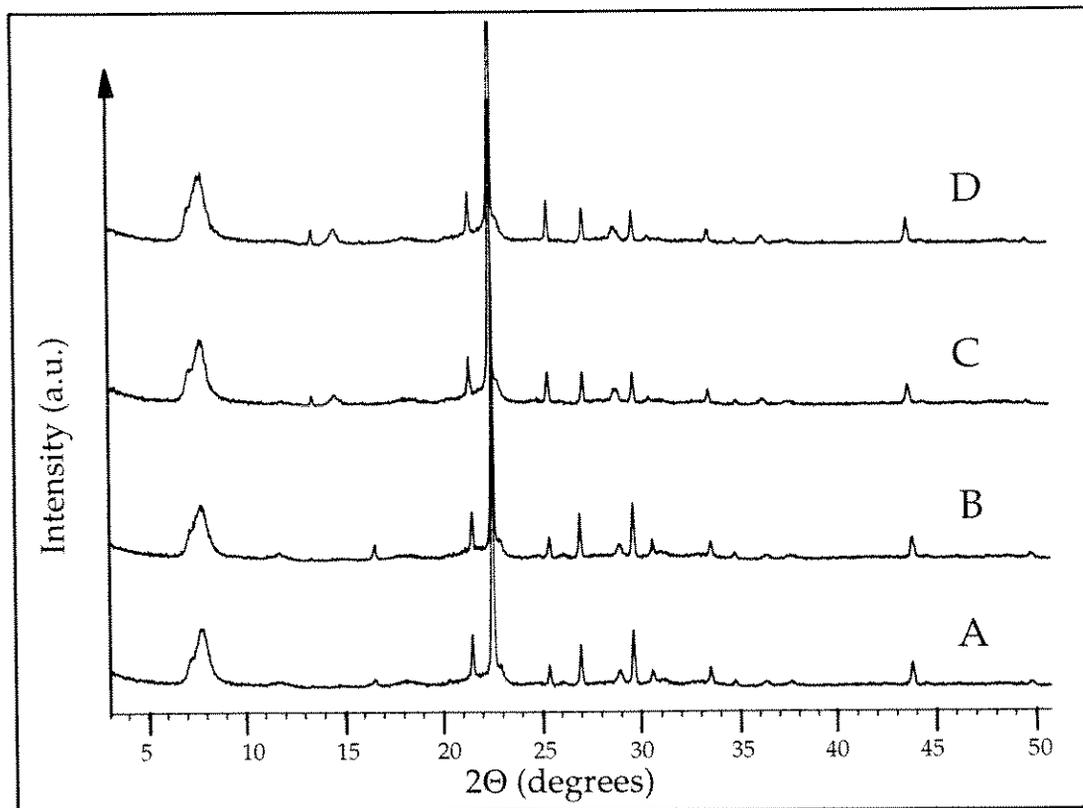
Figure 5.2 XRD patterns of molecular sieves. Beta/PE-S (a), Beta-S
(b), Beta/PE-S extracted by method 2 (c), and Beta-S
extracted by method 2 (d).
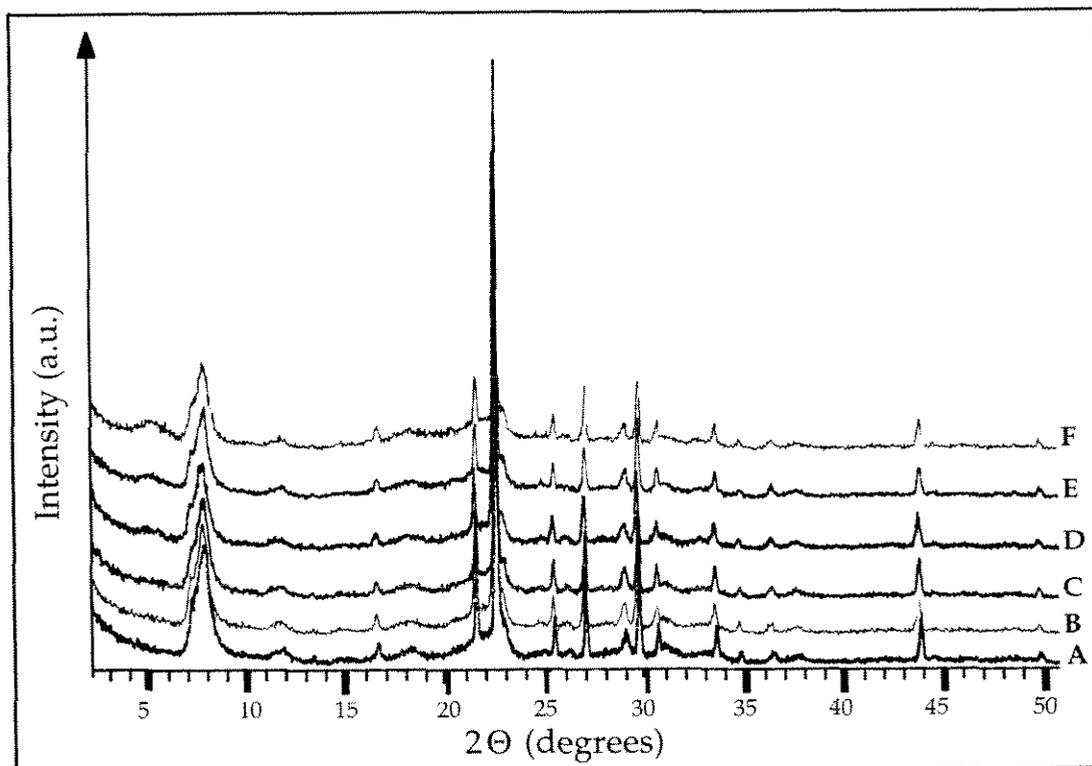
Figure 5.3 XRD patterns of as-synthesized materials. Beta/PE-0.02
(a), Beta/PE-0.05 (b), Beta/PE-0.075 (c), Beta/PE-0.1 (d),
Beta/PE-0.15 (e), and Beta/PE-0.2 (f).
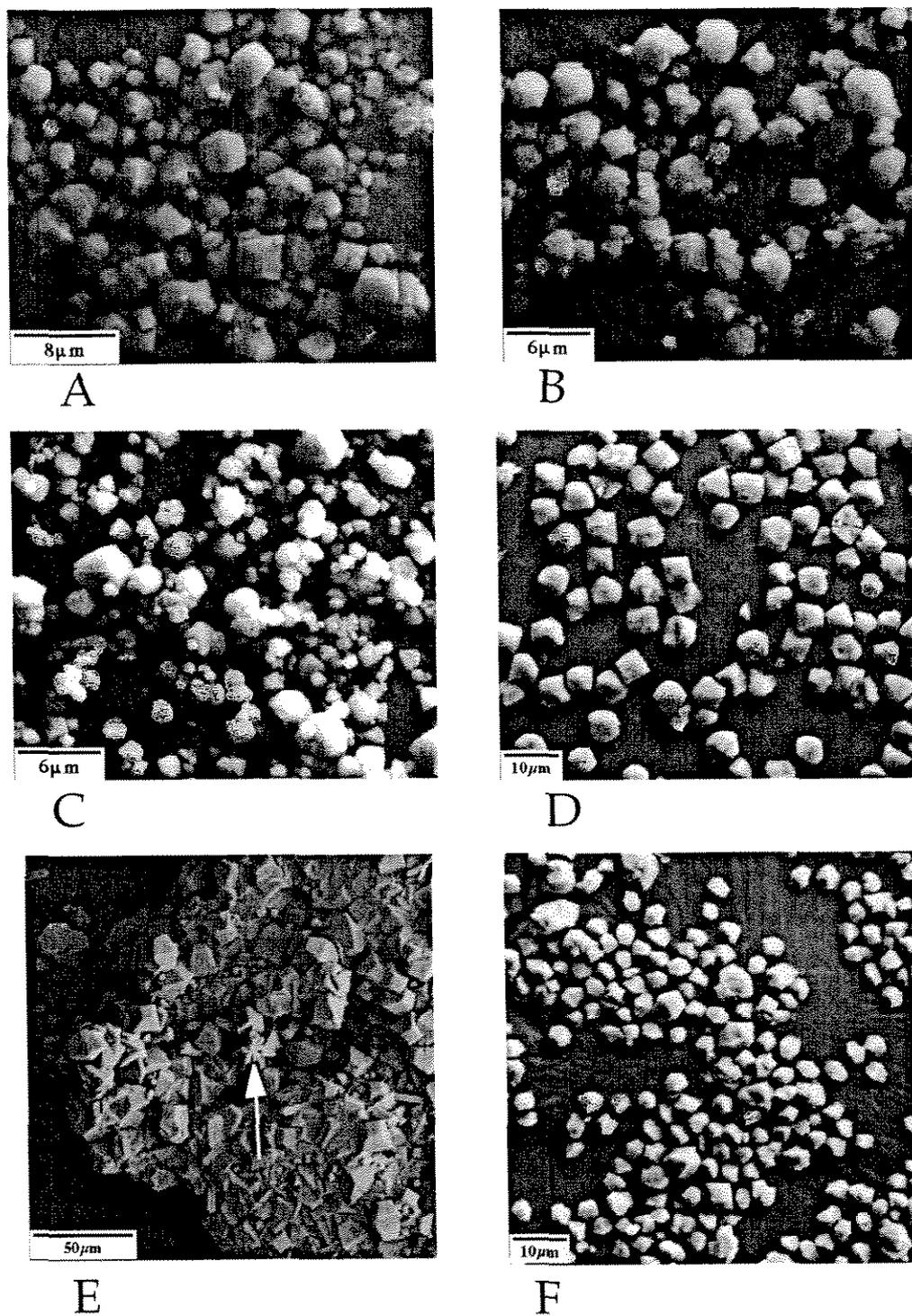
Figure 5.4 SEM images of as-synthesized OFMS's. Beta/PE-NS (a),
Beta/PE-S (b), Beta-S (c), Beta-2/PE (d), Beta/PE-15 (e),
and Beta/PE-16 (f). Arrow denotes MFI phase-impurity
in (e).

A

B

C
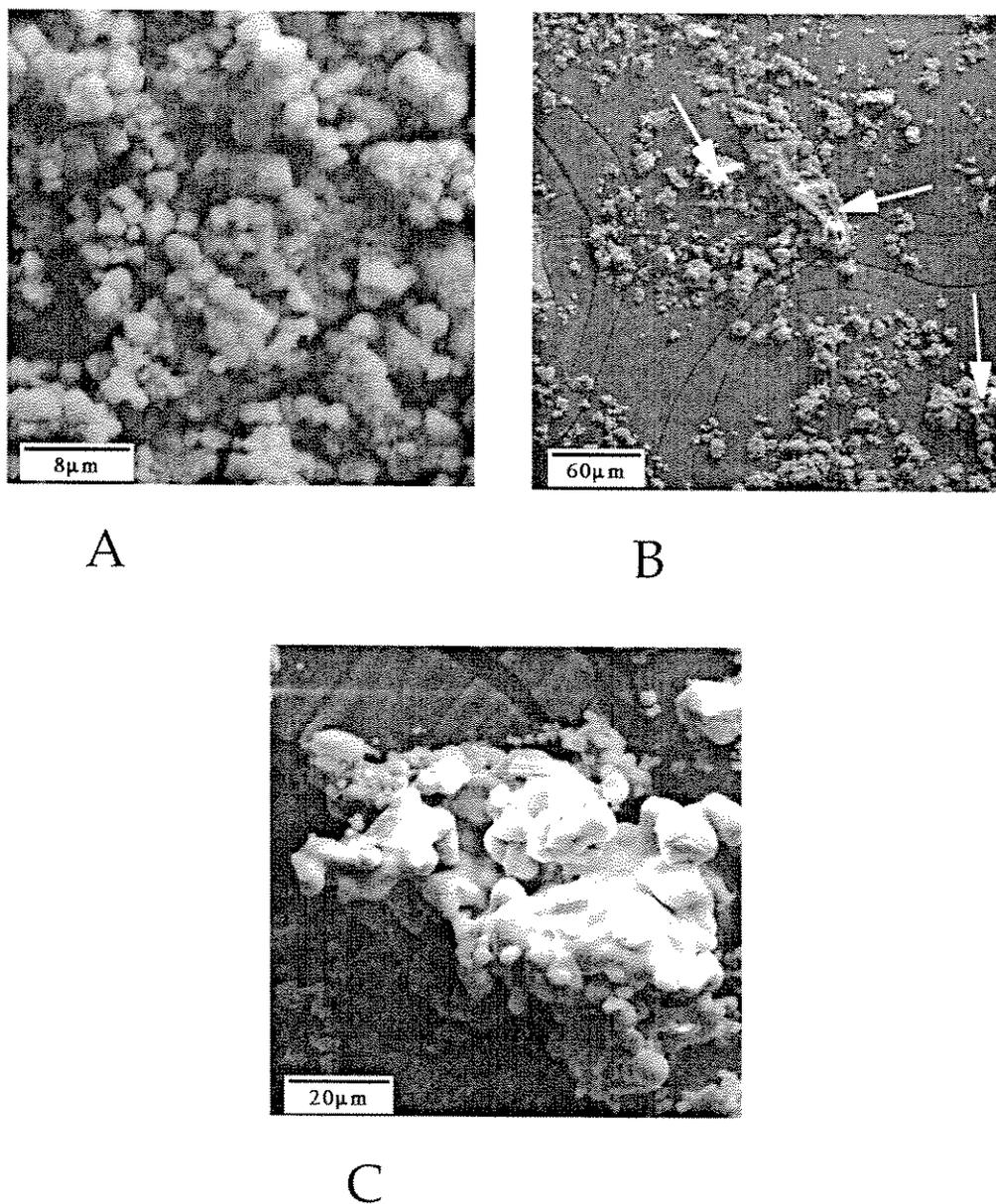
Figure 5.5   SEM images of as-synthesized molecular sieves. Beta/PE-
0.02 (a), Beta/PE-0.2 (b) and amorphous agglomeration in
Beta/PE-0.2 (c). Arrows in (b) highlight large amorphous
masses.
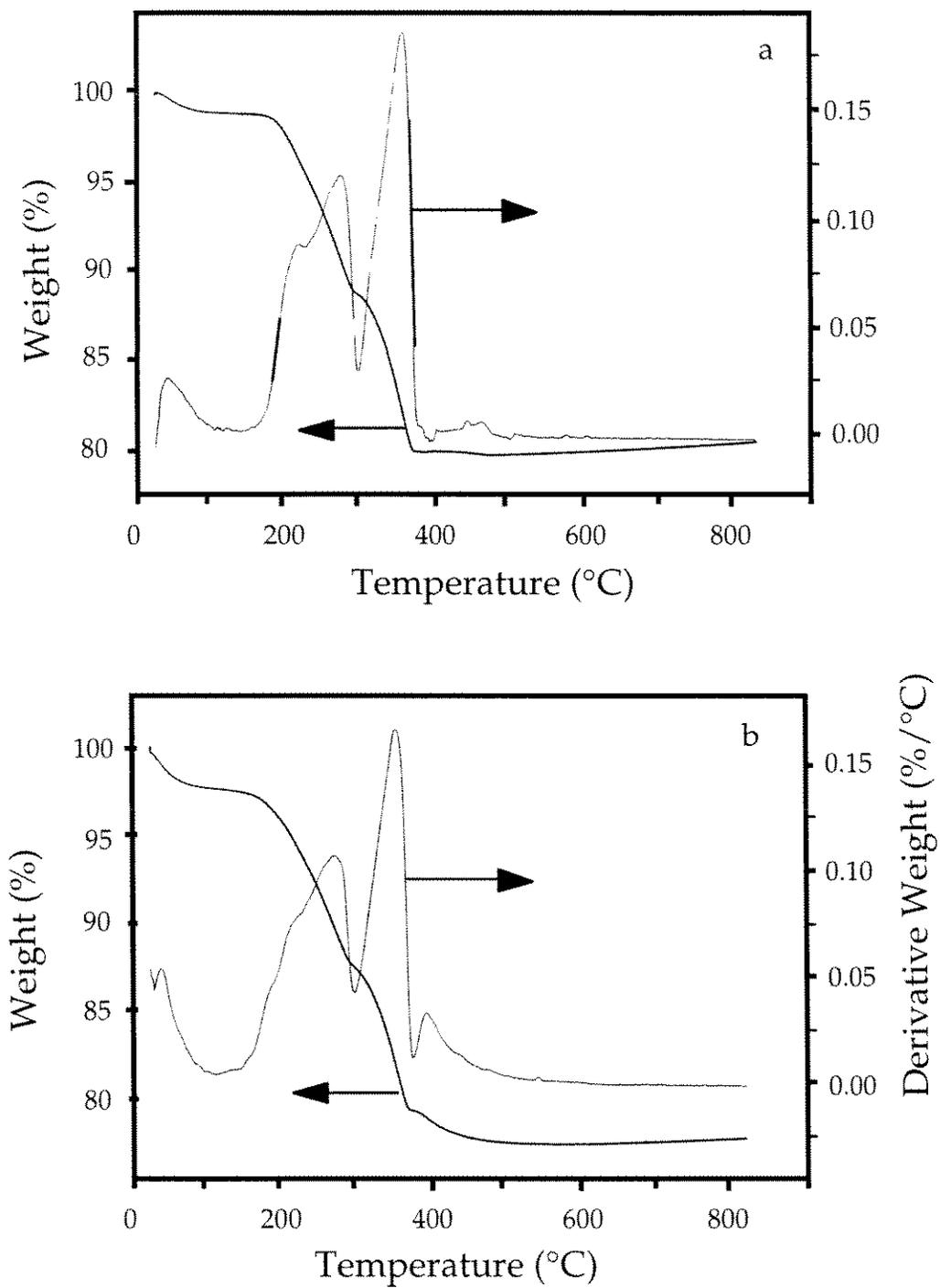
Figure 5.6 TGA results for heating molecular sieves in air. As-synthesized Beta-S (a) and as-synthesized Beta/PE-NS (b).
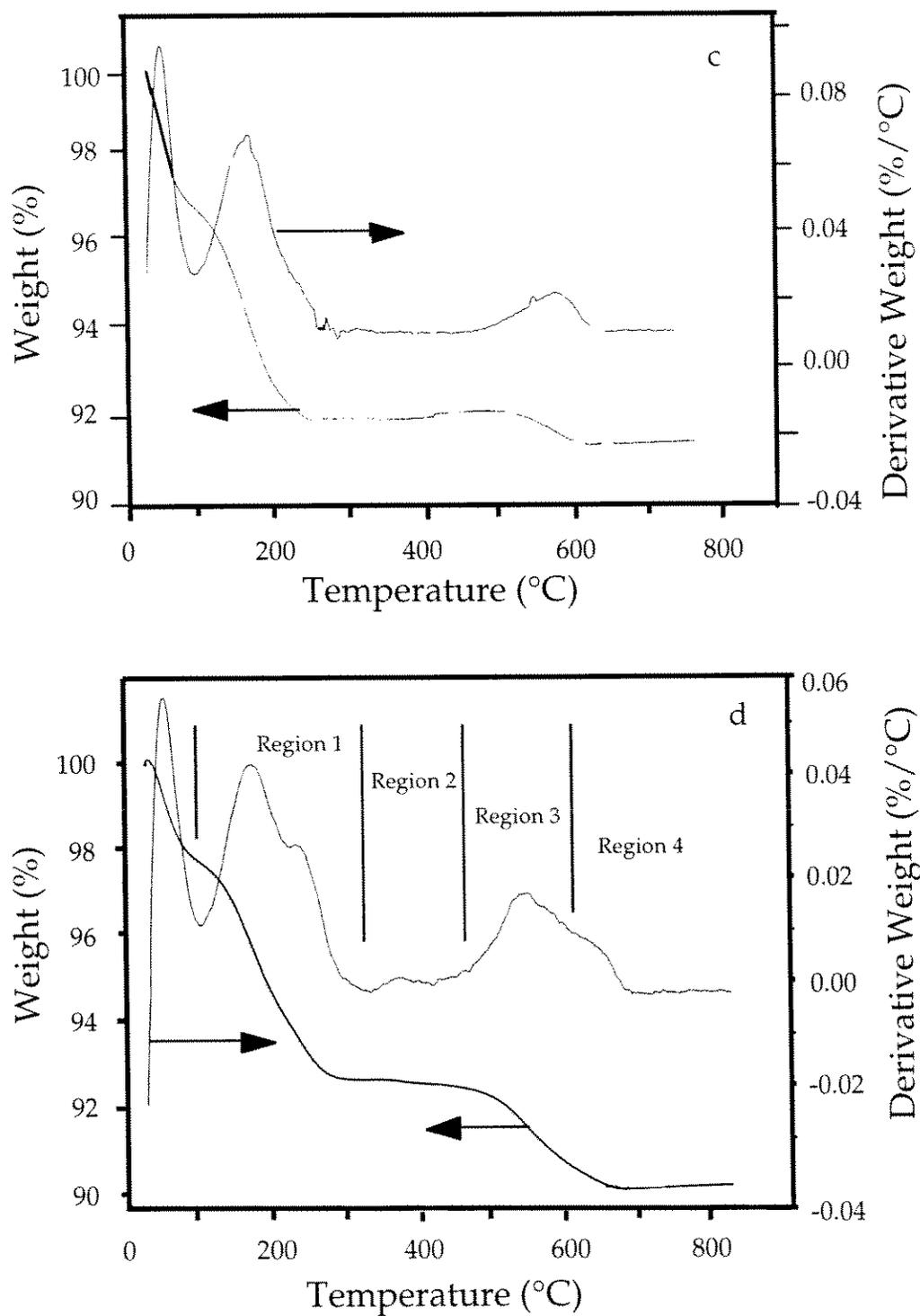
Figure 5.6 (continued)   **Beta-S extracted by method 2 (c) and**

Beta/PE-NS extracted by method 2.
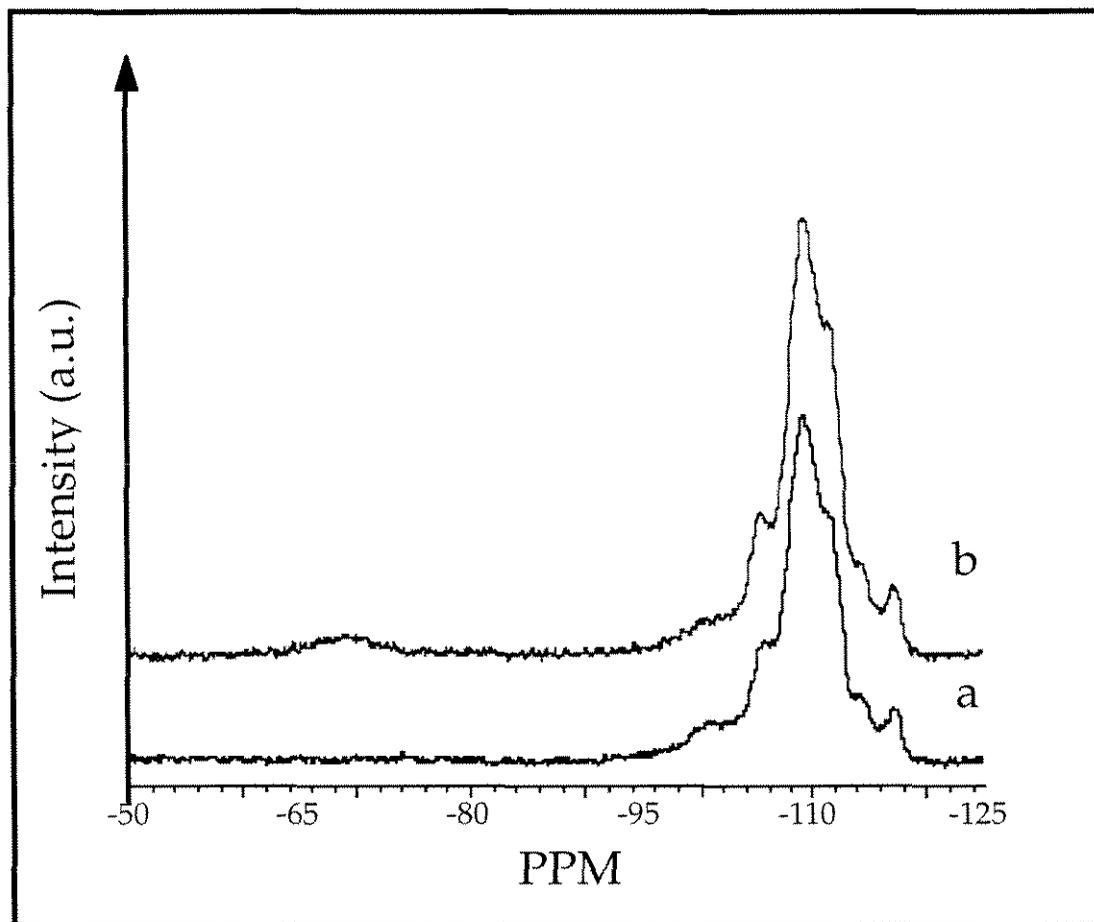
**Figure 5.7** ^{29}Si CPMAS NMR spectra of as-synthesized materials: Beta-S (a) and Beta/PE-S (b).
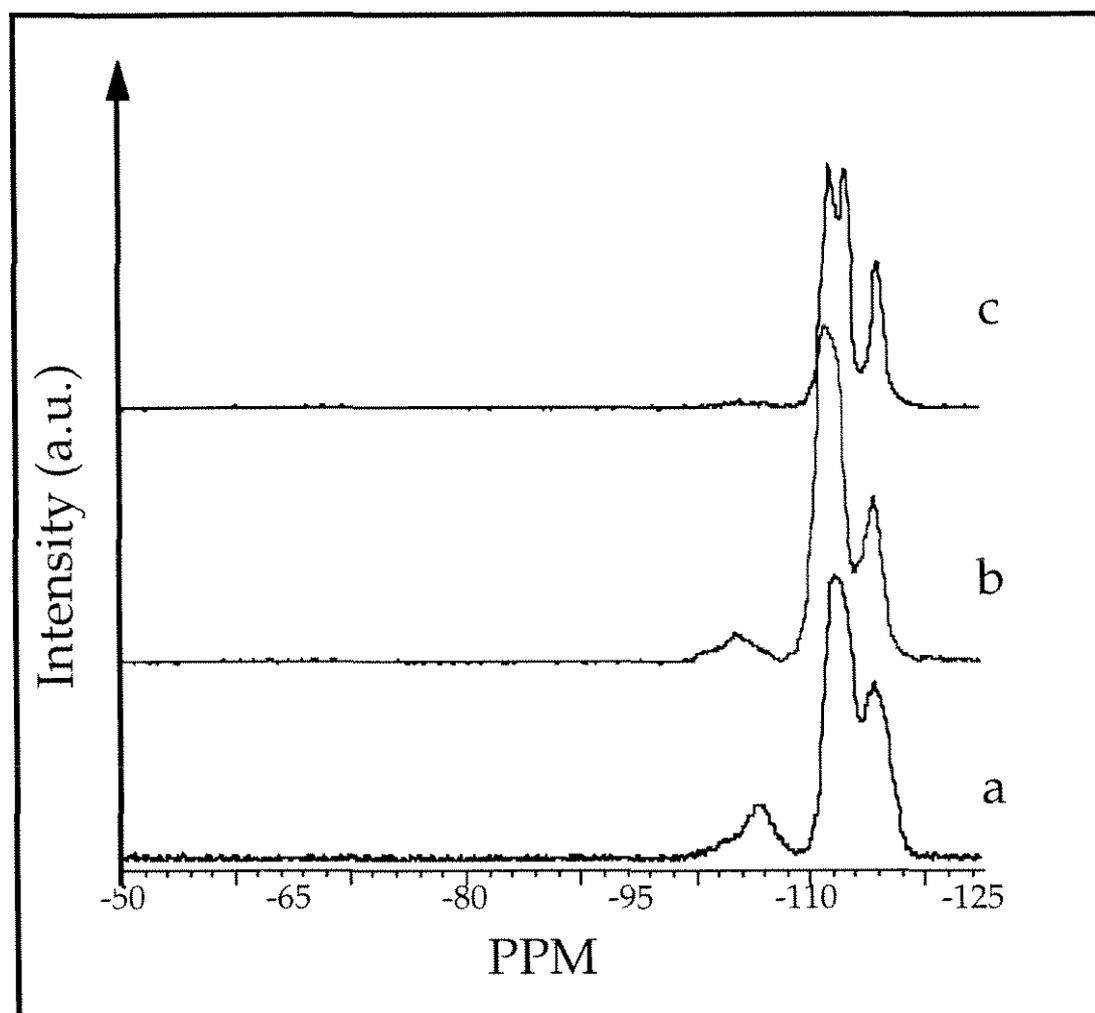
Figure 5.8 ²⁹Si MAS NMR Bloch decay spectra of extracted materials: Beta-S extracted by method 2 (a), Beta/PE-S extracted by method 2 (b), and Beta/PE-S extracted by method 3 at 80°C (c).
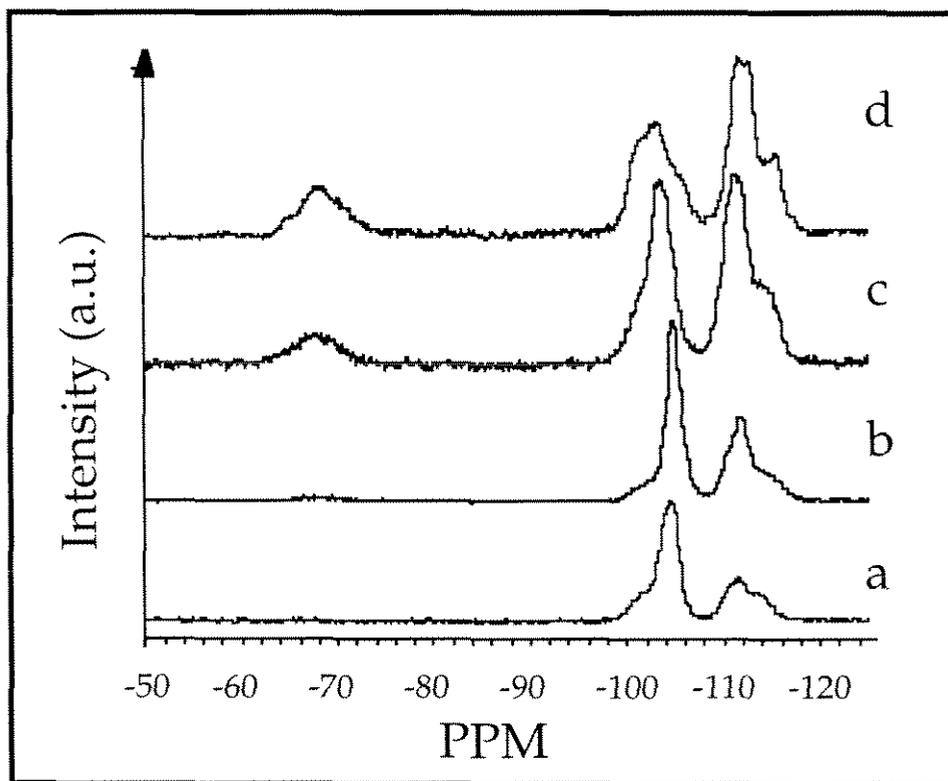
Figure 5.9 ^{29}Si CPMAS NMR spectra of extracted materials: Beta-S extracted by method 2 (a), Beta/PE-S extracted by method 1 (b), Beta/PE-S extracted by method 2 (c), and Beta/PE-S extracted by method 3 at 80°C.
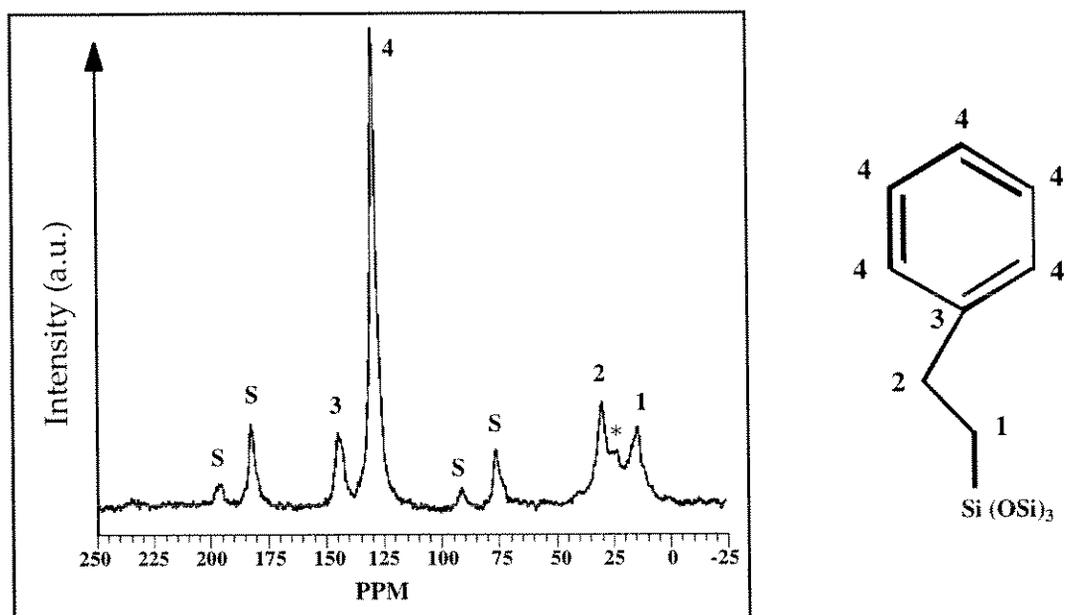
Figure 5.10 ¹³C CPMAS NMR spectra of extracted Beta/PE-0.05. Peaks marked with an S are spinning sidebands. Intensity marked with a * is due to a spinning sideband and some residual TEAF.
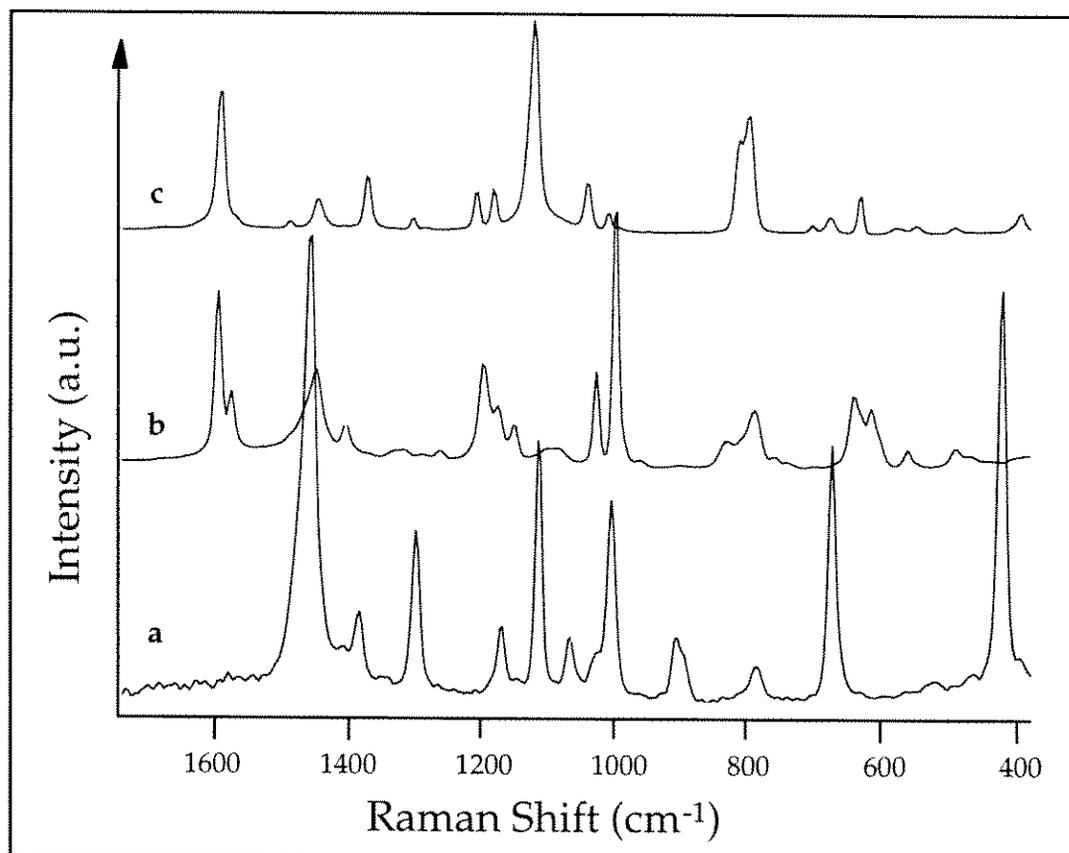
Figure 5.11 FT-Raman spectra of reference compounds: TEAF (a), pure
liquid PE monomer (b), and p-toluenesulfonic acid
hydrate (c).
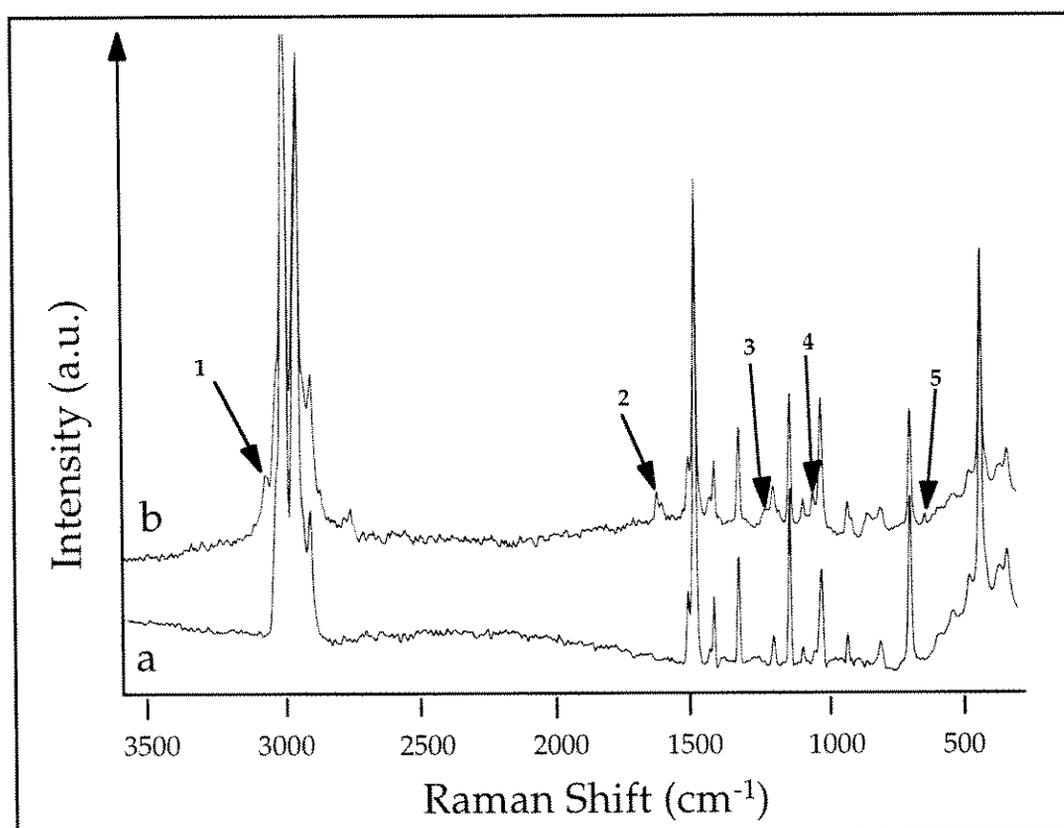
Figure 5.12 FT-Raman spectra of as-synthesized materials: Beta-S (a) and Beta/PE-S (b).
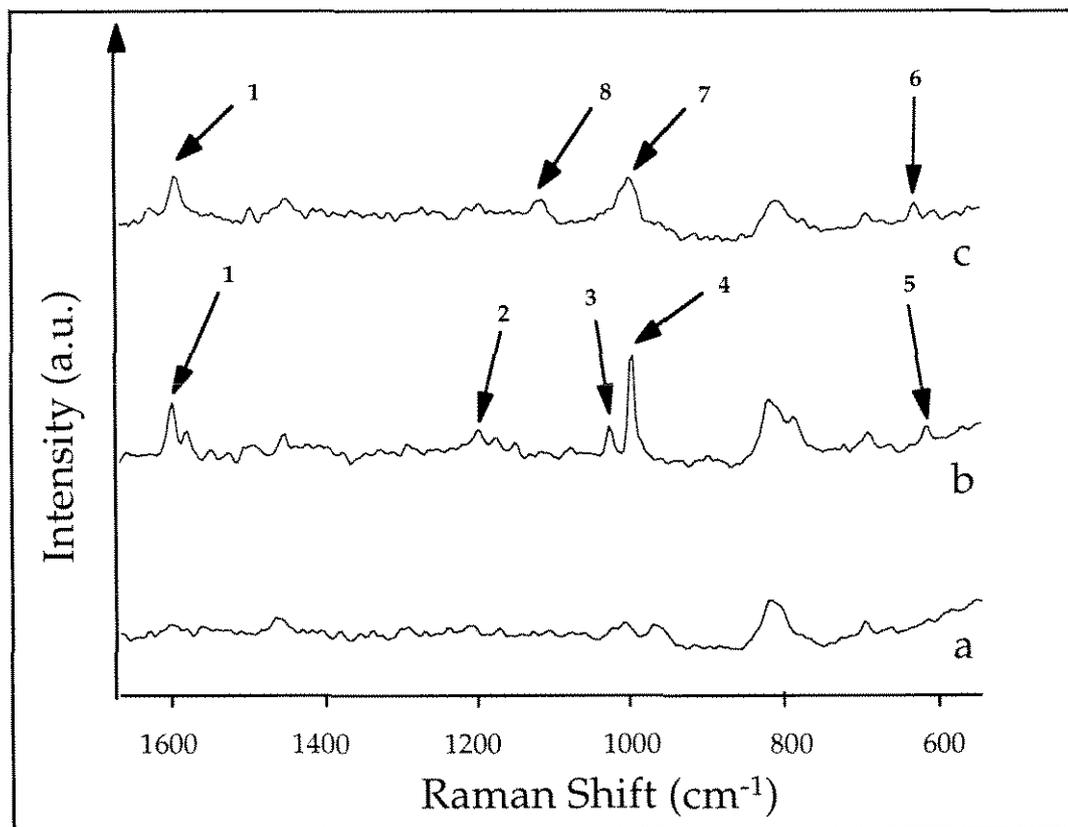
Figure 5.13 FT-Raman spectra of extracted materials: Beta-S extracted by method 2 (a), Beta/PE-S extracted by method 2 (b) and Beta/PE extracted by method 2 and subsequently sulfonated (c).
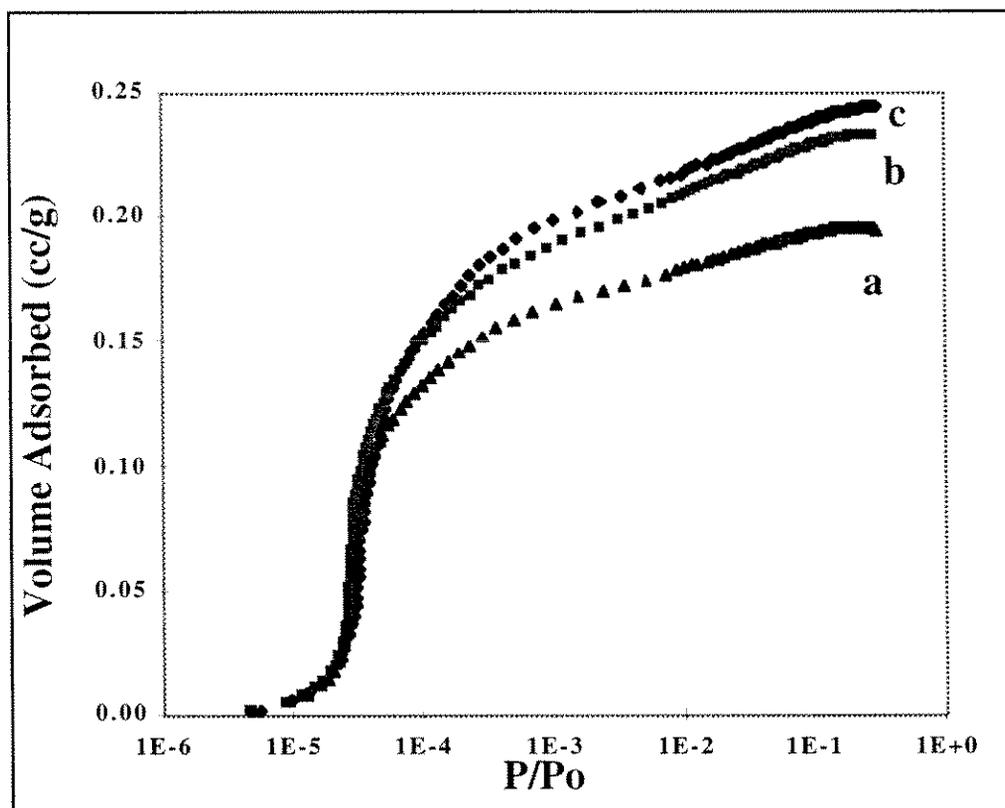
Figure 5.14 Nitrogen adsorption isotherms at 77K: Beta/PE-NS
extracted by method 3 at 120°C (a), Beta/PE-NS extracted
by method 3 at 80°C (b), and Beta/PE-NS calcined at
550°C (c).

CHAPTER SIX

Conclusions

6.1 Concluding Remarks

Investigations into the synthesis of OFMS's from synthetic gels free of organic SDA's showed that this is not a promising route to molecular sieves with tethered intracrystalline organic species. While synthesis of zeolite NaY in the presence of organosilanes routinely produced highly crystalline materials with the FAU topology, the strategy proved to produce organic-functionalized solid materials in only some cases. Additionally, in the nearly all the cases where an organic was incorporated into the solid, this organic was shown to reside in locations other than the zeolite micropores. When ZSM-5 was synthesized from organic SDA-free gels, multiple solid phases were produced in all cases. During preparation of zeolite synthesis gels free of organic SDA's, phase separation of the organosilane from the aqueous gel is observed in several cases. The immiscibility of the organosilane in an organic SDA-free synthesis gel appears to limit the potential of producing OFMS's using these synthetic strategies.

Due to the difficulties encountered when attempting to synthesize OFMS's using organic SDA-free schemes, attention was turned to the synthesis of OFMS's from synthesis gels that included an organic SDA. It was hypothesized that use of an organic SDA should reduce the tendency for phase separation of the organosilane from the other components of the gel by making the entire gel less hydrophilic. By using this approach, the first OFMS was synthesized and described, phenethyl-functionalized pure-silica zeolite beta. Pure-silica zeolite beta was chosen as a host structure because it can be synthesized using an organic SDA (TEAF) that is smaller than the diameter of the molecular sieve's largest pore. Investigations indicated that the TEAF can be extracted by solvent extraction techniques. The organic group can be further functionalized, for example by sulfonation with SO_3, and the product sulfonic acid functions as a shape-selective acid catalyst.

The synthetic technique was shown to be robust and general, as polar organic functional groups such as an aminopropyl moiety can also be incorporated into the framework. The shape-selective formation of imines from the tethered amines demonstrated that the majority of the functional groups were contained within the molecular sieve micropores and that the organic groups can be further transformed using standard organic chemical techniques.

An exhaustive, detailed investigation of the phenethyl-functionalized OFMS's indicated that the materials can be made under a wide variety of synthetic conditions employing TEAF as the organic-SDA. Additionally, it was demonstrated that alteration of the SDA extraction conditions can produce OFMS's with varying porosity and hydrophobicity. An array of polar and non-polar organic functional groups were incorporated into the OFMS's indicating that the synthetic technique is quite general, accommodating many organic groups that are sufficiently small to fit within the molecular sieve micropores.

The utilization of solvent extraction techniques for the removal of the organic SDA has implications for other molecular sieves as well as for OFMS's. In many cases, a significant cost that prevents large scale commercial production of new molecular sieves is the cost of the organic SDA used in the synthesis. The SDA cost is often prohibitively high because it is lost during the calcination step that is generally required for generation of porosity. In particular, highly hydrophobic, pure-silicate molecular sieves, which are sought after for their unique adsorptive properties, are not widely available commercially for this reason. However, this cost could largely be eliminated if the organic SDA could be recovered and reused. Using the methodology described here, it may be possible recover the expensive TEAF from the relatively simple 3 component mixture (water, TEAF, acetic acid) and reuse it in subsequent molecular sieve syntheses. This extraction methodology has been subsequently extended to other molecular sieves [1].

The ability to tether organic species within the micropores of the molecular sieve allows for the creation of a wide array of new types of sites for catalytic and molecular recognition applications. In particular, these materials appear promising for low temperature liquid phase catalytic applications where zeolites are not effective. For example, many species such as nitric acid, acetic acid, or oxalic acid are in many cases not compatible with zeolites, as they are capable of leaching aluminum out of the framework. However, reactions that contain one of these components as a reactant or product are not likely to be detrimental to OFMS's. Furthermore, the ability to tailor the properties of the active site, for example the pKa or pKb of an acid or base site, will enable highly specific catalysts to be designed for a particular application.

The potential to position organic species in the hydrophobic OFMS micropores allows for the possibility to create inorganic catalytic materials with similarities to biological catalysts such as enzymes and catalytic antibodies. Many biological catalysts have active sites where one or more amino acid side chains in a hydrophobic binding pocket are responsible for stabilizing the reaction transition state. With the ability to synthesize inorganic silicates with catalytically active organic residues within the hydrophobic micropores (OFMS's), catalysis with inorganic, heterogeneous catalysts has moved one step closer to true biological catalyst mimics. The potential now exists to take the next step and synthesize OFMS's with multiple organic residues positioned within the micropores.

In summary, by successfully, synthesizing the first OFMS materials, a new class of molecular sieves with attributes unlike any previous types of molecular sieves is now available to catalytic chemist.

6.2 References

[1] T. Takewaki, L. W. Beck and M. E. Davis *J. Phys. Chem. B*. 103 (1999) 2674